BENHA UNIVERSITY
Shoubra Faculty of Engineering
Basic Science Department

Physical Properties for Initial Phase of Nuclear Matter in Terms of Experimental Measurements and Corresponding Predictions of Theoretical Models

A Thesis submitted in partial fulfillment of the requirements of master's degree in engineering physics, Basic Science Department, Faculty of Engineering at Shoubra, Benha University

By

Eng. Ahmed Mostafa Abdelrazik Sayed

M.Sc. Student in Engineering Physics, Basic Science Department, Faculty of Engineering at Shoubra, Benha University

Supervised By

Prof. Dr. Ahmed Mohamed Abdalla

Professor of Engineering Physics, Basic Science Department, Faculty of Engineering at Shoubra, Benha University.

Assoc. Prof. Dr. Abd El-Nasser Saber Abd El-Fattah

Associate Professor of Engineering Physics, Basic Science Department, Faculty of Engineering at Shoubra, Benha University.

Cairo - Egypt
2024

ACKNOWLEDGMENTS

I would like to express my sincere appreciation to everyone who has contributed to the completion of this master's thesis. First and foremost, I am deeply thankful to my main supervisor, Prof. Dr. Ahmed Abdalla, for his valuable guidance, steady support, and insightful feedback throughout this research journey. His expertise, encouragement, and patience have been instrumental in shaping this thesis. I extend my heartfelt appreciation to my friend and supervisor, Assoc. Prof. Dr. Abdelnasser Saber, for his constructive criticism, valuable suggestions, and scholarly visions, which have significantly enriched the quality of this work. In addition, I am grateful for the opportunity to work with the mentioned board as teammates and the weekly meeting from the beginning of this research. I am thankful to my family for their solid love, encouragement, and understanding throughout this academic endeavor, especially my wife, for her unlimited support and cooperation. Her constant support and belief in my abilities has been my source of strength and motivation. Lastly, my huge thanks to my parents for their endless love and support throughout my studies. Without them, I would not have made it this far. I acknowledge with gratitude all those who have directly or indirectly contributed to the completion of this thesis. Their support and encouragement have been indispensable, and I am truly grateful for their assistance.

Ahmed Mostafa

ABSTRACT

Study of internal physical properties for hadrons (protons) is very important in physics. These properties are investigated by using different techniques. Elastic scattering experiments are one of them. Scattering theory using Quantum Electro-Dynamics (QED), is a suitable method especially for high energy experiments. Feynman diagrams are applied for Lepton-Hadron scattering to give a suitable expression for scattering cross-section known as Mott formula. In this thesis we drive it for electron-proton elastic scattering. A comparison between this prediction and experimental measurements is discussed. At low values of momentum transfer, the proton appears as a point-like particle while its constituents appear to be contributed to scattering process with high values. It concludes that there is a modified factor that must be added to Mott formula. This factor is related to electric and magnetic properties of the internal constituents of proton. These factors are called form factors. By comparison with experimental data, the calculated values agreed with that obtained from other groups. The charge radius of proton is expected to be 0.81 fm. Different images for proton are obtained due to different values of momentum transfer and compared with the photon wavelength.

Table of Contents

List of Tables

List of Figures

Chapter 1

Introduction

1.1 Introduction

Nuclear physics represents a basic branch of science, and it developed back to Becquerel's discovery of radioactivity in 1896 in addition to Rutherford's experiment of the existence of the nucleus in 1911. Experimental and theoretical research in nuclear physics has been a significant contributor to the growth in science of the twentieth century. The overall positive charge in the nucleus as well as the total number of mass units define a nuclear species. All elements are characterized by atomic number Z and charge Q where $Q = +Ze$ and $|e| = 1.6 \times 10^{-19}$ C, the magnitude of the electronic charge. The fundamental positively charged particle in the nucleus is the proton, which is considered the nucleus of the simplest atom, hydrogen. Atoms of the elements are electrically neutral charge they must have Z negatively charged electrons. The nucleus must contain additional large mass components called neutrons of number N. This number is independent of Z. The sum of $Z + N = A$ is called mass number or nucleon number. We discover that nuclides with a particular atomic number can have multiple various mass numbers, i.e., a nuclide with Z protons can have a range of different neutron numbers. Isotopes are nuclides that share the same proton number but have different neutron numbers; For instance, the two isotopes $_{17}Cl^{35}$ and $_{17}Cl^{37}$. They have unified chemical properties but differ in nuclear properties because they have different neutron numbers. The term "isotone" is frequently used to describe a group of nuclides that share the same N but have various Z. ^{2}H and ^{3}He are the stable isotones with N = 1. Isobars are nuclides that have the same mass number A; for example, radioactive ^{3}H and stable ^{3}He are both isobars. Because the mass of the electrons is so little in comparison to the mass of the proton (neutron) (m_p=2000 m_e). The electron

may frequently be neglected when talking about the mass of an atom. In nuclear physics we use suitable scale of measuring lengths of the order of 10^{-15}m, which is one femtometer (fm). The proton radius is around 1 fm, and the radius of nuclei increases with mass number to reach about 7 fm. For nuclear mass the used unit is called atomic mass unit u where $1\,u = 1.6605402 \times 10^{-27} Kg$. It defined such that the mass of an atom of ^{12}C is precisely 12 u. As a result, the nucleons have masses of around 1 u. For nuclear energies, we use relativistic mass-energy relation $E=mc^2$ where c is the speed of light. The conversion factor is 1u = 931.502 MeV; so, the nucleons have mass energies of approximately 1000 MeV. Sometimes the masses of nuclear material are represented in terms of their energies [1]

1.2 Natural Units

In high energy and particle physics it is important to introduce suitable units relevant to fundamental constants of relativistic quantum mechanics. The magnitudes of both Plank's constant h and c are used by units' value h = c = 1. Dimensional analysis may always be used to determine precisely where the h's and c's enter any equation. As a result, it is common to speak about mass (m), momentum (mc), and energy (mc^2) all in terms of GeV, also to measure length (ħ/mc) and time (ħ/mc^2) in units of GeV^{-1} where $\hbar = h/2\pi$. We haven't talked about the elementary charge e, which indicates how strongly two electrons interact electromagnetically with one another. We analyze the electromagnetic force of repulsion between two electrons separated by one natural unit of length with the rest mass energy of an electron to derive a dimensionless measure of the intensity of this interaction. The coupling constant α (fine structure constant), for electromagnetic interactions will be often employed and is defined as $\alpha = \frac{e^2}{4\pi\varepsilon_o\hbar c} \approx \frac{1}{137}$

In atomic physics, $4\pi\varepsilon_o = 1$, hence $\alpha = e^2$ in Gauss system of units. while $\alpha = e^2/4\pi$ are more widely employed in particle physics and known as the fine structural constant.[2]

1.3 Nature Fundamental Forces

Our understanding of the fundamental forces of nature, and hence of the fundamental interactions between elementary particles, has developed with our picture of elementary particles. By the end of the nineteenth century, electricity and magnetism were accepted to be expressions of the same force called electromagnetism. Later, it was discovered that atoms have a structure and are made up of a positively charged nucleus and an electron cloud, with the entire kept together by electromagnetic system. Nuclear physics provided; two new short-ranged forces joined the ranks. These are the nuclear force, which operates between nucleons, and the other is the weak force, which reveals itself in nuclear decay[3]. Nuclear force is caused by the strong force bringing quarks together to produce protons and neutrons. These strong and weak forces cause the equivalent basic interactions between elementary particles. The four fundamental interactions on which all physical phenomena are founded are gravity, electromagnetic interaction, strong interaction, and weak interaction. While gravity is necessary for the survival of stars, galaxies, and planetary systems, it has no bearing on subatomic physics since it is simply too weak to impact the interaction of fundamental particles. Some properties of each interaction are summarized and given in table 1.1

Table 1.1: Classification of Fundamental Forces of Nature.

Types of Force	Coupling Constant (α)	Theory	Mediator Particles	Mass (GeV/c^2)	Range (meter)
Strong	1	Chromodynamics	Gluon	0	10^{-15}
Electromagnetic	1/137	Electrodynamics	Photon	0	infinite
Weak	10^{-6}	Flavor dynamics	W , Z	$M_W \approx 80$ $M_Z \approx 91$	10^{-18}
Gravitational	10^{-39}	Geometro dynamic	Graviton	0	infinite

All interactions are explained by considering mediator boson particles characterized by unit spin. In electromagnetic interactions, they are photons, in strong interactions, gluons, and in weak interactions, the W^+, W^-, and Z^0 bosons.

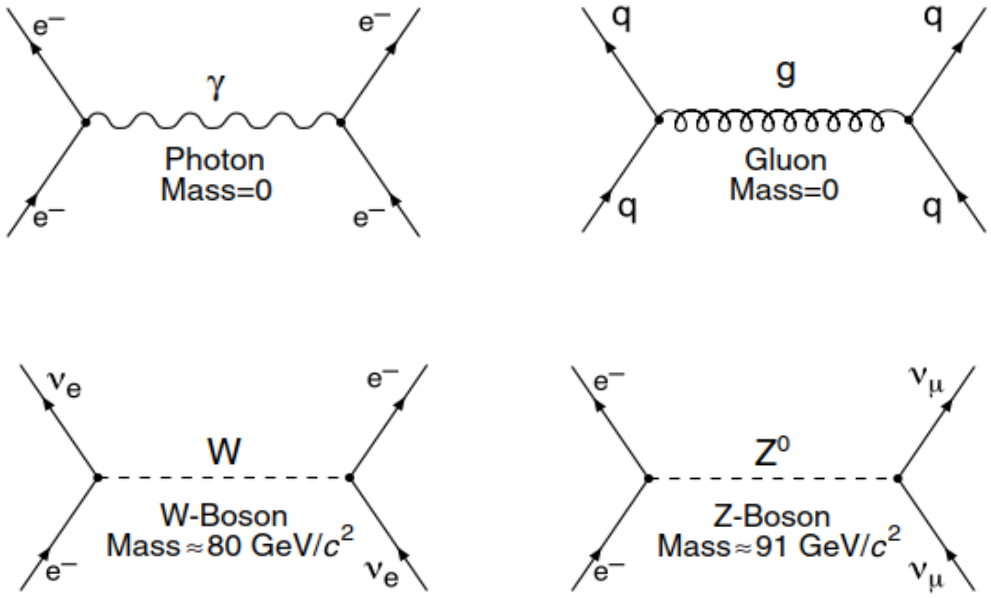

Figure 1.1: Feynman Diagrams for Different Interactions.

Figure (1.1) gives examples of interactions between two particles via boson exchange. These straight lines represent leptons and quarks. The wavy lines represent photons while spirals represent gluons, and dashed lines represent

W and Z^0 bosons. Each of these three interactions has a specific charge attached to it. An interaction occurs when a particle possesses between their charges. The interactions are characterized by a factor called coupling constant (α) which is defined in terms of electromagnetic interactions as the ratio between potential energy and photon energy. The coupling constant is maximum for strong interaction and decreases to zero for gravitational force. In electromagnetic interactions, the intermediate boson particle is the photon which has zero rest mass. As a result, it has an indefinite range. There is a boson particle like photon, called gluon have no rest mass. The gluon particle is responsible for strong interaction. Photons have no electrical charge while gluons hold a color charge responsible for interaction with one other. The W and Z bosons, with masses of $M_W \approx 80$ GeV/c^2 and $M_Z \approx 91$ GeV/c^2, are extra ordinary heavy particles.[4]

1.4 Proton Structure

Electron is elementary particle which has a single charge e and has magnetic momentum $\mu_e = \frac{e\hbar}{2m_e}$ associated to it and has been measured experimentally [4]. When protons and neutrons were discovered in 1919 and 1931, respectively, they were thought to be like electrons. Proton was intended to be point-like, with similar electron charge and mass m_p as represented by:

$$\mu_p = \frac{e\hbar}{2m_p} \tag{1.1}$$

The expected value for neutron is zero because it is a neutral particle.

$$\mu_n = 0 \tag{1.2}$$

Further measurements of the magnetic moments of these nucleons are

$$\mu_{\mathrm{p}} = 2.7928444\,\frac{e\hbar}{2m_p} \quad , \quad \mu_{\mathrm{n}} = -1.91304308\,\frac{e\hbar}{2m_p} \tag{1.3}$$

which contradicts the expected values. It gives the first evidence to confirm the presence of the nucleon substructure. The Second evidence is the analogy between behavior of the measurements of scattering experiments for both Rutherford scattering of alpha particles on gold nucleus and which carried for electron on single proton. The scattering data is shown in figure (1.2).

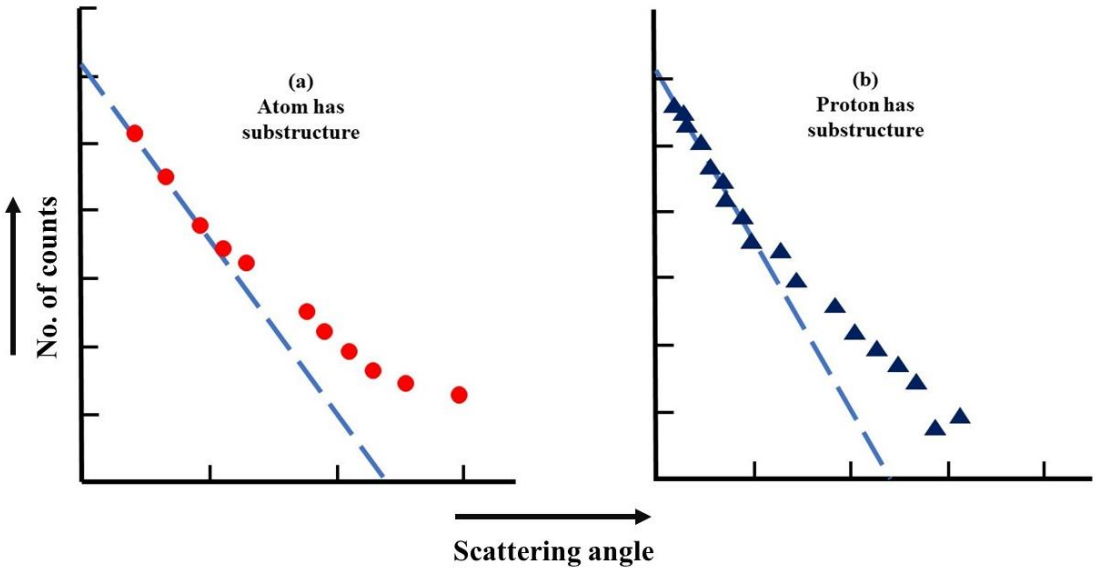

Figure 1.2: Scattering Experiments of gold nucleus and proton.

The experimental data for both scattering processes is assumed due to scattering off point-like particles with specific charge and mass to agree the dashed lines, but it deviated. This confirms the proton is not an elementary particle and has internal structure of partons latterly known as quarks which are collected to give proton properties.

After discovering the substructure of nucleons (protons and neutrons), we now live with the notion of the standard model, and it will be quickly explained that all matter is made up of three types of fundamental particles: leptons, quarks, and mediators. There are six leptons, each with its own charge (Q),

electron number (L_e), muon number (L_m), and tau number (L_τ). They are naturally divided into three families:

Table 1.2: Lepton Classification.

L	Q	L_e	L_μ	L_τ
e	-1	1	0	0
ν_e	0	1	0	0
μ	-1	0	1	0
ν_μ	0	0	1	0
τ	-1	0	0	1
ν_τ	0	0	0	1

There are six antileptons, which have all their signs inverted. For example, the positron has a charge of +e and an electron number of -e. So, in total, there are 12 leptons. Similarly, quarks are classified into three quarks called up quark u has charge $+\frac{2}{3}$, down quark d has charge $-\frac{1}{3}$ and strange s its charge is $-\frac{1}{3}$. The theory of standard model proposed proton is composed of uud combination and neutron is udd. The antiquarks take inverted sign.

The first explanation of strong interaction was by Yukawa theory (1934) to explain the nuclear force [4]. He assumed a mediator boson called π-meson of mass ≈ 139 MeV/c^2 and coming with charge ± e and natural. So, the issue becomes, what particle is transferred between two quarks in a strong process of nucleon? Now, nuclear force is explained by quark-quark interaction rather than nucleon-nucleon interaction. The Standard Model has eight of these mediators, known as gluons. Quarks and gluons carry color charges red, green, and blue in addition to their anti-colors. Nucleons are a combination of these colors to form colorless particles. Quarks should not exist as independent particles. At high energy nuclear collisions of hadron-hadron, hadron-nucleus and nucleus -nucleus, there is creation of a large number of

mesons (combination of quark and antiquark) with high multiplicities depending on collision energies. It explained by assumptions that there is quark-quark, quark- gluon and gluon-gluon interactions. These are responsible for the creation of high multiplicities of quarks and anti-quarks to form hadrons that appear as new mesons which experimentally recorded. The predicted mathematical theory which is used for this analysis is called quantum chromodynamics.

In order to reach a complete description of the nuclear force we must study the fine properties of the internal constituents of hadrons like proton and neutron. This requires many scattering experiments using lepton particles as electrons scattered off hadron such as proton. In this thesis, we will be interested in electron-proton scattering in terms of theoretical predictions by quantum electrodynamic theory at wide range of energy. Then comparing these predictions with experiments.

In the next chapter we will study the theory of quantum electrodynamic and scattering process using Feynman diagram and Fermi-Golden rule to derive the elastic cross-section of electron proton scattering called Mott's formula.

Chapter 2

Scattering Theory

2.1 Primitives

Scattering process between two bodies reveals information about the microscopic details of the materials specially at high energy and scattering among elementary particles against each other can reveal information about the existence of new fundamental particles. Scattering theory is the mechanical formalism in which one body is called projectile and the other is target. Scattering process can be explained in different ways according to the nature of both projectile and target in addition to the scattering energies. One of these techniques is classical mechanics which treats bodies as rigid ones with defined mass and momentum. There is another formalism, quantum mechanics which deals with the wave nature of particles that accompanied the particle during its motion. An important treatment called Quantum Electro Dynamics QED that deals with high energy scattering among elementary particles. There are two types of scattering one is the elastic scattering at which the energy and nature for both projectile and target are conserved. The other type is the inelastic scattering to which the conservation laws are not applicable. Figure (2.1) gives a simple diagram of the basic idea of scattering mechanism. A small projectile with specific physical properties (charge, mass, energy) is directed towards a fixed target with a relatively large size and a suitable value of impact parameter b (the distance between the centers interacting particles). The projectile will interact in some way and deviate by an angle called scattering angle θ, measured from the direction of incidence. In the following sections, we will give short notes on some possible treatment of this process according to different assumptions.[5]

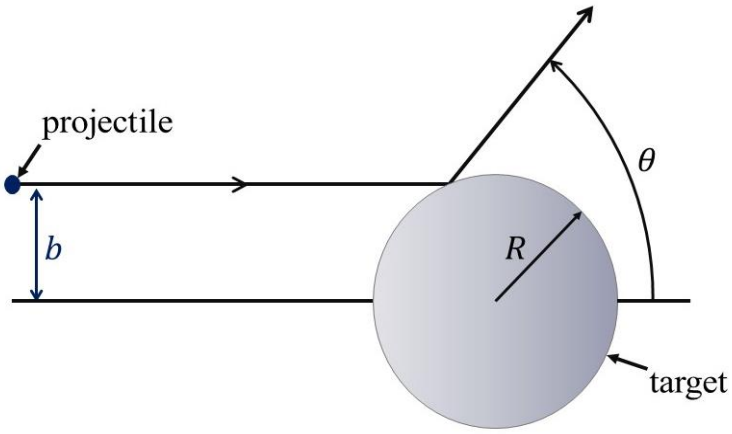

Figure 2.1: An illustration of hard sphere scattering.

2.2 Classical Mechanics in Scattering Theory

Classical theory of scattering considers both projectile and target are hard spheres. They will not orbit each other but approach before the repulsive potential U(r) causes them to move away and never meet again. This type of behavior is shown in figure (2.1). The parameter r is the distance between the center of scattering and the center of the target. In this mechanism a projectile is directed from distance of infinity where $r > R$ and U(r) = 0 in which there is no forces exerts on its motion. The projectile doesn't suffer any deviation and continues along its direction. When projectile collides with the target surface r = R it will be exerted by a force due to potential energy U(r) and suffers a deflection by angle θ. The possible magnitudes of θ depend on the projectile energy, potential energy, and the impact parameter b. In this mechanism, a collision between two particles conserves total energy; we typically refer to the scattering as being elastic. The scattering angle is taken to range anywhere between zero and π radians, where zero radians correspond to absolutely no scattering, and π radians correspond to complete backward scattering. Most scattering experiments involve firing many particles at a

collection of targets, measuring the outgoing angles, and then comparing the results against a set of statistical predictions. For this reason, there is some additional terminology we need to develop beyond what we have been discussing for far in the simple two-body problem, terminology related to the concept of a cross-section. The concept of cross-section, as its name suggests, is that of effective area for collision. In aiming a beam of particles at a target which is much smaller than the beam, as in the Rutherford scattering experiment, the cross-section takes on a statistical nature. To understand the basic concept of a cross-section, we will start by considering a very simple model of scattering, where the potential experienced by the projectile is given by.

$$U(r) = \begin{cases} 0, & r > R \\ \infty, & r < R \end{cases} \tag{2.1}$$

This type of scattering potential is known as hard sphere scattering and is illustrated in figure (2.1). Notice that the solid sphere has an overall cross-sectional area of

$$\sigma = \pi R^2 \tag{2.2}$$

There is a region of space, with cross-sectional area σ, that projectiles cannot pass through. If the incoming path of a projectile passes through this cross-sectional area, it will be deflected off at some angle. For this reason, we define σ to be the scattering cross-section for this potential. The scattering cross-section gives us an intuitive sense of how much area is blocked out by the target during a scattering event. To see how this notion is useful to us, let's imagine that instead of one target, we have devised an experiment which in fact contains many targets, as shown in figure (2.2).

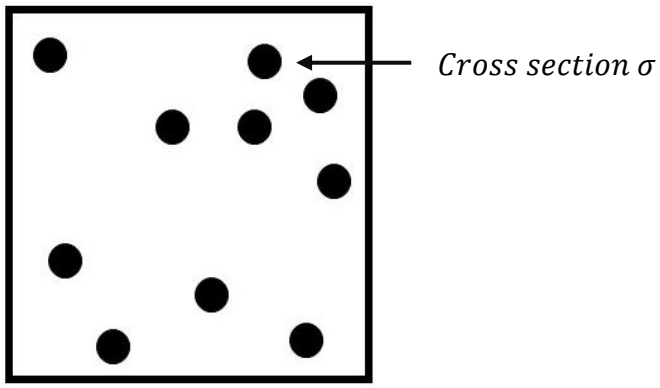

Figure 2.2: A sheet containing many hard sphere targets, each with a scattering cross-section σ.

Figure (2.2) shows a "head-on view" as seen by an incoming projectile. If we describe the surface density of targets by the quantity n_{tar} , then the total number of targets in the sheet is given by An_{tar} , where A is the total area of the target assembly. If we now imagine that our target assembly contains many targets, while still remaining dilute, and that we are interested in describing a large number of scattering events, we can apply statistical considerations when discussing the number of deflections that occur. For any given projectile that is fired at the target assembly, the probability that it will hit one of the spheres and scatter is given by the total cross-sectional area of all the targets, divided by the total area of the assembly, so that.

$$P = \frac{An_{\text{tar}}\,\sigma}{A} = n_{\text{tar}}\,\sigma \tag{2.3}$$

If we now imagine that the number of incident projectiles, we fire at the sheet is N_{inc}, then statistically speaking, the number of scattered particles, N_{sc}, should be given by

$$N_{\text{sc}} = PN_{\text{inc}} = N_{\text{inc}}\ n_{\text{tar}}\ \sigma \tag{2.4}$$

To derive an expression of the cross-section in terms of the experimental parameters, let's return to our single hard sphere target, and consider the motion of a single projectile which strikes it with impact parameter b. This is indicated in figure (2.3).

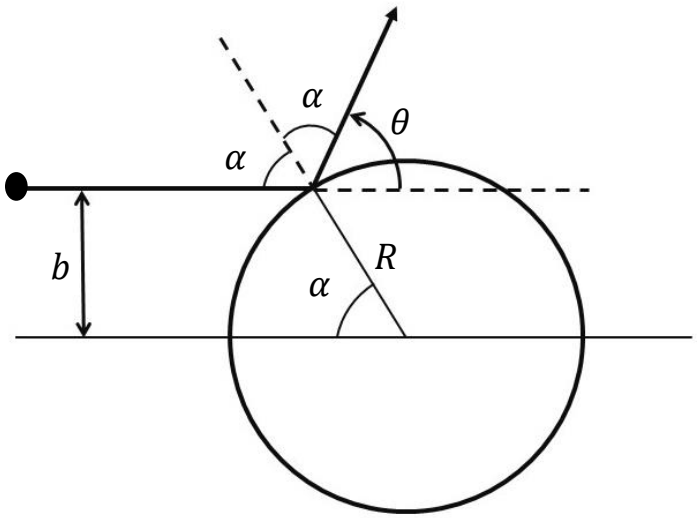

Figure 2.3: The motion of a projectile which strikes a hard sphere with impact parameter b.

In this simple model, it is relatively straight-forward to determine the scattering angle as a function of the impact parameter. The trick is to make use of the fact that the angle of incidence on the surface of the sphere must be the same as the angle of reflection, with respect to the surface tangent of the sphere. This certainly seems "obvious" for scattering off of a hard surface, although we could in fact prove this claim if we wanted to, based on angular momentum and energy conservation. If we denote this angle as α (as is done in the figure), then some simple geometric reasoning and some trigonometry led us to the conclusion that.

$$b = R\sin\alpha \tag{2.5}$$

This is due to the fact that various theorems in geometry about parallel lines tell us that all of the angles marked as α must in fact be the same. Further study of figure (2.3) also indicates that

$$\pi = \theta + 2\alpha \tag{2.6}$$

since these angles add up to a full 180 degrees. Combining these two results, we have

$$b = R \sin\left(\frac{\pi}{2} - \frac{\theta}{2}\right) = R \cos\frac{\theta}{2} \Rightarrow \theta = 2 \arccos\left(\frac{b}{R}\right) \tag{2.7}$$

Notice that this expression becomes undefined when b > R, which makes physical sense in which there is no scattering. When we are interested in particles that scatter only within an infinitesimal range of angles, say dθ, what range of impact parameters, db, is necessary to achieve such a scattering? The result we have just derived tells us that if we want our projectile to scatter into an angle θ + dθ, it must have an impact parameter.

$$\begin{aligned} b + db = R \cos\left(\frac{\theta}{2} + \frac{d\theta}{2}\right) &\approx R \cos\left(\frac{\theta}{2}\right) - \frac{R}{2}\sin\left(\frac{\theta}{2}\right) d\theta \\ &= b - \frac{R}{2}\sin\left(\frac{\theta}{2}\right) d\theta \end{aligned} \tag{2.8}$$

Thus, we find that in order to increase the scattering angle by an amount dθ, we must increase the impact parameter by db where, db is

$$db = -\frac{R}{2}\sin\left(\frac{\theta}{2}\right) d\theta \tag{2.9}$$

We can consider this quantity db as the amount of "infinitesimal cross-section" which determines the area within which a particle's path would need to pass for it to scatter into a range of angles dθ. Now it is possible to integrate this quantity over all possible outgoing angles. Before performing this integration, we need to admit the possibility of multiple projectiles coming along multiple paths and scattering off one target in a wide range of angles

from the central axis. This is illustrated in figure (2.4). In this case, the infinitesimal amount of scattering area is not db, but rather.

$$d\sigma = 2\pi b db \tag{2.10}$$

The extra factor of 2πb comes from the circumference around the central scattering axis. Integrating this expression over all angles, we find

$$\int d\sigma = -\pi R^2 \int_0^{\pi} \sin\left(\frac{\theta}{2}\right) \cos\left(\frac{\theta}{2}\right) d\theta = -\pi R^2 \tag{2.11}$$

Aside from a minus sign, this is simply the total cross-section for scattering by the hard sphere.

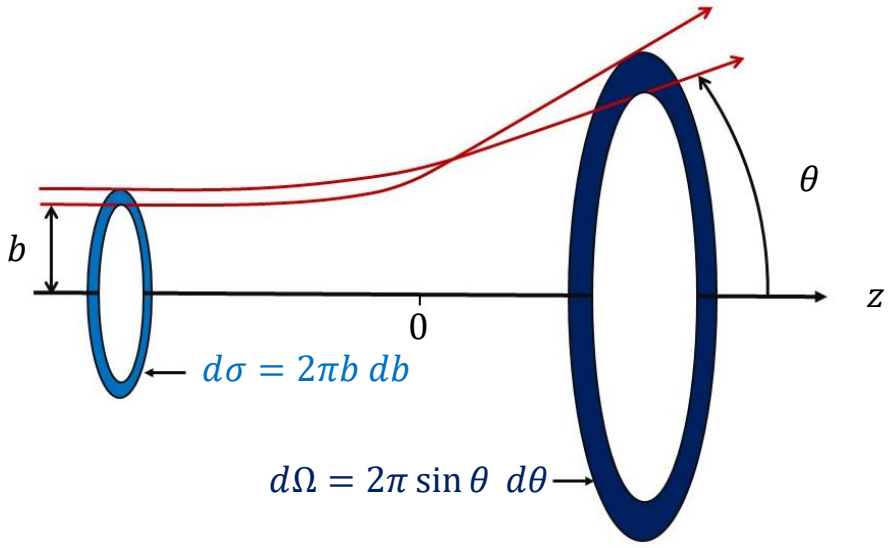

Figure 2.4 : The scattering of multiple projectiles off of a hard sphere, all with an impact parameter which lies between b and b + db.

That is to say, the result for b as a function of the scattering angle θ did not depend on the angle around the central scattering axis φ. In three dimensions the impact parameter and the infinitesimal dσ are function of both angels θ and φ. The formed area corresponding these angles described by solid angle dΩ and shown in figure (2.5).

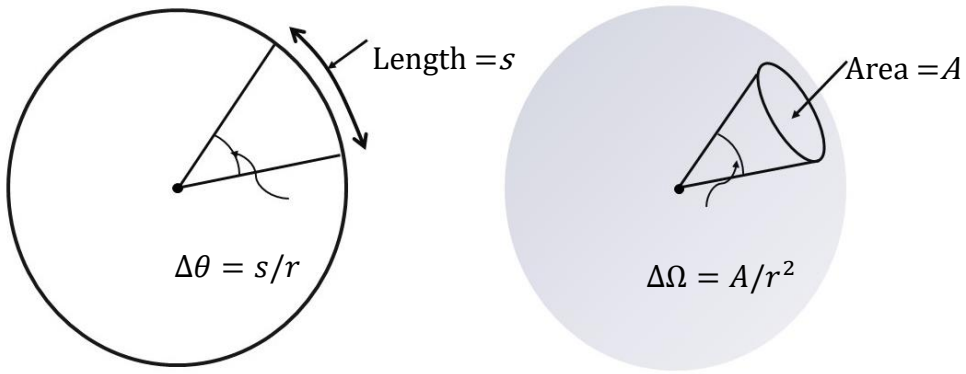

Figure 2.5: a.) The definition of an angle in two dimensions. b.) The definition of solid angle in three dimensions.

In two dimensions, the angular difference between two points on a circle can be defined as

$$\Delta\theta = \frac{s}{r} \tag{2.12}$$

where s is the arc length between the two points, and r is the radius of the circle. In three dimensions, we can similarly define the amount of solid angle corresponding to a patch of area on the surface of a sphere. Analogously to the two-dimensional case, the amount of solid angle is defined as

$$\Delta\Omega = \frac{A}{r^2} \tag{2.13}$$

The unit of solid angle is the steradian, as opposed to the radian which describes regular angles. Notice that since the surface area of a sphere is $4\pi r^2$, the solid angle corresponding to all possible directions in three-dimensional space is given by 4π steradians. In particular, we will often be interested in knowing the amount of infinitesimal solid angle surrounding a set of angles θ and φ which describe a spherical coordinate system. The volume element is given by

$$dV = r^2 \sin\theta \, dr \, d\theta \, d\phi \tag{2.14}$$

so that the infinitesimal amount of area on the surface of a sphere with radius r is given by

$$dA = \frac{dV}{dr} = r^2 \sin\theta \, d\theta \, d\phi \tag{2.15}$$

Thus, the infinitesimal amount of solid angle surrounding a given direction in spherical coordinates is given by

$$d\Omega = \frac{dA}{r^2} = \sin\theta \, d\theta \, d\phi \tag{2.16}$$

Having introduced the idea of solid angle, we are now ready to define differential cross-section D(θ), which is illustrated in figure (2.6).

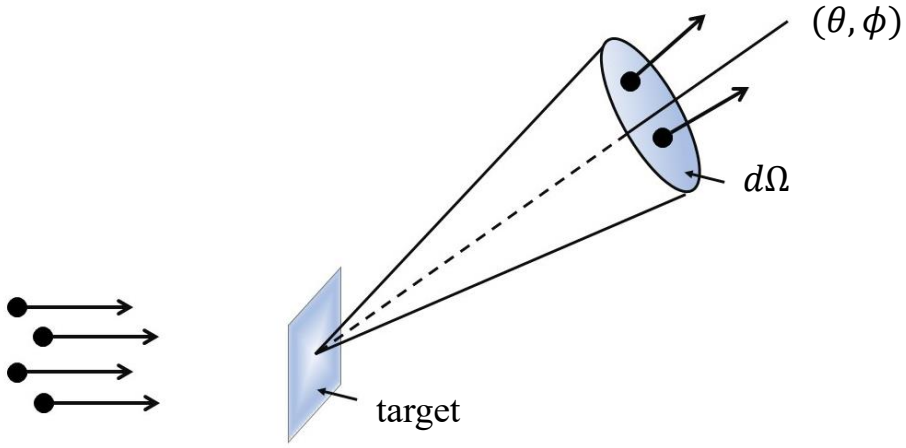

Figure 2.6: The notion of a differential cross-section.

We again imagine that we have fired a sequence of projectiles at a large sheet full of many targets, with some density n_{tar}. Instead of asking about the total cross-section for scattering, we can ask about the infinitesimal amount of cross-section dσ that is required for a particle to scatter off at some angle into a small amount of solid angle dΩ. By the same reasoning as before, if we think

in statistical terms, then the total number of particles scattered into this small region of solid angle should be

$$N_{\mathrm{sc}}(d\Omega) = N_{\mathrm{inc}}\ n_{\mathrm{tar}}\ d\sigma(d\Omega) \tag{2.17}$$

The total cross-section can then be found by integrating.

$$\sigma = \int d\sigma = \int \frac{d\sigma}{d\Omega} d\Omega \tag{2.18}$$

The quantity appearing in the integral,

$$D(\theta) = \frac{d\sigma}{d\Omega} \tag{2.19}$$

The results of scattering experiments cannot determine the initial impact parameter of a given projectile, but they can detect the number of particles being scattered into a certain region of solid angle with great accuracy. The differential cross-section can be determined from experimental measurements on the number of incident particles, the density of targets in our material, and the number of particles scattered off at some angle. In many areas of physics, a given model describing the interactions between particles will result in a theoretical prediction for the differential cross-section in a given experiment. This prediction can then be tested against experiments, in order to verify the given model. In this case, assuming that we have found the function b (θ), the amount of infinitesimal scattering cross-section will again be given by

$$d\sigma = 2\pi\ b\ db \tag{2.20}$$

In this case, the total amount of solid angle, integrated over all values of φ, is given by

$$d\Omega = 2\pi \sin\theta\ d\theta \tag{2.21}$$

Dividing these two expressions, we have

$$D(\theta) = \frac{d\sigma}{d\Omega} = \frac{b}{\sin\theta}\left|\frac{db}{d\theta}\right| \tag{2.22}$$

where we have added the absolute value signs to ensure that the result is positive. Notice that for the case of hard sphere scattering, this gives.

$$D(\theta) = \frac{R^2}{4} \tag{2.23}$$

which is completely independent of angle (as we would expect for a sphere). Integrated over all solid angles, we find.

$$\sigma = \frac{R^2}{4} \int d\Omega = \frac{R^2}{4} \int \sin\theta \, d\theta \, d\phi = \pi R^2 \tag{2.24}$$

2.3 Coulomb Scattering

In the following section, we will be concerned by the Coulomb scattering which is sometimes called Rutherford scattering. In this type of scattering, both projectile of atomic number Z_1 and target Z_2 are electrically charged. The projectile reaches the closest approach of the target before it deflects away due to the electrical potential of the target. It can be shown in figure (2.7) the projectile has the chance to get closer to the target then it starts bending away after it suffers an electrical potential from the target making an angle θ measured from the initial direction. The conservation laws of momentum are applicable in this mechanism. [6]

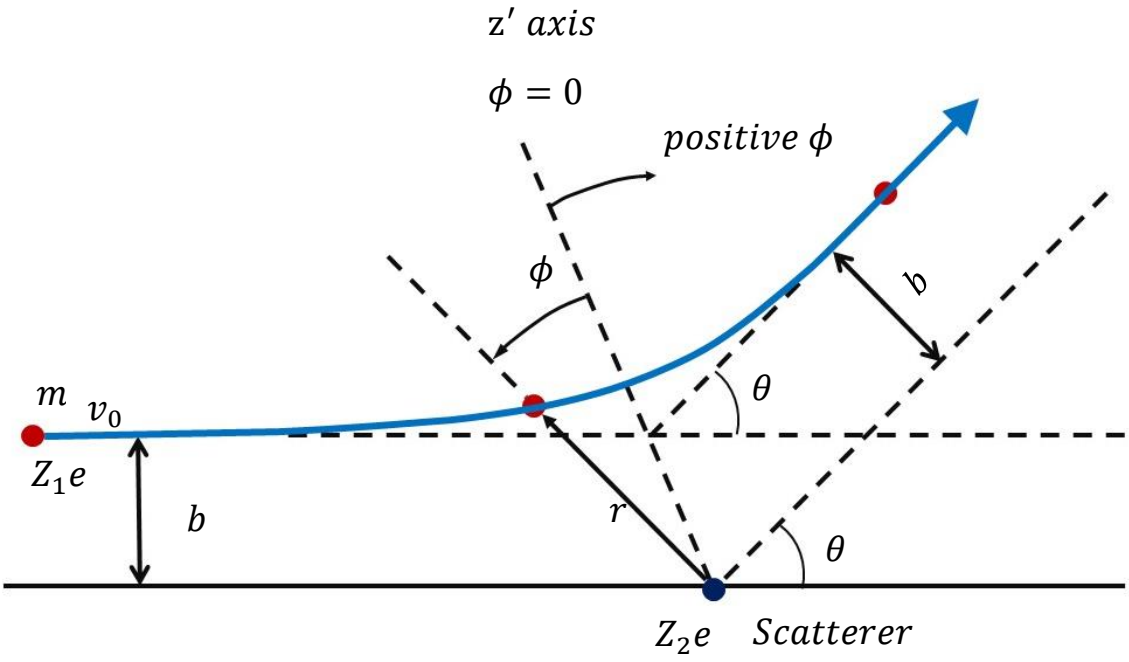

Figure 2.7 : A schematic diagram represents Coulomb scattering.

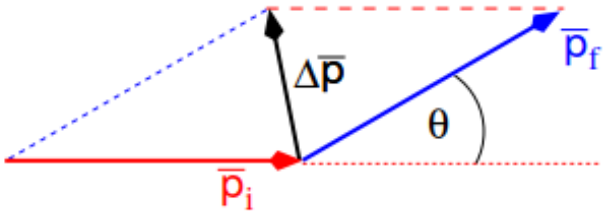

$$|\overrightarrow{p_i}| = |\overrightarrow{p_f}| = p \tag{2.25}$$

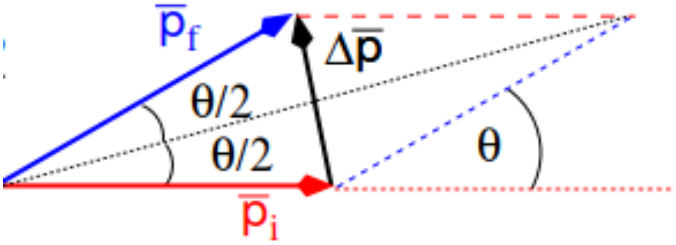

$$\sin\left(\frac{\theta}{2}\right) = \frac{\frac{1}{2}\Delta p}{p} = \frac{\Delta p}{2p} \tag{2.26}$$

$$\Delta p = 2p \sin\left(\frac{\theta}{2}\right) \tag{2.27}$$

$$|\Delta\vec{p}| = \Delta p \tag{2.28}$$

The projectile suffers a change in the direction resulting from Coulomb repulsion force from target and directed in z axis which known as:

$$\vec{F} = \frac{1}{4\pi\varepsilon_0}\frac{Z_1 Z_2 e^2}{r^2}\frac{\vec{r}}{r} \tag{2.29}$$

where e is the electron charge. The force can be written from the second law of Newton.

$$\vec{F} = \frac{d\vec{p}}{dt} \Longrightarrow \Delta\vec{p} = \int \vec{F} dt \tag{2.30}$$

$$\Delta\vec{p} = \int \vec{F} dt \Longrightarrow \Delta p = \int F \cos\phi \, dt \tag{2.31}$$

$$\Delta p = \frac{Z_1 Z_2 e^2}{4\pi\varepsilon_0}\int \frac{1}{r^2}\cos\phi \, dt \tag{2.32}$$

In this integral there are two varying parameters which made it difficult to calculate so we will use the laws of conservations of angular momentum because the scattering is elastic. Since the angular momentum L is

$$L = |\vec{L}| = mr^2\frac{d\phi}{dt} \tag{2.33}$$

In the initial condition, there is no angular velocity it is linear so the angular momentum can be written as

$$L = mv_0 b \tag{2.34}$$

Since the angular momentum is conserved

$$mr^2\frac{d\phi}{dt} = mv_0 b \Longrightarrow \frac{dt}{r^2} = \frac{d\phi}{v_0 b} \tag{2.35}$$

Thus, the change of momentum is

$$\Delta p = \frac{Z_1 Z_2 e^2}{4\pi\varepsilon_0}\int \frac{dt}{r^2}\cos\,\phi = \frac{Z_1 Z_2 e^2}{4\pi\varepsilon_0} = \int \frac{d\phi}{v_0 b}\cos\phi$$
$$= \frac{Z_1 Z_2 e^2}{4\pi\varepsilon_0}\frac{1}{v_0 b}\int_{\phi_1}^{\phi_2}\cos\phi\, d\phi \qquad (2.36)$$

The limits for integration are defined by

$$\phi_1 + \phi_2 + \theta = \pi \;\; \& \;\; \phi_1 = -\phi_2$$
$$\text{So } \phi_1 = -\tfrac{1}{2}(\pi - \theta)\ \&\ \phi_2 = \tfrac{1}{2}(\pi - \theta) \qquad (2.37)$$

The negative and positive φ are equal in magnitude. the solution to these equations is

$$\Delta p = \frac{Z_1 Z_2 e^2}{4\pi\varepsilon_0}\frac{1}{v_0 b}\int_{\phi_1}^{\phi_2} cos\phi\, d\phi \qquad (2.38)$$
$$= \frac{Z_1 Z_2 e^2}{4\pi\varepsilon_0}\frac{1}{v_0 b}\,(sin\phi_2 - sin\phi_1)$$
$$= \frac{Z_1 Z_2 e^2}{4\pi\varepsilon_0}\frac{1}{v_0 b}\,2\sin\left(\frac{\pi-\theta}{2}\right)$$
$$= \frac{Z_1 Z_2 e^2}{4\pi\varepsilon_0}\frac{2}{v_0 b}\,cos\,\left(\frac{\theta}{2}\right)$$

Apply the conservation of momentum then combine two equations 2.27 and 2.38

$$\Delta p = 2p\sin\,(\theta/2) = \frac{Z_1 Z_2 e^2}{4\pi\varepsilon_0}\frac{2}{v_0 b}cos\,\left(\frac{\theta}{2}\right) \qquad (2.39)$$

This equation gives the relation between the impact parameter and the scattering angle. Then we need to get $\frac{db}{d\theta}$

$$b = \frac{Z_1 Z_2 \mathrm{e}^2}{4\pi\varepsilon_0}\frac{1}{pv_0}\frac{1}{tan\left(\frac{\theta}{2}\right)} \qquad (2.40)$$

$$\text{Let } c = \frac{z_1\, z_2\, e^2}{4\,\pi\,\varepsilon_0\, p\, v_0}$$

$$\text{So} \qquad b = c\, cot\left(\frac{\theta}{2}\right)$$

$$db = -c\, csc^2\left(\frac{\theta}{2}\right)\frac{d\theta}{2}$$

$$\left|\frac{db}{d\theta}\right| = \frac{c\, csc^2\left(\frac{\theta}{2}\right)}{2}$$

$$\left|\frac{db}{d\theta}\right| = \frac{c}{2\, sin^2\left(\frac{\theta}{2}\right)}$$

From the equation of differential cross-section (2.22)

$$\frac{d\sigma}{d\Omega} = \frac{b}{\sin(\theta)}\left|\frac{db}{d\theta}\right|$$

$$\frac{d\sigma}{d\Omega} = \frac{b}{\sin(\theta)}\frac{c}{2\, sin^2\left(\frac{\theta}{2}\right)}$$

$$\frac{d\sigma}{d\Omega} = \frac{b}{2\, sin\left(\frac{\theta}{2}\right)\, cos\left(\frac{\theta}{2}\right)}\frac{c}{2\, sin^2\left(\frac{\theta}{2}\right)}$$

Substitute with b and c to get the final equation.

$$\frac{d\sigma}{d\Omega} = \frac{z_1 z_2\, e^4}{64\,\pi^2\,{\varepsilon_0}^2\, m^2\, v^4\, sin^4\left(\frac{\theta}{2}\right)} \qquad (2.41)$$

This equation is called the Rutherford scattering formula. This formula agrees with experimental data for scattering alpha particles off gold nucleus up to 27.5 MeV as shown in figure (2.8).[6]

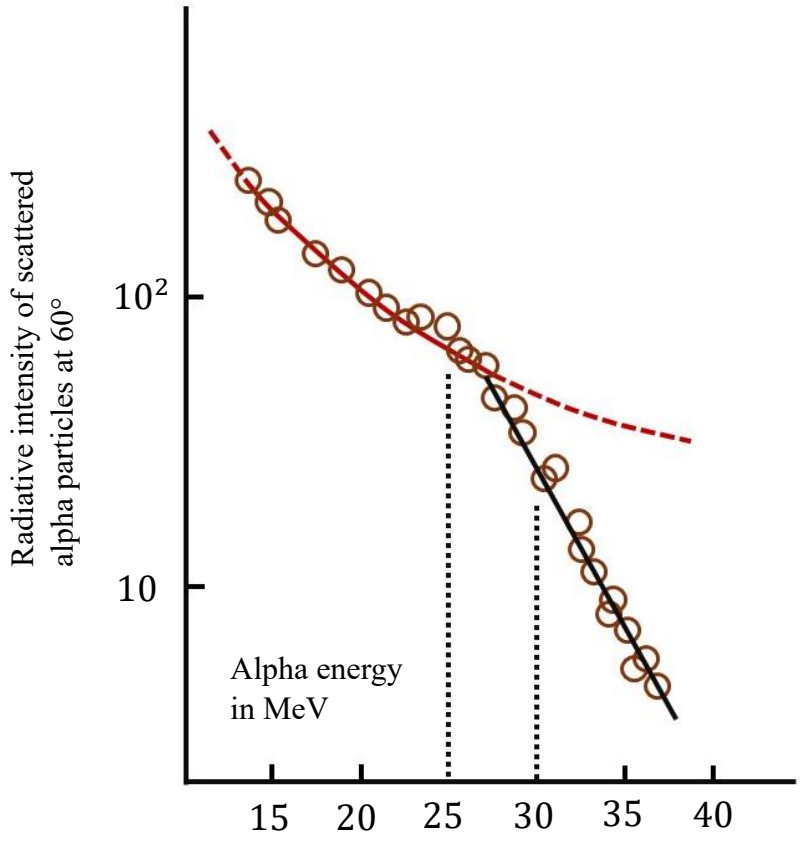

Figure 2.8: Limitations of Rutherford formula.

For higher energy other theoretical techniques will be applied such as quantum theory of scattering and will be explained in detail in the following section.

2.4 Quantum Scattering Theory

In the quantum theory of scattering[7], we imagine an incident particle associated by a plane wave, traveling in the z direction, which encounters a scattering potential, producing an outgoing spherical wave as shown in figure (2.9). That is, we look for solutions to the Schrödinger equation of the generic form.

$$\psi(r,\theta) \approx A\left\{e^{ikz} + f(\theta)\frac{e^{ikr}}{r}\right\}, \quad \text{for large r} \tag{2.42}$$

The spherical wave carries a factor of $\frac{1}{r}$ because this portion of $|\psi|^2$ must go like to conserve probability and the scattering amplitude $f(\theta)$. The wave number k is related to the energy of the incident particles in the usual way

$$k \equiv \frac{\sqrt{2mE}}{\hbar} \tag{2.43}$$

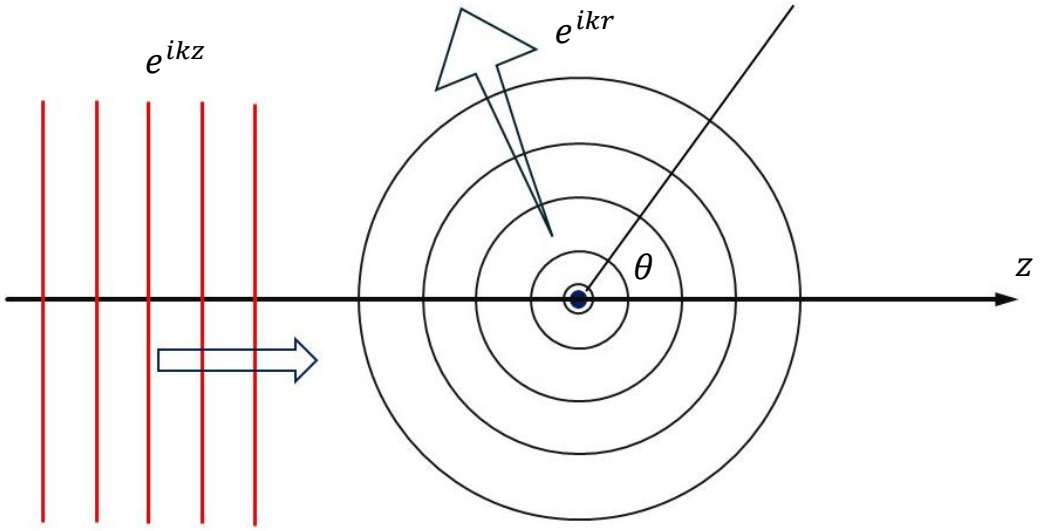

Figure 2.9: Scattering of waves; an incoming plane wave generates a spherical wave.

The whole problem is to determine the scattering amplitude; it indicates the probability of scattering in each direction θ, and hence is related to the differential cross-section. Indeed, the probability that the incident particle, traveling at speed v, passes through the infinitesimal area $d\sigma$, in time dt, is (see figure 2.10)

$$dP = |\psi_{\text{incident}}|^2 dV = |A|^2 (vdt)d\sigma. \tag{2.44}$$

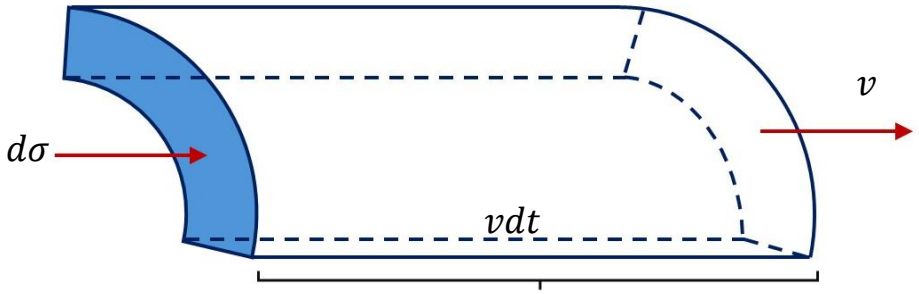

Figure 2.10: The volume dV of incident beam that passes through area dσ in time dt.

But this is equal to the probability that the particle scatters into the corresponding solid angle:

$$dP = |\psi_{\text{scattered}}|^2 dV = \frac{|A|^2|f|^2}{r^2}(vdt)r^2 d\Omega \tag{2.45}$$

from which it follows that $d\sigma = |f|^2 d\Omega$

$$D(\theta) = \frac{d\sigma}{d\Omega} = |f(\theta)|^2 \tag{2.46}$$

Evidently the differential cross-section which is the quantity of interest to the experimentalist is equal to the absolute square of the scattering amplitude. It is obtained by solving the Schrödinger equation. There are different mathematical analyses for this solution to obtain the scattering amplitude $f(\theta)$. First, the partial wave analysis using the phase shift. Second, the Born approximation.

(a) Partial Wave Analysis

In partial wave analysis, the wave function $\psi(\mathrm{r}, \theta)$ takes the form

$$\psi(r, \theta) \approx A\left\{e^{ikz} + f(\theta)\frac{e^{ikr}}{r}\right\} \tag{2.47}$$

and the scattering amplitude is obtained in terms of partial wave amplitudes as

$$f(\theta) = \sum_{\ell=0}^{\infty}(2\ell + 1)a_\ell P_\ell(\cos\ \theta) \tag{2.48}$$

where P_ℓ is the ℓ-state Legendre polynomial and a_ℓ is the partial wave amplitude. The differential cross-section $D(\theta)$ is.

$$D(\theta) = |f(\theta)|^2$$
$$D(\theta) = \sum_\ell \sum_{\ell'}(2\ell + 1)(2\ell' + 1)a_\ell^* a_{\ell'} P_\ell(\cos\ \theta)P_{\ell'}(\cos\ \theta) \tag{2.49}$$

and the total cross-section is

$$\sigma = 4\pi\sum_{\ell=0}^{\infty}(2\ell + 1)|a_\ell|^2 \tag{2.50}$$

In the phase shift analysis, the scattering amplitude of the reflected wave is same as that of the incident wave$|B| = |A|$, due to conservation of probability. But they have not the same phase. The phase shift δ between the incident and scattered waves depending on magnitude of potential. In addition, it depends on the nature of the scattering center. The solution of Schrödinger equation takes the form

$$\psi^{(\ell)} \approx A\frac{(2\ell + 1)}{2ikr}\left[e^{i(kr+2\delta_\ell)} - (-1)^\ell e^{-ikr}\right]P_\ell(\cos\theta) \tag{2.51}$$
$$\text{at } (V(r) \neq 0)$$

The first term in bracket represents the outgoing wave with the phase shift δ_l. The combination of the two methods of scattering analysis gives the partial wave amplitude a_ℓ with the phase shift δ_l as

$$a_\ell = \frac{1}{2ik}\left(e^{2i\delta_\ell} - 1\right) = \frac{1}{k}e^{i\delta_\ell}\sin\left(\delta_\ell\right) \tag{2.52}$$

and the scattering amplitude $f(\theta)$ becomes

$$f(\theta) = \frac{1}{k}\sum_{\ell=0}^{\infty}(2\ell + 1)e^{i\delta_\ell}\sin\left(\delta_\ell\right)P_\ell(\cos\ \theta) \tag{2.53}$$

The scattering cross-section becomes

$$\sigma = \frac{4\pi}{k^2}\sum_{\ell=0}^{\infty}(2\ell+1)\sin^2(\delta_\ell) \tag{2.54}$$

where $l = 0,1,2,....$

(b) The Born Approximation

The Born approximation [7] is a mathematical treatment to solve Schrödinger equation at points of scattering center where time independent is

$$-\frac{\hbar^2}{2m}\nabla^2\psi + V\psi = E\psi \tag{2.55}$$

The previous equation can be written as

$$(\nabla^2 + k^2)\psi = Q \tag{2.56}$$

where

$$k \equiv \frac{\sqrt{2mE}}{\hbar} \text{ and } Q \equiv \frac{2m}{\hbar^2}V\psi \tag{2.57}$$

This has superficial appearance of the Helmholtz equation; note, however, that the inhomogeneous term (Q) itself depends on ψ. Suppose we could find a function G(r) that solves the Helmholtz equation with a delta function 'source'

$$(\nabla^2 + k^2)G(\mathbf{r}) = \delta^3(\mathbf{r}) \tag{2.58}$$

then we could express ψ as an integral:

$$\psi(\mathbf{r}) = \int G(\mathbf{r}-\mathbf{r}_0)Q(\mathbf{r}_0)d^3\mathbf{r}_0 \tag{2.59}$$

For it easy to show that this satisfies Schrodinger equation

$$\begin{aligned}(\nabla^2 + k^2)\psi(\mathbf{r}) &= \int [(\nabla^2 + k^2)G(\mathbf{r}-\mathbf{r}_0)]Q(\mathbf{r}_0)d^3\mathbf{r}_0 \\ &= \int \delta^3(\mathbf{r}-\mathbf{r}_0)Q(\mathbf{r}_0)d^3\mathbf{r}_0 = Q(\mathbf{r})\end{aligned} \tag{2.60}$$

$G(\mathrm{r})$ is called the green function for the Helmholtz equation. (In general, the green function for linear differential equations represents the response to delta function source. The solution of Green function is analysed and given as

$$G(\mathbf{r}) = \frac{i}{8\pi^2 r}\left[\left(i\pi e^{ikr}\right) - \left(-i\pi e^{ikr}\right)\right] = -\frac{e^{ikr}}{4\pi r} \tag{2.61}$$

and general solution of schrodinger equation takes the form

$$\psi(\mathbf{r}) = \psi_0(\mathbf{r}) - \frac{m}{2\pi\hbar^2}\int \frac{e^{ik|\mathbf{r}-\mathbf{r}_0|}}{|\mathbf{r}-\mathbf{r}_0|} V(\mathbf{r}_0)\psi(\mathbf{r}_0) d^3\mathbf{r}_0 \tag{2.62}$$

where ψ_0 satisfies the free-particle Schrödinger equation,

$$(\nabla^2 + k^2)\psi_0 = 0 \tag{2.63}$$

It is looks like an explicit solution to the Schrödinger equation (for any potential) which is too good to be true.

In the case of scattering, we want.

$$\psi_0(\mathbf{r}) = Ae^{ikz} \tag{2.64}$$

representing an incident plane wave. For large r, then,

$$\psi(\mathbf{r}) \approx Ae^{ikz} - \frac{m}{2\pi\hbar^2}\frac{e^{ikr}}{r}\int e^{-i\mathbf{k}\cdot\mathbf{r}_0}\, V(\mathbf{r}_0)\, \psi(\mathbf{r}_0)\, d^3\mathbf{r}_0. \tag{2.65}$$

This is in the standard from (equation 2.47), and we can read off the scattering amplitude

$$f(\theta,\phi) = -\frac{m}{2\pi\hbar^2 A}\int e^{-i\mathbf{k}\cdot\mathbf{r}_0}\, V(\mathbf{r}_0)\, \psi(\mathbf{r}_0)\, d^3\mathbf{r}_0 \tag{2.66}$$

This is exact. Now we invoke the Born approximation: Suppose the incoming plane wave is not substantially altered by the potential; then it makes sense to use

$$\psi(\mathbf{r}_0) \approx \psi_0(\mathbf{r}_0) = A\, e^{ikz_0} = A\, e^{i\mathbf{k}'\cdot\mathbf{r}_0} \tag{2.67}$$

where $\mathbf{k}' \equiv k\hat{z}$ inside the integral. (This would be the exact wave function, if V were zero; it is essentially a weak potential approximation. In the Born approximation, then,

$$f(\theta,\phi) \approx -\frac{m}{2\pi\hbar^2}\int e^{i(\mathbf{k}'-\mathbf{k})\cdot\mathbf{r}_0}\, V(\mathbf{r}_0)\, d^3\mathbf{r}_0. \qquad (2.68)$$

The two vectors k and k' are the wave numbers of the incident and outgoing waves respectively and are shoen in figure (2.11).

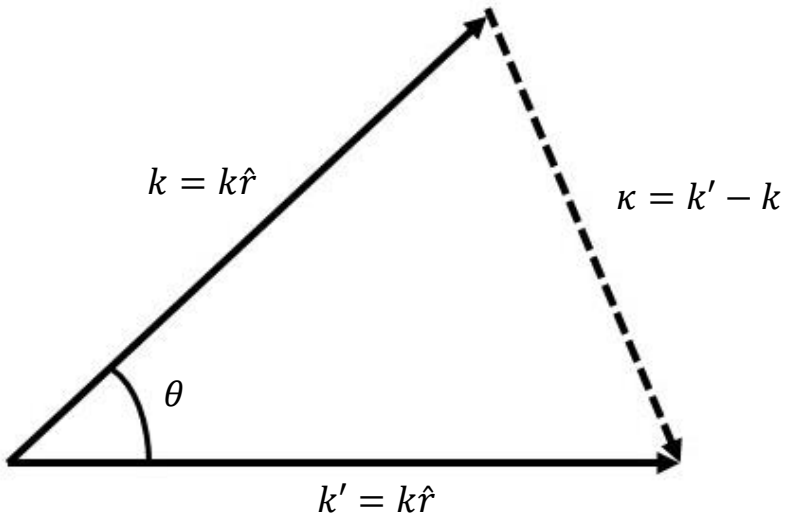

Figure 2.11: Two wave vectors in the Born approximation: k' points in the incident direction, k in the scattered direction.

For **low energy** (long wavelength) **scattering**, the exponential factor is essentially constant over the scattering region, and the Born approximation simplifies to

$$f(\theta,\phi) \approx -\frac{m}{2\pi\hbar^2}\int V(\mathbf{r})\, d^3\mathbf{r} \qquad \text{(low energy)} \qquad (2.69)$$

For spherical symmetrical potential, $V(\mathbf{r}) = V(r)$ but not nessairly at low energy and the Born approximation again reduces to a simpler form,

$$\kappa \equiv k' - k \qquad (2.70)$$

And let the polar axis for the $\mathbf{r}_0$ integral lie along κ, so that

$$(\mathbf{k}' - \mathbf{k}) \cdot \mathbf{r}_0 = \kappa\, r_0 \cos\theta_0. \tag{2.71}$$

Then

$$f(\theta) \approx -\frac{m}{2\pi\hbar^2} \int e^{i\kappa r_0 \cos\,\theta_0}\, V(r_0)\, r_0^2\, \sin\theta_0\, dr_0\, d\theta_0\, d\phi_0. \tag{2.72}$$

The ϕ_0 integral is trivial (2π), and the θ_0 integral is one. Dropping the subscript on r, we are left with

$$f(\theta) \approx -\frac{2m}{\hbar^2\kappa} \int_0^\infty r\, V(r)\, \sin(\kappa r)\, dr \quad \text{(spherical symmetry).} \tag{2.73}$$

The angular dependence of $f(\theta)$ is carried by κ; as shown in figure 2.11.

$$\kappa = 2k \sin\left(\frac{\theta}{2}\right). \tag{2.74}$$

An application to Born approximation is Rutherford scattering between two charged points q_1 and q_2 at Couomb's potential. The Born approximation gives

$$f(\theta) \approx -\frac{2m\beta}{\hbar^2\kappa} \int_0^\infty e^{-\mu r}\, \sin(\kappa r)\, dr = -\frac{2m\beta}{\hbar^2(\mu^2 + \kappa^2)} \tag{2.75}$$

where β and μ are constants. If we put $\beta = q_1 q_2 / 4\pi\epsilon_0$ and $\mu = 0$ the scattering amlitude is

$$f(\theta) \approx -\frac{2mq_1q_2}{4\pi\epsilon_0\hbar^2\kappa^2} \tag{2.76}$$

or (using Equations 2.74 and 2.57):

$$f(\theta) \approx -\frac{q_1q_2}{16\pi\epsilon_0 E\, \sin^2\left(\frac{\theta}{2}\right)} \tag{2.77}$$

the differential creoss-section is the square of this

$$\frac{d\sigma}{d\Omega} = \left[\frac{q_1 q_2}{16\pi\epsilon_0 E \sin^2\left(\frac{\theta}{2}\right)}\right]^2 \tag{2.78}$$

which is precisely the Rutherford formula. It happens that for Coulomb potential classical mechanics, the Born approximation, and quantum field theory all yield the same result. [7]

2.5 Quantum Electro-Dynamics

In this section, we will investigate the scattering process in terms of quantum electrodynamics QED. This theory describes the electromagnetic interactions between leptons (like electron) and hadrons (like proton, neutron, muon). The following are the technical issues that must be addressed in any estimation of the cross-sections in terms of their transition rates: First, is dealing with a many-particle situation. Second, is handling a relativistic problem. We calculate the one-particle wave equations for free leptons (or quarks) and then investigate the scattering of one particle by another. At first glance, it is unexpected that single-particle wave equations may be used to explain interactions in which particles can be created and annihilated. QED theory is applied in terms of Feynman diagrams, using Golden rules where the exchange boson is photon (γ) with energy q. In the following sections, we will explain the mathematical tools used in QED in terms of relativistic mechanics.

2.6 Lorentz Covariance and Four-Vector Notation

The fact that the basic laws have the same form in all Lorentz frames, that is, reference frames with uniform relative velocity, is a cornerstone of modern physics. Lorentz covariance describes the fundamental equations. The theory of special relativity is founded on the assumption that the velocity of light, c,

is constant in all Lorentz frames. A Lorentz transformation connects the coordinates of two such frames. $c^2t^2 - x^2$ is the basic invariant. A four-vector is defined as any collection of four values that transform as (ct, x) under Lorentz transformations. We use the abbreviation.

$$(ct, \mathbf{x}) \equiv (x^0, x^1, x^2, x^3) \equiv x^\mu \tag{2.79}$$

According to special relativity theory, the total energy E and momentum p of an isolated system transform as components of a four-vector.

$$\left(\frac{E}{c}, \mathbf{p}\right) \equiv (p^0, p^1, p^2, p^3) = p^\mu \tag{2.80}$$

with the basic invariant $(E^2/c^2) - p^2$. The simplest system is a free particle, for which

$$\frac{E^2}{c^2} - \mathbf{p}^2 = m^2c^2 \tag{2.81}$$

where m is the particle's rest mass.We will now return to the usage of natural units with c = 1. We may apply the scalar product of two four-vectors in three-dimensional space, just as we can in two-dimensional space. $A^\mu = (A^0, A)$ and $B^\mu = (B^0, B)$

$$A \cdot B \equiv A^0B^0 - \mathbf{A} \cdot \mathbf{B} \tag{2.82}$$

which is left invariant under Lorentz transformations. Due to the minus sign, it is convenient to introduce a new type of four-vector, $A_\mu = (A^0, - A)$, so that the scalar product is

$$A \cdot B = A_\mu B^\mu = A^\mu B_\mu = g_{\mu\nu}A^\mu B^\nu = g^{\mu\nu}A_\mu B_\nu \tag{2.83}$$

Here, we have introduced the (metric) tensor $g_{\mu\nu}$ which is defined by $g_{00} = 1$, $g_{11} = g_{22} = g_{33} = - 1$, other components = 0

$$g_{\mu\nu} = \begin{pmatrix} +1 & 0 & 0 & 0 \\ 0 & -1 & 0 & 0 \\ 0 & 0 & -1 & 0 \\ 0 & 0 & 0 & -1 \end{pmatrix} \tag{2.84}$$

Upper (lower) index vectors are called contravariant (covariant) vectors. The rule for forming Lorentz invariants is to make the upper indices balance the lower indices. If an equation is Lorentz covariant, we must ensure that all unrepeated indices (upper and lower separately) balance on either side of the equation, and that all repeated indices appear once as an upper and once as a lower index. the following are examples of scalar products of two four vectors positions x and momentum p are

$$p^{\mu}x_A \equiv p \cdot x = Et - \mathbf{p} \cdot \mathbf{x} \tag{2.85}$$

And also, for two momentum vectors

$$P^{\mu}P_{\mu} \equiv p \cdot p = p^2 = E^2 - p^2 \tag{2.86}$$

These quantities are Lorentz invariants. For a free particle, we have $p^2 = m^2$. We say that the particle is on its mass shell. The collision of two particles, each of mass M, is viewed in a Lorentz frame in which they hit head-on with momenta equal in magnitude but opposite in direction. We speak of this as the "center-of-mass" frame (though the name "center-of-momentum" would be more appropriate).

The total energy of the system is E_{cm}

$$s \equiv (p_1 + p_2)_{\mu}(p_1 + p_2)^{\mu} \equiv (p_1 + p_2)^2 = E_{cm}^2 \tag{2.87}$$

If the collision is viewed in the "laboratory" frame where one of the particles is at rest, then show, by evaluating the invariant s, that the other has energy.

$$E_{lab} = \frac{E_{cm}^2}{2M} - M \tag{2.88}$$

This study shows that colliding-beam accelerators have a huge advantage compared to fixed-target accelerators in terms of reaching a given total center of mass energy $\sqrt{s}$. List some of the benefits of fixed-target accelerators. It is worth noting that the space-like components of A^{μ} and A_{μ} are A and - A, respectively. The exception is

$$\partial^{\mu} = \left(\frac{\partial}{\partial t}, -\nabla\right) \quad \text{and} \quad \partial_{\mu} = \left(\frac{\partial}{\partial t}, \nabla\right) \tag{2.89}$$

which can be shown to transform like x^{μ} = (t, x) and x_{μ}= (t, -x). respectively. Thus. the covariant form of $E \rightarrow ih\frac{\partial}{\partial t}$, $\mathbf{p} \rightarrow -i\hbar\nabla$ is

$$p^{\mu} \rightarrow i\,\partial^{\mu} \tag{2.90}$$

From ∂_{μ} and ∂^{μ} we can form the invariant (D'Alembertian) operator

$$\Box^2 \equiv \partial_{\mu}\,\partial^{\mu} \tag{2.91}$$

In classical quantum mechanics Schrödinger equations can be modified in relativistic which is known as Klein-Gordon equation.

2.7 The Klein-Gordon Equation

Wave equation violates Lorentz covariance and is not suitable for a particle moves in a relativistic motion. Starting from the relativistic energy-momentum relation equation. (2.81)

$$E^2 = p^2 + m^2 \tag{2.92}$$

Making the operator substitutions $E \rightarrow ih\frac{\partial}{\partial t}$, $\mathbf{p} \rightarrow -i\hbar\nabla$ into Schrodinger equation, we obtain

$$-\frac{\partial^2\phi}{\partial t^2}+\nabla^2\phi=m^2\phi \tag{2.93}$$

It is known as the Klein-Gordon equation (but might be expressed more precisely. Known as the relativistic Schrodinger equation). The complex conjugate equation and the Klein-Gordon equation are multiplied by - iϕ and - iϕ*, respectively, then we get.

$$\frac{\partial}{\partial t}\underbrace{\left[i\left(\phi^*\frac{\partial\phi}{\partial t}-\phi\frac{\partial\phi^*}{\partial t}\right)\right]}_{\rho}+\nabla\cdot\underbrace{[-i(\phi^*\nabla\phi-\phi\nabla\phi^*)]}_{\mathbf{j}}=0 \tag{2.94}$$

When comparing with the variables in square brackets to the equation of continuity equation (2.95) where ρ is the probability density and j is the flux density

$$\frac{\partial\rho}{\partial t}+\nabla\cdot\mathrm{j}=0 \tag{2.95}$$

The probability and flux densities can be identified. For instance, consider a free particle with energy E and momentum p that is characterized by the Klein-Gordon solution.

$$\phi=Ne^{i\mathbf{p}\cdot x-\mathrm{i}Et} \tag{2.96}$$

We find from equation (2.94) that the probability density ρ and the current density j are given as

$$\rho=i(-2iE)|N|^2=2E|N|^2 \tag{2.97}$$

$$\mathrm{j}=-i(2i\mathrm{p})|N|^2=2\mathrm{p}|N|^2 \tag{2.98}$$

We can observe that the probability density grows in proportion to E, the particle's relativistic energy. The Klein-Gordon equation yields when the D'Alembertian operator equation (2.91) is used.

$$(\Box^2 + m^2)\phi = 0 \tag{2.99}$$

Moreover, the probability and the flux densities form a four-vector.

$$j^\mu = (\rho, \mathbf{j}) = i(\phi^* \partial^\mu \phi - \phi \partial^\mu \phi^*) \tag{2.100}$$

which satisfies the (covariant) continuity relation:

$$\partial_\mu \mathrm{j}^\mu = 0 \tag{2.101}$$

Taking the free particle solution

$$\phi = Ne^{-i\mathbf{p}\cdot x} \tag{2.102}$$

we have

$$j^\mu = 2p^\mu |N|^2 \tag{2.103}$$

We noted that the probability density ρ is the time-like component of a four-vector; ρ is proportional to E. This result may be anticipated since under a Lorentz boost of velocity v, a volume element suffers a Lorentz contraction $d^3x \to d^3x\ \sqrt{1-v^2}$; and so, to keep ρ d^3x invariant, we require ρ to transform as the time-like component of a four-vector $\rho \to \rho\sqrt{1-v^2}$. To obtain the energy eigenvalues of the Klein-Gordon equation must substitute of (2.102) into (2.99).

$$E = \pm(\mathrm{p}^2 + m^2)^{\frac{1}{2}} \tag{2.104}$$

As a result, we have negative energy solutions in addition to acceptable E > 0 options. This appears to be an unavoidable trouble at first glance, because transitions to lower and lower (more negative) energies might occur. Another problem is that the E < 0 solutions have a negative probability density from equation (2.97). To summarize, the problems are $E < 0$ solutions with $\rho < 0$

This problem cannot be simply ignored. We cannot simply discard the negative energy solutions as we have to work with a complete set of states, and this set inevitably includes the unwanted states.[2]

2.8 Dirac Equation

To avoid the negative energy problems, Dirac proposed a relativistic wave equation linear in $\partial/\partial t$ and ∇. He was successful in solving the problem of the negative probability density, and the equation also described spin -1/2 particles, which was an unexpected bonus. However, $E < 0$ solutions did arise, as seen in figure (2.12) energy spectrum for a free Dirac electron. Dirac avoided negative energy solutions by employing the exclusion principle. He proposed that the vacuum is an endless sea of $E < 0$ electrons, and that all negative energy states are inhabited. The exclusion principle now prevents positive energy electrons from collapsing into lower (negative) energy levels. However, a "hole" in the sea may be created by exciting an electron from a negative energy (- E) state to a positive energy (E') state, as shown. The lack of a charge - e and energy - E electron is interpreted as the existence of a charge +e and energy +E antiparticle (a positron). As a result of this excitation, a pair of particles are produced.

$$e^{-}(E') + e^{+}(E) \tag{2.105}$$

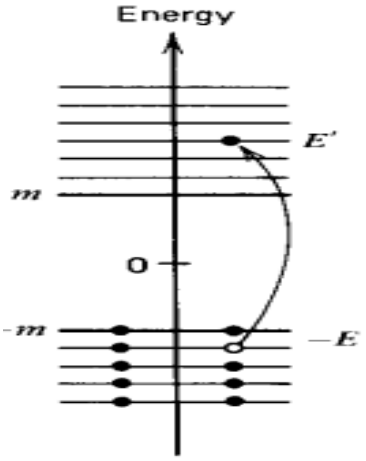

Figure 2.12: Energy level spectrum for the electron. Dirac's picture of the vacuum has all the negative energy states occupied. It shows two states per level to account for the two spin states of the electron.

It obviously demands energy $E + E' \geq 2m$ (see diagram). The Dirac equation was thought to be only valid relativistic wave equation until 1934. Pauli and Weisskopf reintroduced the Klein-Gordon equation in 1934 by introducing the charge -e into j^{μ} and interpreting it as the electron's charge-current density.

$$j^{\mu} = -ie(\phi^* \partial^{\mu}\phi - \phi \partial^{\mu}\phi^*) \tag{2.106}$$

Now that $\rho = j^0$ reflects a charge density rather than a probability density, the fact that it can be negative is no longer an issue. In certain ways, as we will see later, the $E < 0$ solutions can thus be considered as $E > 0$ solutions for particles of a reverse charge (antiparticles). Unlike "hole theory," this interpretation applies to bosons as well as fermions. The Dirac Sea cannot be filled with bosons because there is no exclusion principle to stack the particles. To build the antiparticle concept and introduce Feynman diagrams, it is necessary to initially neglect the difficulties caused by electron spin. To begin, we extract the Feynman rules for "spinless" electrons and employ them to compute scattering amplitudes and cross-sections for interacting particles. Only then do we resort to the Dirac equation and the Feynman rules for the physically relevant situation of spin 1/2 electron electromagnetic interactions.[2]

2.9 The Dirac Equation and Spinors

In this section we develop the appropriate wave functions for fundamental fermions and bosons. In covariant form, Dirac equation can be written as:

$$\left(i\gamma^0\frac{\partial}{\partial t}+i\overrightarrow{\gamma}.\,\vec{\nabla}-m\right)\psi=0 \qquad\qquad \left(i\gamma^\mu\partial_\mu-m\right)\psi=0 \quad (2.107)$$

where we have introduced the coefficients $\gamma^\mu = (\gamma^0, \vec{\gamma}) = (\gamma^0, \gamma^1, \gamma^2, \gamma^3)$, which must be determined. Dirac equation is simply four coupled differential equations, describing a wavefunction ψ with four components. To find gamma matrices γ^μ, μ = 0, 1, 2, 3, we first multiply the Dirac equation by its conjugate equation:

$$\psi^\dagger\left(-i\gamma^0\frac{\partial}{\partial t}-i\overrightarrow{\gamma}.\,\vec{\nabla}-m\right)\left(i\gamma^0\frac{\partial}{\partial t}+i\overrightarrow{\gamma}.\,\vec{\nabla}-m\right)\psi=0 \quad (2.108)$$

it is consistent with the Klein-Gordon equation, this leads to the following conditions on the γ^μ:

$$(\gamma^0)^2=1, \quad \left(\gamma^i\right)^2=-1, \quad \gamma^\mu\gamma^\nu+\gamma^\nu\gamma^\mu=0 \text{ for } \mu\neq\nu$$

$$\text{with } i=1,2,3 \qquad \mu,\nu=0,1,2,3$$

Equivalently in terms of anticommutation relations and the metric tensor equation (2.84):

$$\{\gamma^\mu,\gamma^\nu\}=\gamma^\mu,\,\gamma^\nu+\gamma^\nu,\,\gamma^\mu=2g^{\mu\nu} \qquad \mu,\nu=0,1,2,3$$

The simplest solution for the γ^μ, that satisfies these anticommutation relations, are 4 × 4 unitary matrices. We will use the following representation for the γ matrices:

$$\gamma^0=\begin{pmatrix}\mathrm{I} & 0\\ 0 & -\mathrm{I}\end{pmatrix} \qquad\qquad \gamma^i=\begin{pmatrix}0 & \sigma^i\\ -\sigma^i & 0\end{pmatrix} \qquad (2.109)$$

Where $\mathrm{I} = \begin{pmatrix} 1 & 0 \\ 0 & 1 \end{pmatrix}$ and $-\mathrm{I} = \begin{pmatrix} -1 & 0 \\ 0 & -1 \end{pmatrix}$

where I denote a 2 × 2 identity matrix which described by unit diagonal matrices, 0 denotes a 2 × 2 null matrix, and the σ^i are the Pauli spin matrices:

$$\sigma_x = \begin{pmatrix} 0 & 1 \\ 1 & 0 \end{pmatrix} \qquad \sigma_y = \begin{pmatrix} 0 & -i \\ i & 0 \end{pmatrix} \qquad \sigma_z = \begin{pmatrix} 1 & 0 \\ 0 & -1 \end{pmatrix}$$

Let's write out the gamma matrices in full:

$$\gamma^0 = \begin{pmatrix} 1 & 0 & 0 & 0 \\ 0 & 1 & 0 & 0 \\ 0 & 0 & -1 & 0 \\ 0 & 0 & 0 & -1 \end{pmatrix} \qquad \gamma^1 = \begin{pmatrix} 0 & 0 & 0 & 1 \\ 0 & 0 & 1 & 0 \\ 0 & -1 & 0 & 0 \\ -1 & 0 & 0 & 0 \end{pmatrix} \quad (2.110)$$

$$\gamma^2 = \begin{pmatrix} 0 & 0 & 0 & -i \\ 0 & 0 & i & 0 \\ 0 & i & 0 & 0 \\ -i & 0 & 0 & 0 \end{pmatrix} \qquad \gamma^3 = \begin{pmatrix} 0 & 0 & 1 & 0 \\ 0 & 0 & 0 & -1 \\ -1 & 0 & 0 & 0 \\ 0 & 1 & 0 & 0 \end{pmatrix}$$

Please note, despite the μ superscript, the γ^μ are not four vectors. However, they do remain constant under Lorentz transformations. Finally let's write out the Dirac Equation in full:

$$\begin{pmatrix} i\frac{\partial}{\partial t} - m & 0 & i\frac{\partial}{\partial z} & i\frac{\partial}{\partial x} + \frac{\partial}{\partial y} \\ 0 & i\frac{\partial}{\partial t} - m & i\frac{\partial}{\partial \mathrm{x}} - \frac{\partial}{\partial y} & -i\frac{\partial}{\partial z} \\ -i\frac{\partial}{\partial z} & -i\frac{\partial}{\partial x} - \frac{\partial}{\partial y} & -i\frac{\partial}{\partial \mathrm{t}} - m & 0 \\ -i\frac{\partial}{\partial \mathrm{x}} + \frac{\partial}{\partial y} & i\frac{\partial}{\partial z} & 0 & -i\frac{\partial}{\partial \mathrm{t}} - m \end{pmatrix} \begin{pmatrix} \psi^1 \\ \psi^2 \\ \psi^3 \\ \psi^4 \end{pmatrix} = \begin{pmatrix} 0 \\ 0 \\ 0 \\ 0 \end{pmatrix} \quad (2.111)$$

This form will be used in further calculations in scattering research for electron-proton scattering.

2.10 Spinors

The Dirac equation describes the behavior of spin -1/2 fermions in relativistic quantum field theory. For a free fermion the wavefunction is the product of a plane wave and a Dirac spinor, $u(p^{\mu})$:

$$\psi(x^{\mu}) = u(p^{\mu})\, e^{-ip\cdot x} \tag{2.112}$$

Substituting the fermion wavefunction, ψ, into the Dirac equation:

$$\left(\gamma^{\mu} p_{\mu} - m\right) u(p) = 0 \tag{2.113}$$

For a particle at rest, $\vec{P} = 0$, we find the following equations:

$$\left(i\gamma^{0}\frac{\partial}{\partial t} - m\right)\psi = (\gamma^{0}E - m)\psi = 0$$
$$\hat{E}u = \begin{pmatrix} m\mathbf{I} & 0 \\ 0 & -m\mathbf{I} \end{pmatrix} u \tag{2.114}$$

The solutions are four eigen spinors:

$$u^{1} = \begin{pmatrix} 1 \\ 0 \\ 0 \\ 0 \end{pmatrix} \quad u^{2} = \begin{pmatrix} 0 \\ 1 \\ 0 \\ 0 \end{pmatrix} \quad u^{3} = \begin{pmatrix} 0 \\ 0 \\ 1 \\ 0 \end{pmatrix} \quad u^{4} = \begin{pmatrix} 0 \\ 0 \\ 0 \\ 1 \end{pmatrix} \tag{2.115}$$

and the associated wavefunctions of the fermion is:

$$\psi^{1} = e^{-imt}u^{1} \qquad \psi^{2} = e^{-imt}u^{2}$$
$$\psi^{3} = e^{+imt}u^{3} \qquad \psi^{4} = e^{+imt}u^{4} \tag{2.116}$$

Note that the spinors are, however, not four-vectors representation but they are 1 × 4 column matrices, with four possible states. We would expect only two spin states for a spin 1/2 fermion. The change of sign in the exponents of the plane waves in the states ψ^3 and ψ^4 describe two different spin states (↑

and ↓) with negative energy E = −m. and explained with details in the following section.

2.11 Spinors for Moving Particles

To describe the negative energy states, Dirac postulated that an electron in a positive energy state is produced from the vacuum accompanied by a hole with negative energy. The hole corresponds to a physical antiparticle, the positron, with charge +e. Another interpretation (Feynman-Stuckelberg) is that the E=−m solutions can either describe a negative energy particle which propagates backwards in time, or a positive energy antiparticle propagating forward in time:

$$e^{-i[(-E)(-t)-(-\vec{p})\cdot(-\vec{x})]} = e^{-i[Et-\vec{p}\cdot\vec{x}]} \tag{2.117}$$

For a moving particle, $\vec{P} \neq 0$ the Dirac equation becomes [using equations (2.107) and (2.109)]:

$$(\gamma^{\mu}p_{\mu} - m)(u_A u_B) = \begin{pmatrix} E-m & -\vec{\sigma}\cdot\vec{p} \\ \vec{\sigma}\cdot\vec{p} & -E-m \end{pmatrix}\begin{pmatrix} u_A \\ u_B \end{pmatrix} = 0 \tag{2.118}$$

where u_A and u_B denote the 1 × 2 upper and lower components of u respectively. The equations for u_A and u_B are coupled:

$$u_A = \frac{\vec{\sigma}\cdot\vec{p}}{E-m}u_B \qquad\qquad u_B = \frac{\vec{\sigma}\cdot\vec{p}}{E+m}u_A \tag{2.119}$$

The solutions are obtained for u^1 and u^2 in which describe an electron of energy $E = +\sqrt{m^2 + \overrightarrow{p^2}}$, and momentum $\vec{P}$ and the wave functions represent as

$$\psi^1 = u^1(p^{\mu})e^{-ip\cdot x} \qquad\qquad \psi^2 = u^2(p^{\mu})e^{-ip\cdot x} \tag{2.120}$$

$$u^1 = \begin{pmatrix} 1 \\ 0 \\ p_z/(E+m) \\ (p_x + ip_y)/(E+m) \end{pmatrix} \qquad u^2 = \begin{pmatrix} 0 \\ 1 \\ (p_x - ip_y)/(E+m) \\ -p_z/(E+m) \end{pmatrix} \quad (2.121)$$

$$u^3 = \begin{pmatrix} -p_z/(-E+m) \\ (-p_x - ip_y)/(-E+m) \\ 1 \\ 0 \end{pmatrix} \quad u^4 = \begin{pmatrix} (-p_x + ip_y)/(-E+m) \\ p_z/(-E+m) \\ 0 \\ 1 \end{pmatrix} \quad (2.122)$$

The u^3 and u^4 of equation (2.122) describe a positron of energy $E = -\sqrt{m^2 + \overrightarrow{p^2}}$, and momentum $\vec{P}$. It is usual to change the spinors u^3 and u^4 into $v^2(p) \equiv u^3(-p)$ and $v^1(p) \equiv u^4(-p)$ to describe these positive energy antiparticle states, $E = +\sqrt{m^2 + \overrightarrow{p^2}}$

$$v^2(p^\mu) \equiv u^3(-p^\mu) = \begin{pmatrix} \dfrac{p_z}{E+m} \\ \dfrac{(p_x + ip_y)}{E+m} \\ 1 \\ 0 \end{pmatrix} \quad (2.123)$$

$$\psi^3 = v^2(p^\mu)\, e^{-ip\cdot x} = u^3(-p^\mu)\, e^{i(-p)\cdot x}$$

$$v^1(p^\mu) \equiv u^4(-p^\mu) = \begin{pmatrix} \dfrac{(p_x - ip_y)}{(E+m)} \\ \dfrac{p_z}{(E+m)} \\ 0 \\ 1 \end{pmatrix}$$

$$\psi^4 = v^1(p^\mu)\, e^{-ip\cdot x} = u^4(-p^\mu)\, e^{i(-p)\cdot x}$$

the u and v are the solutions of:

$$(i\gamma^{\mu}p_{\mu} - m)u = 0 \qquad (i\gamma^{\mu}p_{\mu} + m)v = 0 \tag{2.124}$$

The two different solutions for each of the fermions and antifermions correspond to two possible spin states. For a fermion with momentum $\vec{P}$ along the z-axis, $\psi = u^1(p^\mu)\, e^{-ip\cdot x}$ describes a spin-up fermion and $\psi = u^2(p^\mu)\, e^{-ip\cdot x}$ describes a spin-down fermion. For an antifermion with momentum $\vec{P}$ along the z-axis, $\psi = v^1(p^\mu)\, e^{-ip\cdot x}$ describes a spin-up antifermion and $\psi = v^2(p^\mu)e^{-ip\cdot x}$ describes a spin-down antifermion.

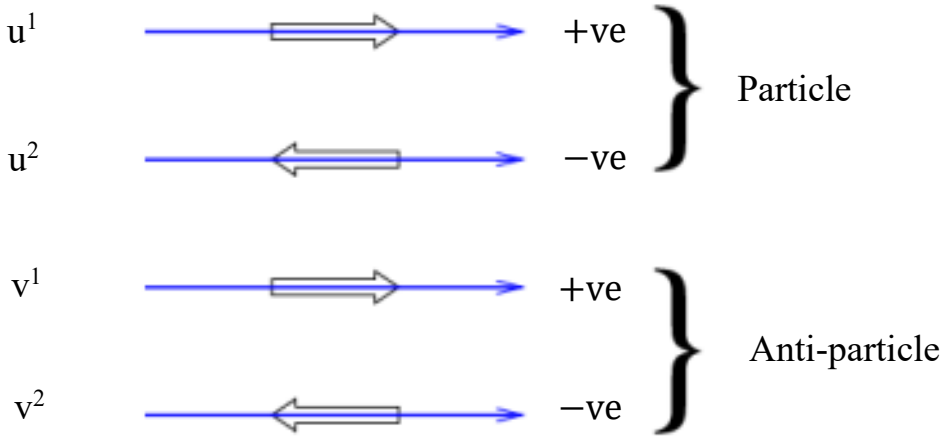

Figure 2.13: Helicity eigenstates for a particle or antiparticle travelling along the +z axis.

The u^1, u^2, v^1 and v^2 spinors are only eigenstates of $\hat{S}_z$ for momentum p along the z-axis. These states take equal probabilities. For our purposes it makes more sense to project the spin along the particle's direction of flight, this defines the helicity, h of the particle.

$$\hat{h} = \frac{\vec{S}\cdot\vec{p}}{|\vec{S}||\vec{p}|} = \frac{2\vec{S}\cdot\vec{p}}{|\vec{p}|} \tag{2.125}$$

For a spin 1/2 fermion, the two possible values of h are h = +1 or h = −1. We call h = +1 right-handed and h = −1 left-handed. The possible states of particles and antiparticles are shown in figure (2.13). As we will see, the concept of left- and right-handedness plays an important role in calculating matrix elements and in the weak force. If it is also worth noting here, massless fermions, are purely left-handed (only u^2 and h = -1); massless antifermions are purely right-handed (only ν^1 and h = +1). [8]

2.12 Fermion currents

We need to define a Lorentz invariant quantity to describe fermion currents for QED. We define the adjoint spinor $\bar{\psi} \equiv \psi^\dagger\gamma^0$, where $\psi^\dagger$ is the Hermitian conjugate (complex conjugate transpose) of ψ:

$$\psi = \begin{pmatrix} \psi_1 \\ \psi_2 \\ \psi_3 \\ \psi_4 \end{pmatrix} \tag{2.126}$$

$$\psi^\dagger = (\psi^*)^T = (\psi_1^*, \psi_2^*, \psi_3^*, \psi_4^*)$$

$$\bar{\psi} \equiv \psi^\dagger\gamma^0 = (\psi_1^*, \psi_2^*, -\psi_3^*, -\psi_4^*)$$

The adjoint Dirac equation can be formed by taking the Hermitian conjugate of the Dirac equation (2.107), and multiplying it from the right by γ^0:

$$i\,\partial_\mu\bar{\psi}\gamma^\mu + m\bar{\psi} = 0 \tag{2.127}$$

Multiplying the adjoint Dirac equation (2.127) by ψ from the right, (or the original Dirac equation by $\bar{\psi}$ from the left) gives the continuity equation which is described by Lorentz invariant quantity.

$$\partial_\mu(\bar{\psi}\gamma^\mu\psi) = \bar{\psi}\gamma^\mu(\partial_\mu\psi) + (\partial_\mu\bar{\psi})\gamma^\mu\psi = 0 \tag{2.128}$$

$$\text{or } \partial_\mu j^\mu = 0 \tag{2.129}$$

Where j^μ is the four-vector fermion current:

$$j^\mu = \bar{\psi}\gamma^\mu\psi = (\bar{\psi}\gamma^0\psi, \bar{\psi}\vec{\gamma}\psi) = (\rho, \vec{j}) \tag{2.130}$$

and ρ is the probability density:

$$\rho = j^0 = \bar{\psi}\gamma^0\psi = \psi^\dagger\psi \tag{2.131}$$

The fermion current $j^\mu = \bar{\psi}\gamma^\mu\psi$ and it has the properties of a Lorentz four-vector, which is what we required. Additionally, the probability density ρ is positive definite for all four possible spinor states. This is only true if we use the adjoint form with $\bar{\psi}$

The previous discussion is characterized for spin ½ fermions like electrons and mesons. For integer spin particles (Bosons) like photons, there are three spin projections corresponding to three possible helicity states s = +1, 0, −1.

s = 0 is known as longitudinal polarization, and the s = ±1 are transverse polarizations (actually left and right-handed circular polarizations). For massless particles, the s = 0 state does not exist. Plane wave solutions can be written as

$$\psi = \epsilon^\mu(p; s)\, e^{-ip\cdot x} \tag{2.132}$$

where $\epsilon^\mu(s)$ is the polarization vector, which depends on the spin, s, of the photon. The polarization vector is Lorentz gauge invariant quantity:

$$p_\mu\epsilon^\mu = 0 \tag{2.133}$$

In scattering theory by QED, the exchange virtual boson like photons have $q^2 \neq 0$, and thus can have both longitudinal and transverse polarization. This is also true for the massive W and Z bosons.[8]

2.13 Feynman Diagrams

In QED theory[4], the electromagnetic interaction is represented by Feynman diagram which is a powerful technique that simplifies the mechanism of interaction. In addition, it is used to calculate the cross-section of scattering process by introducing a very important parameter which is called matrix element $\mathcal{M}$, that indicates the probability of this interaction to happen. Also, it is called scattering amplitude which connects between initial and final states of scattering process. It describes the interactions between boson particles with both projectile and target and carries information like mass, energy, momentum, and spin. The following figure gives a simple form of Feynman diagram of scattering process of two electrons.

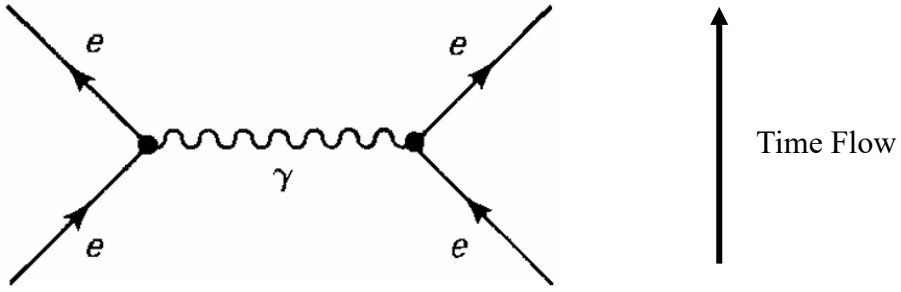

Figure 2.14: shows the scattering process for two electrons in terms QED using Feynman diagram.

In the previous chapter we explained the basic assumption of QED to describe the interactions in terms of exchange boson. In this example it will be photon as a mediated boson between interacting particles. Here, two electrons enter the interaction then a photon passes between them. It is not possible to say

which electron emits the photon and which one absorbs. In classical theory, this interaction is called Coulomb repulsion of like charges when they are at rest. In QED this process is called Moller scattering. The Feynman diagram consists of main parts they will be illustrated as listed below.

1- Fermion lines, it is the line with arrow indication. If the arrow takes the time flow it belongs to fermion propagates in time. Otherwise, it belongs to anti-fermion.

2- Propagator wavy line, it is the line which indicates the exchange boson for the interaction of two electrons. In this case photon represents electromagnetic interaction. It is a photon.

3- Vertices represent the places where particles are created or annihilated. In the case of electromagnetic interaction, the vertex couples a photon to a charged particle with strength proportional to its charge.

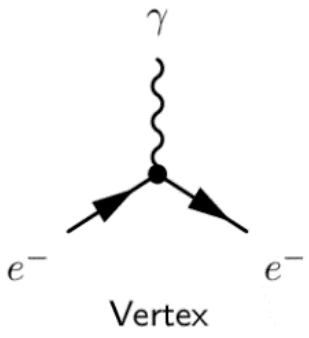

As a conclusion, these diagrams consist of lines representing particles while vertices describe which particles are created or annihilated. The diagrams represent transitions between well-defined 4-momentum states that include the contributions from all possible paths in both time and space. This means that it is not meaningful to ask about the time-ordering of any channel of the internal events, while all possible time-orderings are necessarily included. Each Feynman diagram actually stands for a particular number, which can be calculated using the so-called Feynman rules. It takes different processes as the following:

Firstly, we draw all the diagrams that have the appropriate external lines (it may contain initial channel with two vertices as shown in figure (2.15).

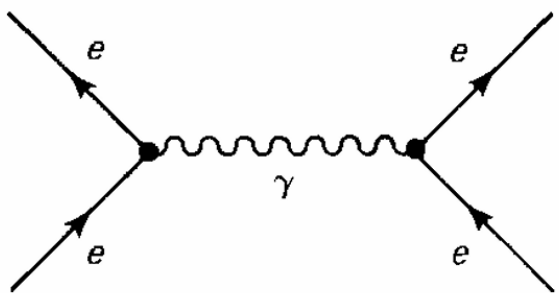

Figure 2.15: Feynman diagram with two vertices.

and may contain another channel with four vertices as shown in figure (2.16) and infinitely so on).

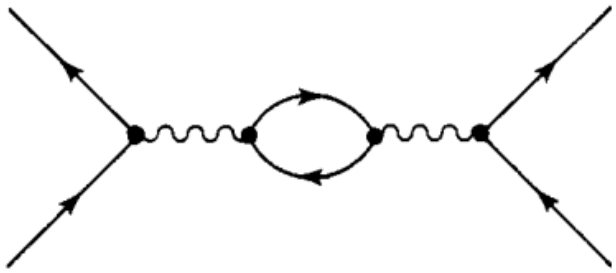

Figure 2.16: Feynman diagram with four vertices (containing a loop).

It is possible to evaluate the contribution of each diagram and add it all up. The sum of all possible Feynman diagrams with the given external lines represents the actual physical process. The total Feynman diagrams give a more accurate description of the interaction with more vertices. Each vertex introduces a constant fraction factor called fine structure constant $\alpha = (e^2/hc)$ so the higher vertices diagrams become less and less effective. Because this is such a small number, diagrams with more and more vertices contribute less and less to the final result and these diagrams may be ignored depending on the accuracy you need. In fact, in QED it is rare to see a calculation that includes diagrams with more than four vertices. The Feynman rules enforce conservation of energy and momentum at each vertex, and hence for the diagram as a whole.

Secondly, to determine the scattering cross-section, by calculating the matrix element using Feynman diagrams then inserting it into Fermi's golden rule relation of two body scattering as

$$\frac{d\sigma}{d\Omega} = \left(\frac{\hbar c}{8\pi}\right)^2 \frac{S|\mathcal{M}|^2}{(E_1 + E_2)^2} \frac{|\mathrm{p}_f|}{|\mathrm{p}_i|} \tag{2.134}$$

where $|P_f|$ is the magnitude of either outgoing momentum and $|P_i|$ is the magnitude of either incoming momentum. S is a product of statistical factors:

l/j! for each group of j identical particles in the final state. Now we need to get the matrix element $\mathcal{M}$ to get the differential cross-section for scattering interaction. This will be calculated according to the following steps:

1- Label the incoming and outgoing four-momenta p_1, p_2 , . .p_n,, and the corresponding spins s_1 , s_2 , . . . , s_n; label the internal four- momenta q_1 , q_2 ,… and it shown in figure (2.17). Assign arrows to the lines as follows: the arrows on external fermion lines indicate whether it is an electron or a positron; arrows on internal fermion lines are assigned so that the "direction of the flow" through the diagram is preserved (i.e., every vertex must have one arrow entering and one arrow leaving). The arrows on external photon lines point "forward"; for internal photon lines the choice is arbitrary. (See figure. 2.17)

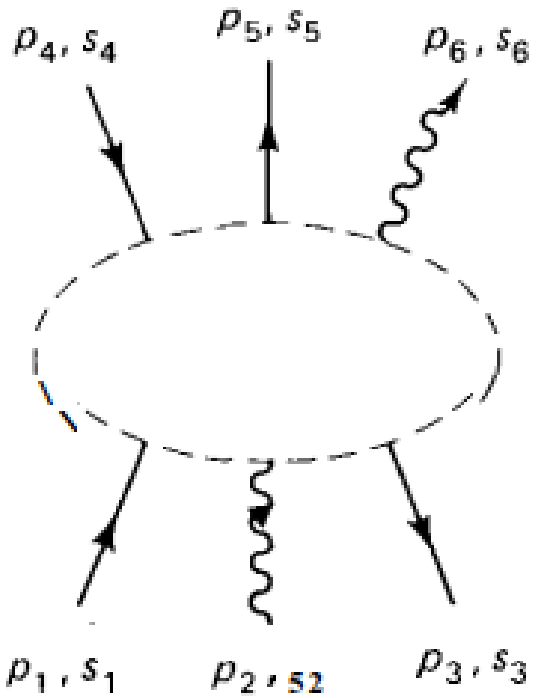

Figure 2.17: A typical QED diagram, with external lines labeled. (Internal lines not shown.

2- External Lines. External lines contribute factors as follows:

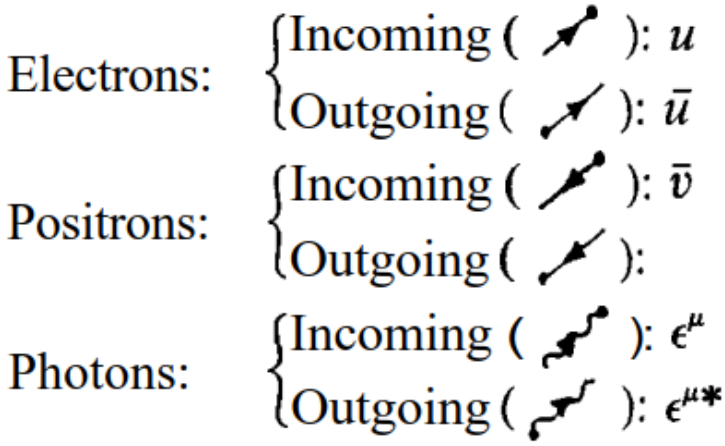

3- Each vertex contributes by a factor called vertex factor.

$$ig_e\gamma^\mu$$

Where g_e is the dimensionless coupling constant which is related to the charge of the positron: $g_e = e\sqrt{4\pi / \hbar c} = \sqrt{4\,\pi\,\alpha}$. In writing the Feynman rules we are dealing with electrons and positrons. In general, the QED coupling constant is $= -q\sqrt{4\pi / \hbar c}$, where q is the charge of the particle (as opposed to the antiparticle).

4- Each internal line contributes a factor called as propagator factor depends on the boson mass and is described as $\frac{i(\gamma^\mu q_\mu + mc)}{q^2 - m^2c^2}$ for massive propagators and takes $\frac{ig_{\mu v}}{q^2}$ for photon.

5- For each vertex the conservation of energy and momentum must be satisfied where a delta function must write in the form

$$(2\pi)^4\delta^4(k_1 + k_2 + k_3)$$

where the k‘s are the three four-momenta coming into the vertex (if an arrow leads outward, then k is minus the four-momentum of that line, except for

external antiparticle). This factor enforces conservation of energy and momentum at the vertex.

6- For each internal momentum q, write a factor $\frac{d^4q}{(2\pi)^4}$ and integrate.

7- Cancel the delta function and the result will include a factor

$$(2\pi)^4\delta^4(p_1 + p_2 + \cdots - p_n)$$

corresponding to overall energy-momentum conservation. Cancel this factor, and what remains is $-i\mathcal{M}$

This can be summarized as

1-write down all diagrams contributing to the process (up to the desired order),
2- calculate the amplitude ($\mathcal{M}$) for each one, and add them up to get the total amplitude,

3- inserted into the appropriate formula for the cross-section.

As we can see, the previous procedure is applied for example electron-muon scattering shown in figure 2.18

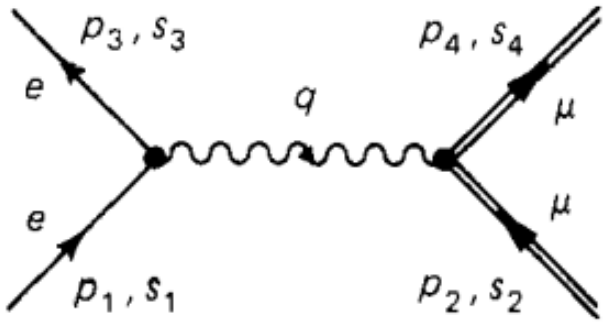

Figure 2.18: Electron-muon scattering.

The simplest case is electron-muon scattering[4], for here only one diagram contributes in lowest order. In applying the Feynman rules, we proceed "backward" along each fermion line

$$(2\pi)^4 \int \left[\bar{u}^{(s_3)}(p_3)(ig_e\gamma^\mu)u^{(s_1)}(p_1)\right]\frac{-ig_{\mu\nu}}{q^2}\left[\bar{u}^{(s_4)}(p_4)(ig_e\gamma^\nu)u^{(s_2)}(p_2)\right] \times \delta^4(p_1 - p_3 - q)\delta^4(p_2 + q - p_4)d^4q \quad (2.135)$$

Notice that the space-time indices on the photon propagator contract with those of the vertex factors at either end of the photon line. Carrying out the (trivial) q integration, and dropping the overall delta function, we can find the matrix element of electron-muon scattering as

$$\mathcal{M} = -\frac{g_e^2}{(p_1 - p_3)^2}\left[\bar{u}^{(s_3)}(p_3)\gamma^\mu u^{(s_1)}(p_1)\right]\left[\bar{u}^{(s_4)}(p_4)\gamma_\mu u^{(s_2)}(p_2)\right] \quad (2.136)$$

After we get the matrix element, we use it to find the scattering differential cross-section by substituting into equation (2.134) (Fermi's Golden Rule) of two body scattering. This will be described in detail in the next chapter as we will apply this theory for electron-proton scattering to get the scattering cross-section for this interaction which is the main objective of this thesis.

Chapter 3

Electron-Proton Elastic Scattering

3.1 Elastic Electron-Proton Scattering

In particle physics[9], scattering experiments are the most effective tool of research and allow studying the interactions between particles. It is a suitable technique for probing the properties of the initial phase of nuclear matter and their structure. A great importance to study electron-proton scattering because it is the best prop to investigate the properties of the internal structure of proton. Electron with a given energy E, and momentum p can resolve distances of De' Brogli wavelength λ where $\lambda = \frac{\hbar}{p}$ compared to proton radius r_p. At very low electron energies where $\lambda \gg r_p$, the electron scattering off proton is equivalent to that from point-like spin-less object as shown in figure (3.1).

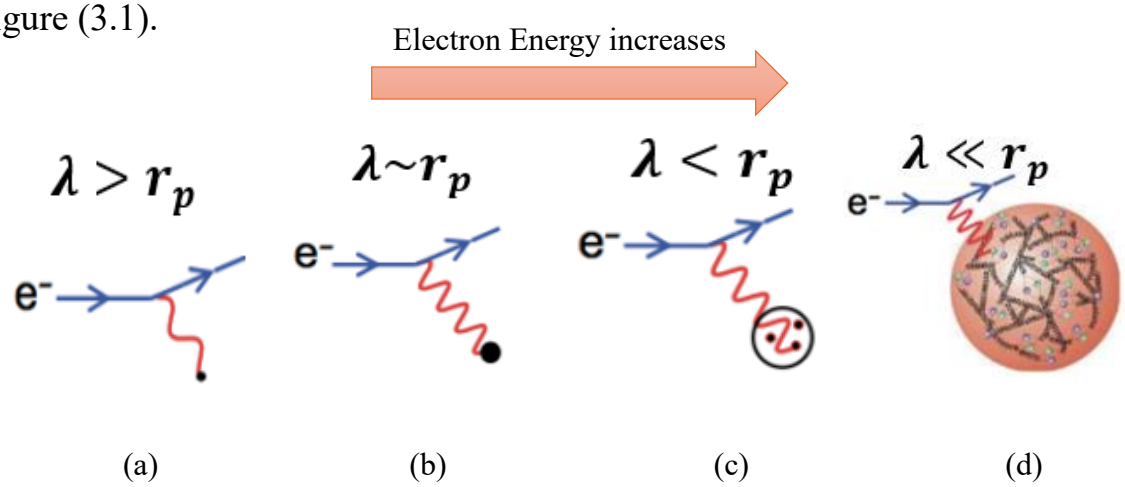

(a) (b) (c) (d)

Figure 3.1: Probing the proton by increasing electron energy.

At low electron energy, $\lambda \sim r_p$ the scattering is equivalent to that from an extended charged object figure (3.1 b). At high electron energies, $\lambda < r_p$ the wavelength is sufficient short to resolve sub-structure to consider the scattering processes are incoherent from that obtained at low energy and are due to proton constituent of quarks figure (3.1 c). At very high electron energies $\lambda \ll r_p$, the proton appears to be a sea of quarks and gluons figure

(3.1 d). The scattering processes are classified into two main categories. The first is elastic-scattering in which the proton is treated as point-like with a single scattering center. Second, is the inelastic-scattering in which proton is considered as a convention of point-like matter called partons or quarks which are treated as a collection of many scattering centers and responsible for production of secondary new hadrons. At low electron energy, the proton is a simple point charge, obeying the Dirac equation given in chapter 2. Consider an elastic scattering for electron-proton at low energies e + p → e + p. The lowest-order Feynman diagram is shown in figure (3.2). This figure shows two vertices diagram first describe the interaction between electron-photon and second is for photon-proton interaction.[4]

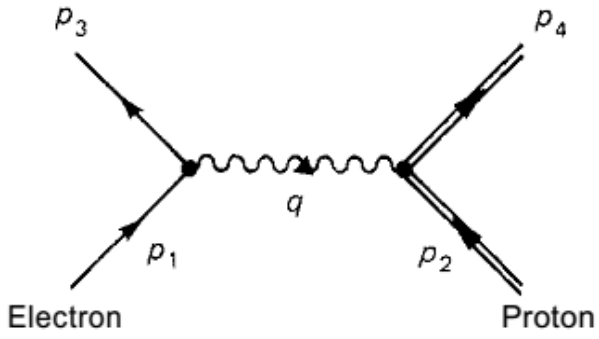

Figure 3.2: Feynman diagram with single photon of electron-proton scattering.

In this section, we will investigate the scattering process in terms of QED. QED theory applied in terms of Feynman diagrams, using Golden rules where the exchange boson is virtual photon (γ) has a four-momentum q. We define the important Lorentz-invariant four-momentum transfer squared represented by Q^2 where $Q^2 = - q^2$

$$Q^2 \sim 4EE' \sin^2\left(\frac{\theta}{2}\right) \tag{3.1}$$

An electron with initial four-momentum $\boldsymbol{p_1}$ scatters from a proton of four-momentum $\boldsymbol{p_2}$ and emerges with a final four-momentum $\boldsymbol{p_3}$ and $\boldsymbol{p_4}$. The virtual photon transfers a four-momentum q to the proton. In the case of elastic scattering, $(p_3 + q)^2 = p_4^2 = M^2$ where M is the mass of the proton. The simplest case in which the spin scattering amplitude is obtained by applying Feynman rules explained in chapter 2 and it has been given by the expression

$$\mathcal{M} = -\frac{g_e^2}{(p_1 - p_3)^2}\left[\bar{u}^{(s_3)}(p_3)\gamma^\mu u^{(s_1)}(p_1)\right]\left[\bar{u}^{(s_4)}(p_4)\gamma_\mu u^{(s_2)}(p_2)\right] \quad (3.2)$$

Where u and $\bar{u}$ represent the four spinors of spin s, for incoming and outgoing particles respectively and eight γ-matrices produced from two vertices. Each vertex contributes a factor $ig_e\gamma^\mu$ where g_e is dimensionless coupling constant, $g_e = e\sqrt{4\pi/\hbar c} = \sqrt{4\pi\alpha}$ which related to the electric charge e. If we know the spins of the incoming and outgoing particles, we can write down the appropriate spinors and do the matrix multiplication. In experiments, beams of electrons have a random spin, we might measure only the number of particles scattered at a particular angle θ measured from direction of incident beam. In this case the relevant cross-section is the average over all initial spin configurations i, and the sum over all final spin configuration f. In principle, we could compute $|\mathcal{M}(i \to f)|^2$ for every possible combination, and then do the summing and averaging. The scattering cross-section of electron of mass m off proton of mass M where M>>m is given by

$$\frac{d\sigma}{d\Omega} = \left(\frac{\hbar}{8\pi Mc}\right)^2 \langle|\mathcal{M}|^2\rangle \quad (3.3)$$

where, $\langle|\mathcal{M}|^2\rangle$ is spin average amplitude. In practice, it is much easier to compute $\langle|\mathcal{M}|^2\rangle$ directly, without ever evaluating the individual amplitudes. Consider, for instance, the electron-proton scattering amplitude given in equation (3.2) and squaring, we have

$$|\mathcal{M}|^2 = \frac{g_e^4}{(p_1 - p_3)^4}[\bar{u}(3)\gamma^\mu u(1)]\big[\bar{u}(4)\gamma_\mu u(2)\big] \times [\bar{u}(3)\gamma^\nu u(1)]^*[\bar{u}(4)\gamma_\nu u(2)]^* \tag{3.4}$$

Applying Casimir's trick twice, (it explained in detail in appendix A) we find $\langle|\mathcal{M}|^2\rangle$ as

$$\langle|\mathcal{M}|^2\rangle = \frac{g_e^4}{4(p_1 - p_3)^4}\mathrm{Tr}\big[\gamma^\mu(\not{p}_1 + mc)\gamma^\nu(\not{p}_3 + mc)\big] \times \mathrm{Tr}\left[\gamma_\mu(\not{p}_2 + Mc)\gamma_\nu(\not{p}_4 + Mc)\right] \tag{3.5}$$

where, the trace for the electron fermion current is

$$\mathrm{Tr}\big[\gamma^\mu(\not{p}_1 + mc)\gamma^\nu(\not{p}_3 + mc)\big] = 4\big[p_1^\mu p_3^\nu + p_3^\mu p_1^\nu + g^{\mu\nu}\big((mc)^2 - (p_1 \cdot p_3)\big)\big] \tag{3.6}$$

For each of the two particles they have two spin states and average must include a factor 1⁄4. So

$$\langle|\mathcal{M}|^2\rangle = \frac{4g_e^4}{(p_1 - p_3)^4}\left[p_1^\mu p_3^\nu + p_3^\mu p_1^\nu + g^{\mu\nu}\big((mc)^2 - (p_1 \cdot p_3)\big)\right] \times \left[p_{2_\mu}p_{4_\nu} + p_{4_\mu}p_{2_\nu} + g_{\mu\nu}\big((Mc)^2 - (p_2 \cdot p_4)\big)\right] \tag{3.7}$$

$$= \frac{8g_e^4}{(p_1 - p_3)^4}[(p_1 \cdot p_2)(p_3 \cdot p_4) + (p_1 \cdot p_4)(p_2 \cdot p_3) - (p_1 \cdot p_3)(Mc)^2 - (p_2 \cdot p_4)(mc)^2 + 2(mMc^2)^2]$$

Apply in equation (3.3) for lab system in which electron is scattered from heavier and fixed proton as shown in figure (3.3).

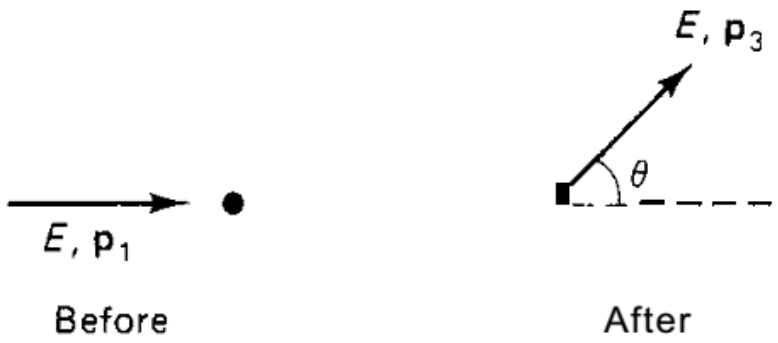

Figure 3.3: Electron scattering from a heavy target.

The unpolarized cross-section is independent of the azimuthal scattering angle φ. Therefore, it has two degrees of freedom, e.g. the energy of the incoming electron E and the scattering angle θ. where

$$p_1 = \left(\frac{E}{c}, \mathbf{p}_1\right), \qquad p_2 = (Mc, \mathbf{0}), \qquad p_3 = \left(\frac{E'}{c}, \mathbf{p}_3\right), \qquad p_4 = (Mc, \mathbf{0})$$

Where $\mathbf{p_1}$ and $\mathbf{p_3}$ are the incident and scattered electron momenta and E's are the corresponding energies where $p1.p3 = \ p^2\ cos\theta$ and

$$(p_1 - p_3)^2 = -(\mathrm{p}_1 - \mathrm{p}_3)^2 = -\mathrm{p}_1^2 - \mathrm{p}_3^2 + 2\mathrm{p}_1 \cdot \mathrm{p}_3 \ = -2\mathrm{p}^2(1 - \cos\ \theta)$$

$$= -4\mathrm{p}^2 \sin^2\ \frac{\theta}{2}$$

and $(p_1 \cdot p_3) = \frac{E^2}{c^2} - \mathbf{p}_1 \cdot \mathbf{p}_3 = \mathbf{p}^2 + m^2c^2 - \mathbf{p}^2 \cos\ \theta = m^2c^2 + 2\mathbf{p}^2 \sin^2\ \frac{\theta}{2}$

$$(p_1 \cdot p_2)(p_3 \cdot p_4) = (p_1 \cdot p_4)(p_2 \cdot p_3) = (ME)^2$$

$$(p_2 \cdot p_4) = (Mc)^2$$

Use previous equations in equation (3.7) to write spin average amplitude as

$$\langle|\mathcal{M}|^2\rangle = \left(\frac{g_e^2 Mc}{p^2 \sin^2\ (\theta/2)}\right)^2 \left((mc)^2 + p^2 \cos^2\ \frac{\theta}{2}\right) \qquad (3.8)$$

Then substitute with equation (3.8) in equation (3.3) to get differential cross-section where $g_e = \sqrt{4\pi\alpha}$

$$\frac{d\sigma}{d\Omega} = \left(\frac{\alpha\hbar}{2p^2\sin^2(\theta/2)}\right)^2 \{(mc)^2 + p^2\cos^2(\theta/2)\} \tag{3.9}$$

This is called Mott formula and gives a good approximation to study the differential cross-section for elastic electron-proton scattering. This equation will be used to calculate the theoretical cross-section and will be compared with corresponding values that obtained in experiments at different ranges of energy. It gives regular disagreement with experimental data and will be given in detail in chapter 4. This is explained due to new effects related to the internal components of proton and will modify the Mott formula as the following section.

3.2 Proton Form Factors

An additional treatment is applied by considering two effects of momentum transfer q where $q=p_1-p_3$ on both electron and proton in terms of tensors between electron-photon $L^{\mu\nu}_{\text{electron}}$ and the corresponding tensor for photon-proton $L_{\mu\nu\,\text{proton}}$. The scattering amplitude will take the form

$$\langle|\mathcal{M}|^2\rangle = \frac{g_e^4}{q^4} L^{\mu\nu}_{\text{electron}} L_{\mu\nu\,\text{proton}} \tag{3.10}$$

and equation. (3.6) becomes

$$L^{\mu\nu}_{\text{electron}} = 2\{p_1^\mu p_3^\nu + p_3^\nu p_1^\mu + g^{\mu\nu}[(mc)^2 - (p_1 \cdot p_3)]\} \tag{3.11}$$

By the same way the proton tensor is $L_{\mu\nu\,\text{proton}}$ is obtained by replacing electron mass m by proton mass M and momenta of proton p_2 and p_4 before and after scattering process respectively

$$L_{\mu\nu\,\text{proton}} = 2\{p_{2\mu}p_{4\nu} + p_{4\mu}p_{2\nu} + g_{\mu\nu}[(\text{M}c)^2 - (p_2 \cdot p_4)]\} \tag{3.12}$$

The obtained cross-section is similar to Mott formula given before in equation (3.9). In order to study the effect of proton components, a second additional formalism is applied on process at high electron energy elastic scattering. This is by considering proton is not a simple point charge, and so, more additional formalism is introduced according to the internal physical properties. The incident electron has a chance to see an extended and a clear image of the proton for its constituents which are affected by electric and magnetic form factors. So, there must be a modification which called Form Factor *F(q)* added to the Mott formula to match this behavior. This modification describes the charge distribution inside the proton and is represented by electric form factor. The cross-section for an electron scattering from a static charge distribution of density $\rho(\vec{x})$, in the non-relativistic limit is given as:[3,10]

$$\frac{d\sigma}{d\Omega} = \frac{d\sigma}{d\Omega}\Big|_{\text{point}} |F(q^2)|^2 \tag{3.13}$$

where $F(q^2)$ is the Fourier transform of the charge distribution $\rho(\vec{x})$. The form factor can be expressed as the Fourier transform as follows:

$$F(\vec{q}) = \int d^3x \rho(x) e^{i\vec{q}\cdot\vec{x}} \tag{3.14}$$

It can be shown that $F(q^2)$ can be identified as the electric form factor, $G_E(q^2)$. Similarly, if the source has an extended magnetic moment distribution, then the Fourier transform of that distribution is the magnetic form factor $G_M(q^2)$. At low electron energy where $\lambda \gg r_p$ and no sensitivity for charge distributions inside proton $F(q^2)=1$. At large q^2 the electron is sensitive to charge distribution inside proton and $F(q^2)<1$. At relativistic electron energy, the electron props the extended proton and strong sensitive to electric and magnetic distributions due to spin and orientation for both electron and proton

in addition to the recoil energy of proton. In the lowest-order QED, an additional process is represented as shown in figure (3.4).

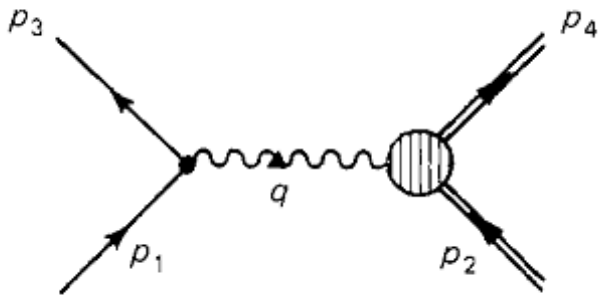

Figure 3.4: Feynman diagram for electron elastic scattering off extended proton constituents.

The blob on the right describes the mechanism of interaction of the photon with the proton. Now, the left vertex describes the interaction of electron with photon and photon propagator is unchanged as before. The average spin amplitude $\langle|\mathcal{M}|^2\rangle$ becomes sensitive to process at photon-proton vertex and equation (3.10) rewritten as

$$\langle|\mathcal{M}|^2\rangle = \frac{g_e^4}{q^4} L^{\mu\nu}_{\text{electron}}\, K_{\mu\nu\ \text{proton}} \tag{3.15}$$

where $K_{\mu\nu\ \text{proton}}$ is hadronic tensor and unknown quantity describing the photon-proton vertex. The complete information about the target response is contained in $K_{\mu\nu}$ with the nucleon spin, gauge invariance and symmetry properties allow a parameterization of the hadronic tensor. The quantity $q = p_4 - p_2$ and will represent p_2 to the initial proton momentum p. There are different ways used to describe this tensor depending on the possible mechanisms of photon-proton interaction. Energy of the experiments controls the most and general tensor of the two vectors p and q is

$$K^{\mu\nu}_{\text{proton}} = -K_1 g^{\mu\nu} + \frac{K_2}{(Mc)^2} p^\mu p^\nu + \frac{K_4}{(Mc)^2} q^\mu q^\nu + \frac{K_5}{(Mc)^2}(p^\mu q^\nu + p^\nu q^\mu) \qquad (3.16)$$

where K_i are investigated and unknown functions of the scalar variable q^2 only and $p^2=(Mc)^2$ is constant where M is proton mass and $q.p=-q^2/2$. The $K's$ functions are not independent and will have the same dimensions where

$$q_\mu K^{\mu\nu} = 1 \qquad (3.17)$$

$$K_4 = \frac{(Mc)^2}{q^2} K_1 + \frac{1}{4} K_2 \quad \text{and} \quad K_5 = \frac{1}{2} K_2 \qquad (3.18)$$

The hadronic tensor $K^{\mu\nu}$ can be expressed in terms of just two unknown functions say $K_1(q^2)$ and $K_2(q^2)$ where

$$K^{\mu\nu}_{\text{proton}} = K_1\left(-g^{\mu\nu} + \frac{q^\mu q^\nu}{q^2}\right) + \frac{K_2}{(Mc)^2}\left(p^\mu + \frac{1}{2}q^\mu\right)\left(p^\nu + \frac{1}{2}q^\nu\right) \qquad (3.19)$$

The two functions K_1 and K_2 are fundamental to describe the structure of the proton and obtained from experimental data, which measure the cross-section of elastic scattering. According to equations (3.11) and (3.19), the average scattering amplitude is

$$\langle|\mathcal{M}|^2\rangle = \left(\frac{2g_e^2}{q^2}\right)^2 \left\{K_1[(p_1 \cdot p_3) - 2(mc)^2] + K_2\left[\frac{(p_1 \cdot p)(p_3 \cdot p)}{(Mc)^2} + \frac{q^2}{4}\right]\right\} \qquad (3.20)$$

In the laboratory frame, proton is at rest with momentum components $p=(Mc,0,0,0)$ and incident electron with energy E scatters with emerging energy E' at angle θ. Neglect electron mass compared to E and E'. Electron components are

$$p_1 = \frac{E}{c}(1, \hat{p}_i) \quad \text{and} \quad p_3 = \frac{E'}{c}(1, \hat{p}_f) \quad \text{where} \quad \hat{p}_i \cdot \hat{p}_f = cos\theta$$

It is customary for space-like (the meaning of space-like: it means that the interaction of scattering between electron and proton has only difference in

space not time, so they called space like) processes to refer to the momentum transfer squared as $Q^2=-q^2$, which is a positive quantity. We find

$$\langle|\mathcal{M}|^2\rangle = \frac{g_e^4 c^2}{4EE'\sin^4(\theta/2)}\left(2K_1\sin^2\frac{8}{2} + K_2\cos^2\frac{\theta}{2}\right) \qquad (3.21)$$

The energy of the scatter electron E' is determined from incident electron energy E and scattering angle θ where

$$E' = \frac{\mathrm{E}}{1+(2E/Mc^2)\sin^2(\theta/2)} \qquad (3.22)$$

The cross-section for particles with reduces mass is given as

$$\frac{d\sigma}{d\Omega} = \left(\frac{\hbar E'}{8\pi McE}\right)^2 \langle|\mathcal{M}|^2\rangle \qquad (3.23)$$

Here the elastic cross-section for electron-proton is

$$\frac{d\sigma}{d\Omega} = \left(\frac{\alpha\hbar}{4\mathrm{ME}\sin^2(\theta/2)}\right)^2 \frac{E'}{\mathrm{E}}[2K_1\sin^2(\theta/2) + K_2\cos^2(\theta/2)] \qquad (3.24)$$

Equation (3.24) is known as Rosenbluth formula.[4] Notice that its analogy to Mott cross-section in equation (3.9). Here the term *E′/E* is due to the proton recoil, called Mott correction in cross-section and the new term which is directly with $sin^2(\theta/2)$ is due to the magnetic interaction produced from spin-spin interactions.

In the next chapter, we will compare the results of theoretical predictions and corresponding experimental data to investigate the contribution of electric and magnetic form factors.

Chapter 4

Comparison between Theoretical Predictions and Experimental Data

4.1 Scattering Experiments

The search for fine properties of nuclear materials requires different experiments, especially at very-high energies. In this section we will briefly talk about some laboratories which deal with scattering experiments and their ranges of energy which help to compare the results of the theoretical predictions obtained from this research. The scattering experiments at high-energy are concentrated in a small number of places. The large accelerator facilities employ a variety of acceleration devices and have sophisticated arrays of detectors to permit analysis of the results. One of the most well-known laboratories or colliders that deals with scattering experiments is SLAC (Stanford Linear Accelerator Center) has a 2-mile linear accelerator. In a single pass, it accelerates electrons to 25 GeV. Research at SLAC is interested in the internal structure of proton and the properties of elementary particles as charm quark, quark structure and the tau lepton. Another important laboratory is Fermilab located near Chicago specializing in high-energy particle physics. Fermilab's main injector is 3.3 km in circumference. It had the Tevatron, one of the most powerful colliders. It was designed to reach 1 TeV. The third laboratory is the Brookhaven national laboratory in New York. It was the first facility to employ a proton synchrotron up to 250 GeV. The Relativistic Heavy Ion Collider (RHIC) at Brookhaven is a synchrotron particle accelerator with a circumference of 4 kilometers. The search for nuclear phase, called quark-gluon plasma, is achieved from high energy collisions hadron-hadron, hadron-nucleus and nucleus-nucleus. The experiments to date have involved accelerating two beams of gold ions in opposite directions around the circle and then directing them together for a

collision experiment which may produce the quark-gluon plasma state. The last laboratory is the European organization for nuclear research known as CERN laboratory for particle physics is located just outside Geneva, Switzerland. It has a 27-kilometer circumference circular tunnel which houses the Large Electron-Positron Collider (LEP). And the Large Hadron Collider (LHC) which should produce proton-proton collisions in the energy range 10-14 TeV. [11]

4.2 Theoretical Prediction and Experimental Data

In the following sections, we will calculate the cross-section for electron-proton scattering at different values of electron energies using the derived Mott formula as given in equation (3.9). These calculations are compared with experimental data which were carried out in global laboratories at the same energies to check the postulates which are assumed during these calculations. These comparisons will be interested by elastic cross-section and their modifications. Also, checkup of the proton electric and magnetic form factors which are assumed for relatively high energy experiments.

4.2.1 Cross-section Calculations

This section studies the calculations of cross-section using Mott formula for e-p scattering at wide range of energies and comparing them with experiments. During scattering process of electron proton, the momentum transfer Q^2 $(GeV/c)^2$ by photon is calculated from the corresponding experimental values measured from incident electron energy E, scattered electron energy E', and the angle of scattering θ, where Q^2 is calculated as

$$Q^2 = 4EE' \sin^2\left(\frac{\theta}{2}\right) \tag{4.1}$$

First, at low-values of Q^2 in the range 0.2-1 $(GeV/c)^2$, Elastic e-p scattering cross-section is classified according to the magnitude of scattering angle into forward in which $\theta \leq 90°$ and backward at $\theta > 90°$.These comparisons at different angles are shown in figure (4.1).

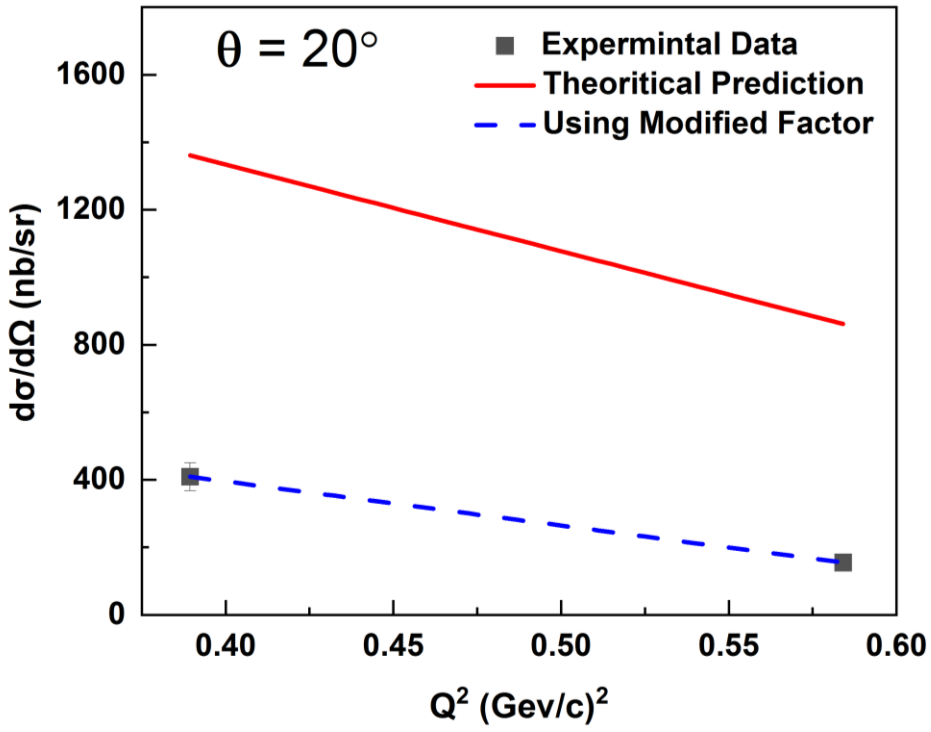

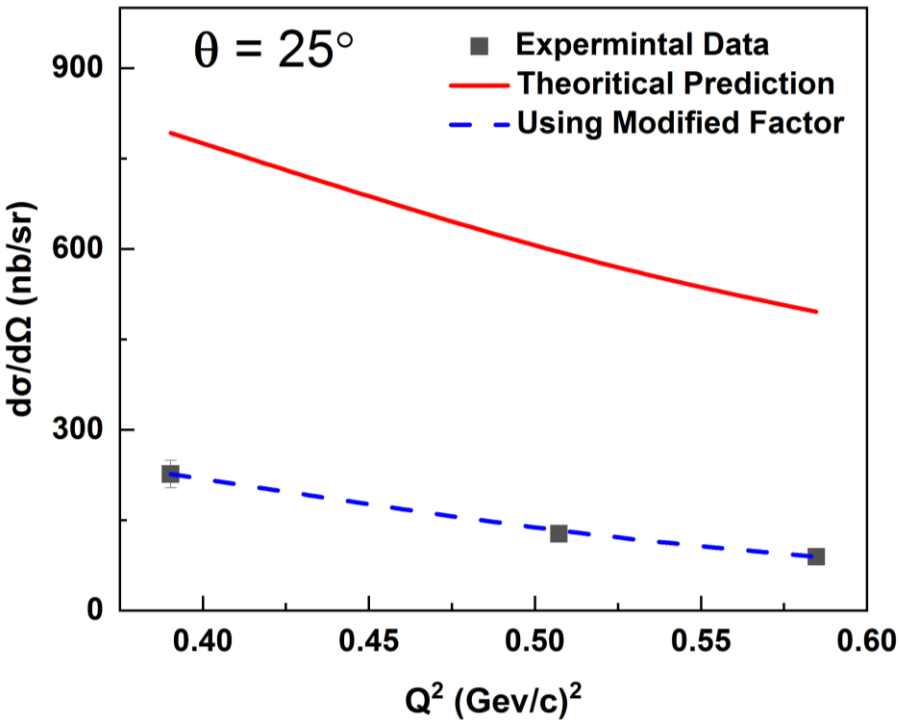
θ = 25°
Expermintal Data
Theoritical Prediction
Using Modified Factor
dσ/dΩ (nb/sr)
900
600
300
0
0.40
0.45
0.50
0.55
0.60
Q² (Gev/c)²

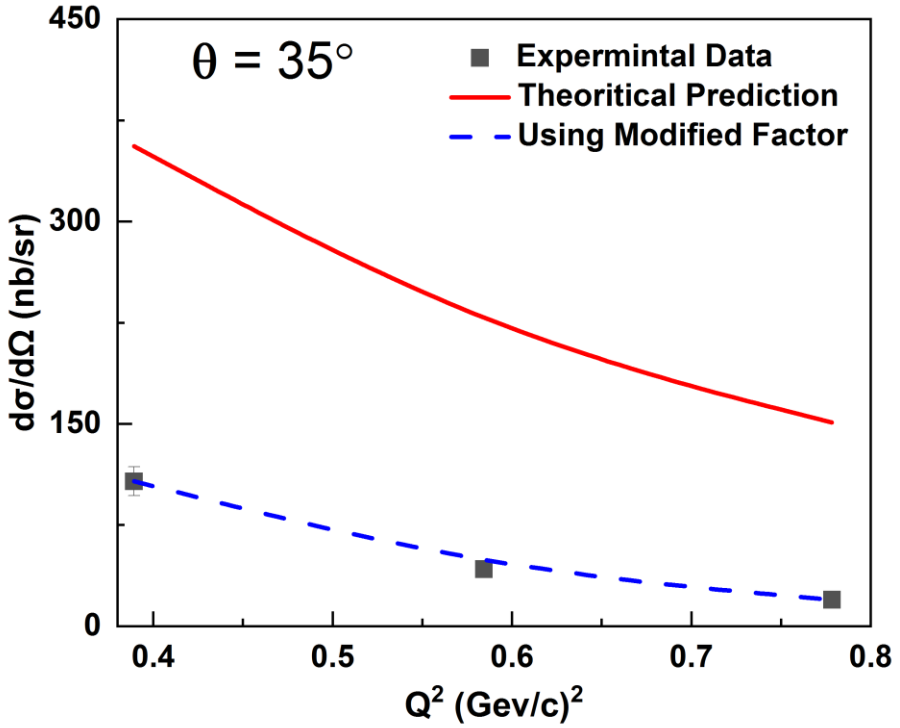
θ = 35°
Expermintal Data
Theoritical Prediction
Using Modified Factor
dσ/dΩ (nb/sr)
450
300
150
0
0.4
0.5
0.6
0.7
0.8
Q² (Gev/c)²

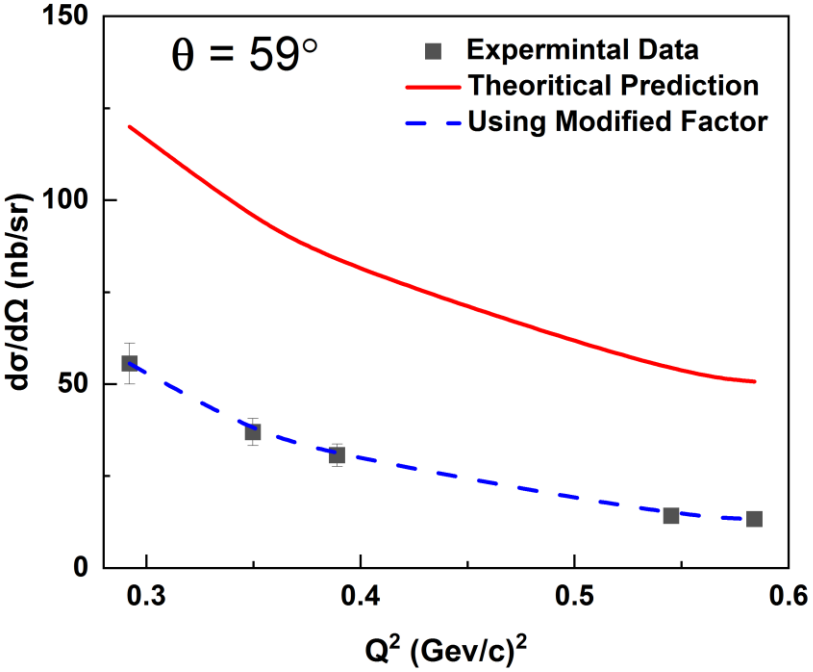
θ = 59°
Expermintal Data
Theoritical Prediction
Using Modified Factor
dσ/dΩ (nb/sr)
150
100
50
0
0.3
0.4
0.5
0.6
Q² (Gev/c)²

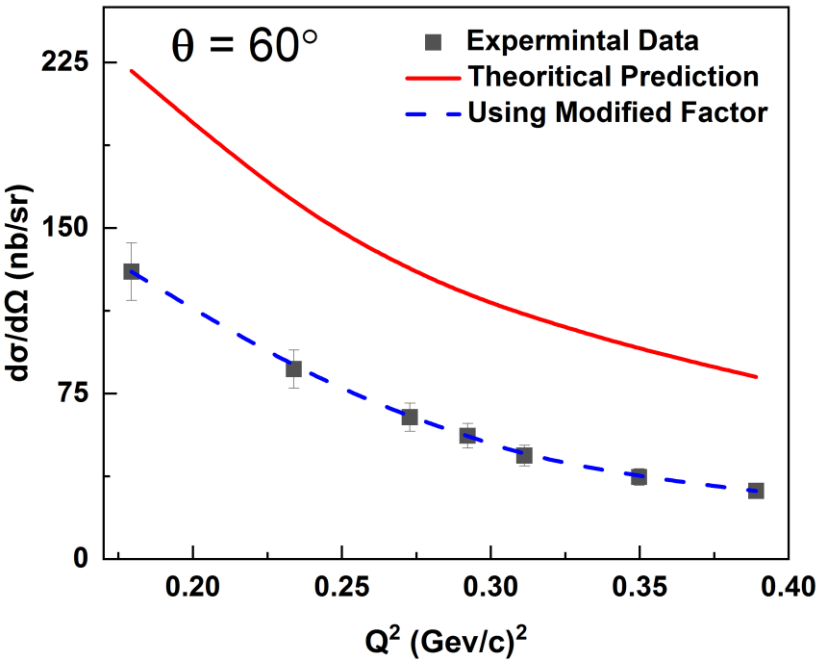
θ = 60°
Expermintal Data
Theoritical Prediction
Using Modified Factor
dσ/dΩ (nb/sr)
225
150
75
0
0.20
0.25
0.30
0.35
0.40
Q² (Gev/c)²

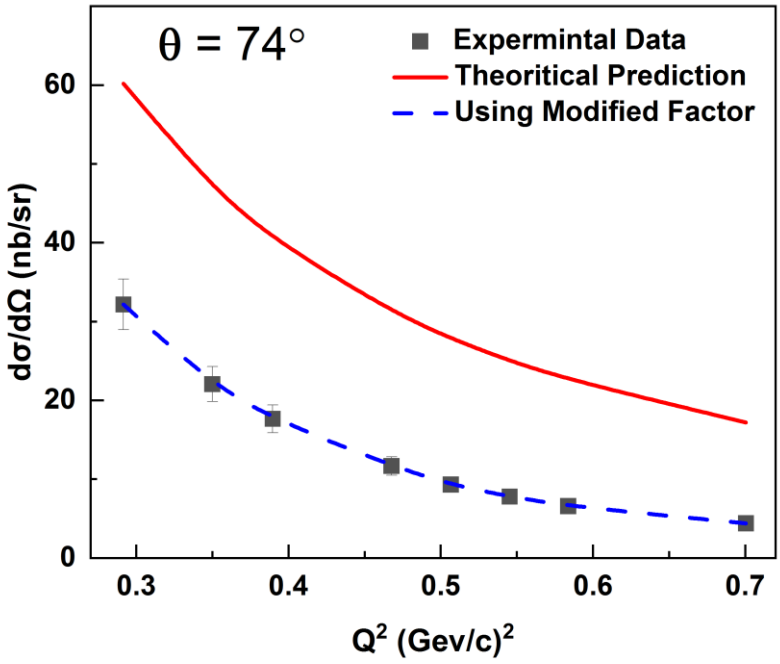
θ = 74°
Expermintal Data
Theoritical Prediction
Using Modified Factor
dσ/dΩ (nb/sr)
0
20
40
60
0.3
0.4
0.5
0.6
0.7
Q² (Gev/c)²

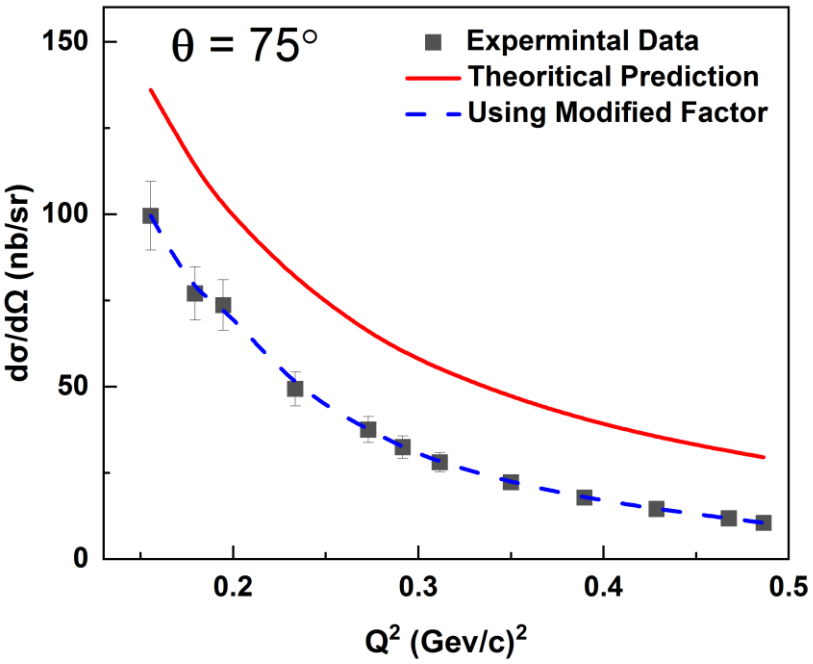
θ = 75°
Expermintal Data
Theoritical Prediction
Using Modified Factor
dσ/dΩ (nb/sr)
0
50
100
150
0.2
0.3
0.4
0.5
Q² (Gev/c)²

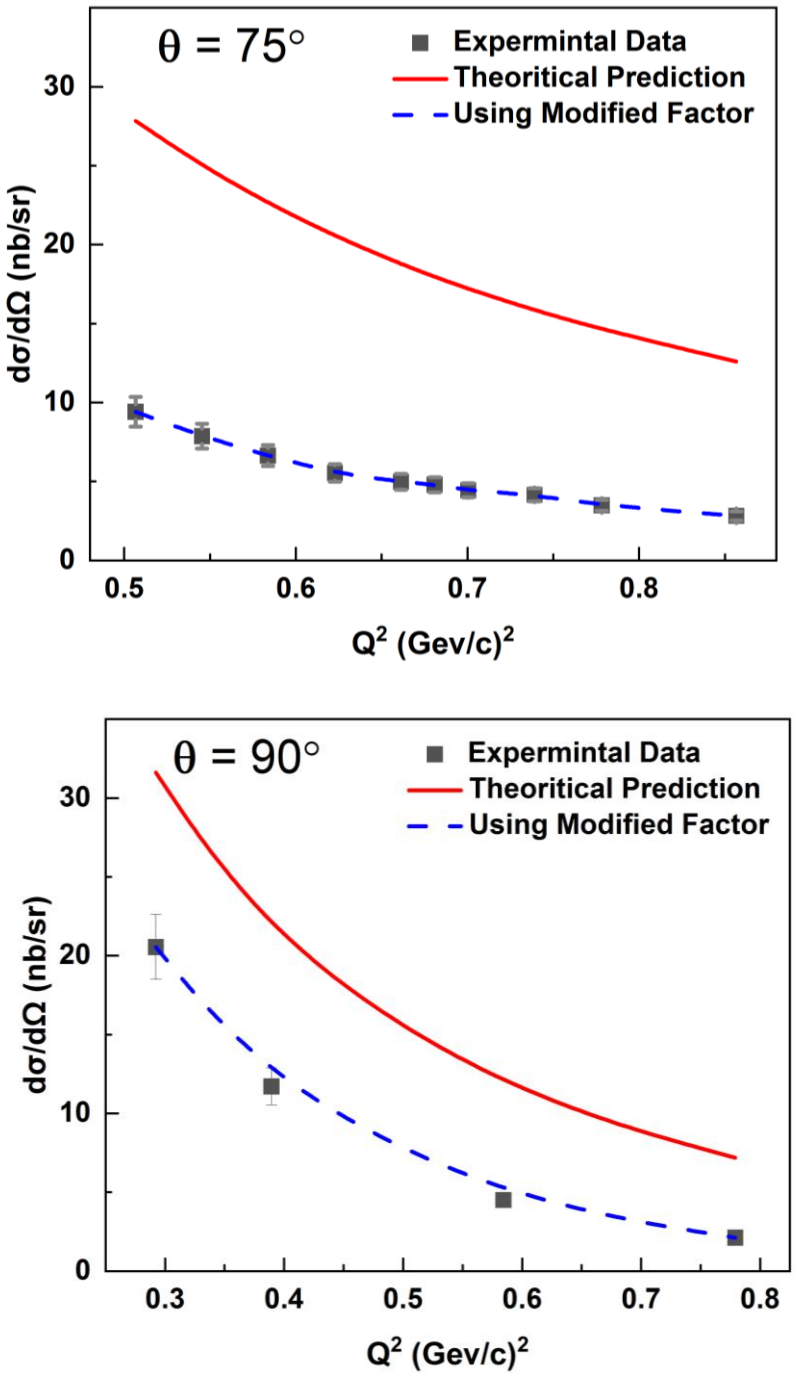

Figure 4.1: Variation of cross-section of e-p elastic scattering with Q^2 at different scattering angles in forward directions. The solid line is the prediction of Mott formula while the dashed line represents the modified factor.

Figure (4.1) shows the variation of the cross-section of e-p elastic scattering with Q^2 at different scattering angles in the forward directions. The solid line represents the prediction of Mott formula and solid square represents the experimental data measure and is given in references[12] and [13]. For both theoretical and experimental data, the common observations enable us to conclude that the cross-section decreases with Q^2 for all possible values of angles θ. Theoretical predictions are similar but not identical with experiments. The calculated values are greater than the experimental data in the forward angels. From this, we can conclude that Mott formula can give good physical analysis of scattering process but not identical due to a regular spacing between experiments and theoretical predictions. This spacing requires an additional modification to be matched with experimental data by a suitable factor called modified factor MF. This factor reduces the spacing to be in agreement with experiments and is shown by a dashed line shown in figure (4.1). It is important to study this remark for the backward angles at the same range momentum transfer Q^2. Figure (4.2) shows the same comparisons but for backward angles $\theta > 90^o$.

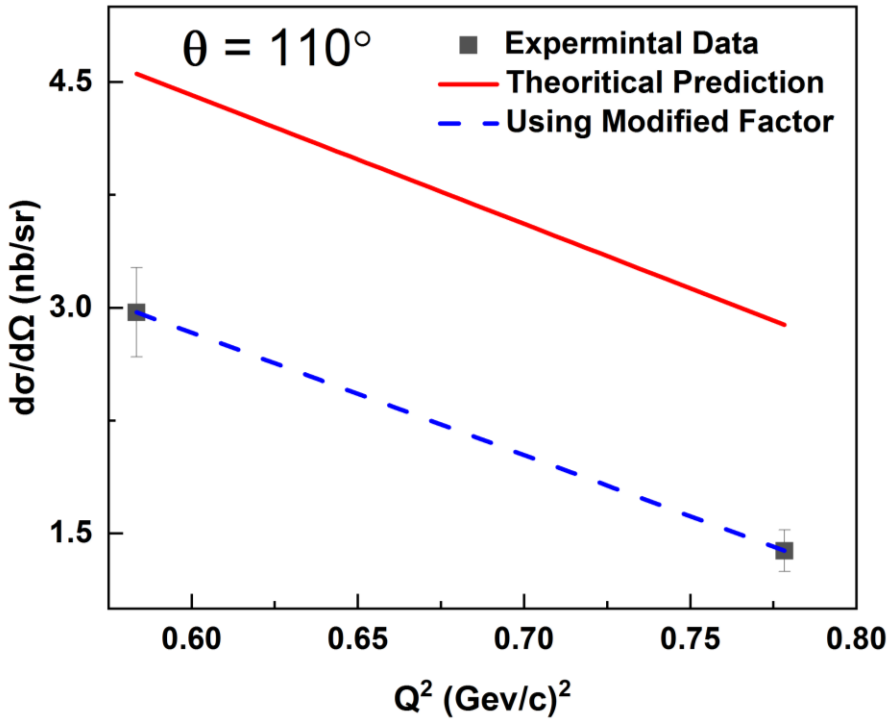
θ = 110°
Expermintal Data
Theoritical Prediction
Using Modified Factor
dσ/dΩ (nb/sr)
4.5
3.0
1.5
0.60
0.65
0.70
0.75
0.80
Q² (Gev/c)²

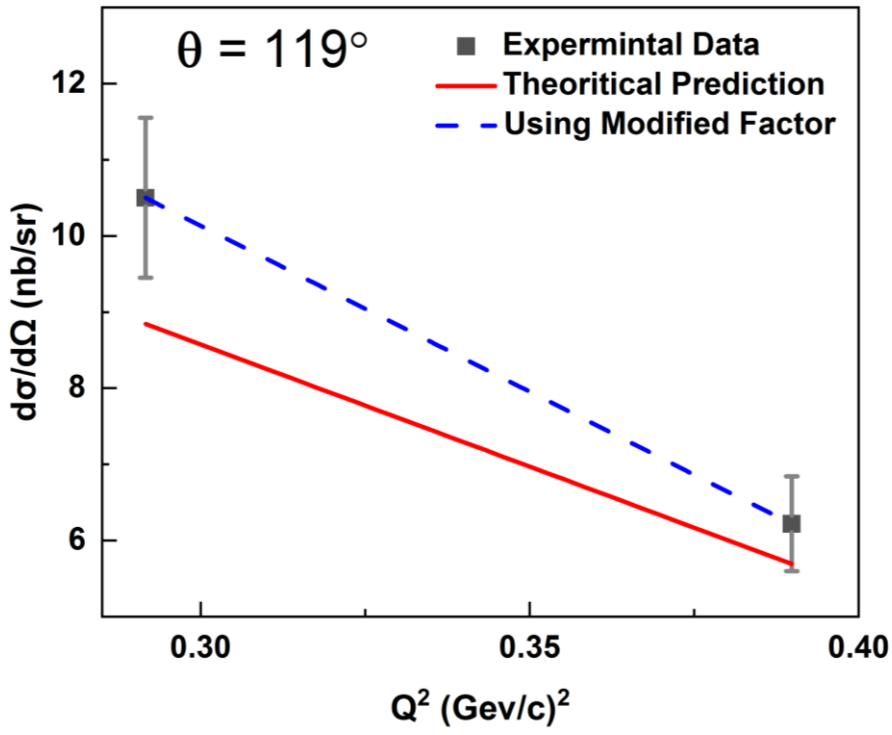
θ = 119°
Expermintal Data
Theoritical Prediction
Using Modified Factor
dσ/dΩ (nb/sr)
12
10
8
6
0.30
0.35
0.40
Q² (Gev/c)²

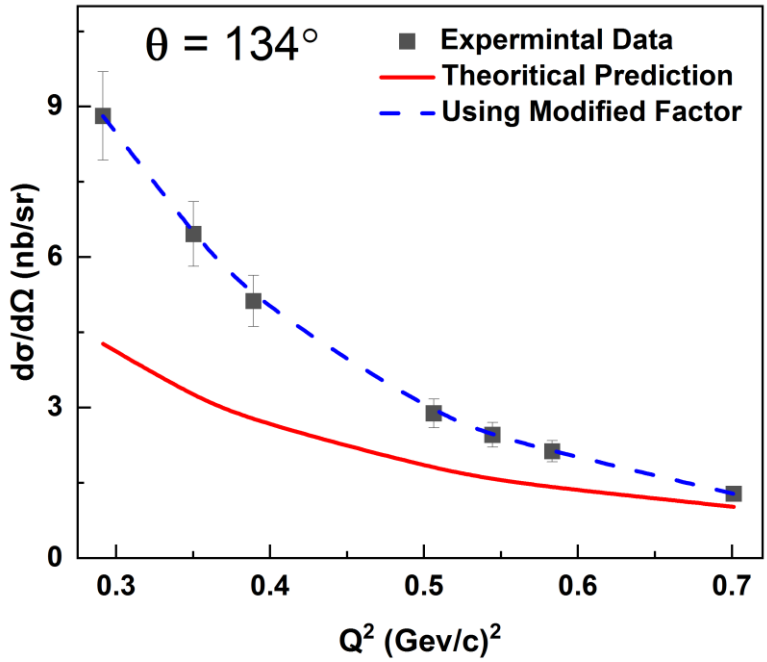
θ = 134°
Expermintal Data
Theoritical Prediction
Using Modified Factor
dσ/dΩ (nb/sr)
0
3
6
9
0.3
0.4
0.5
0.6
0.7
Q² (Gev/c)²

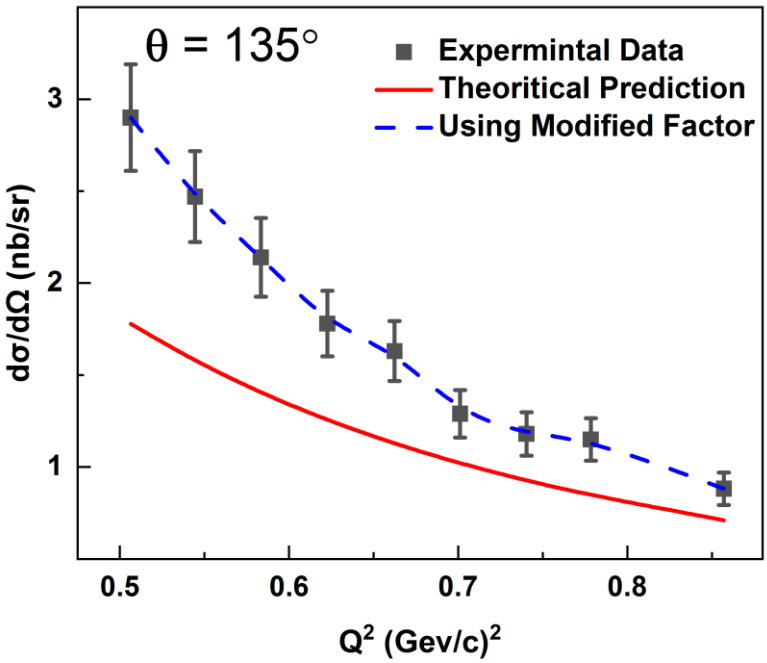
θ = 135°
Expermintal Data
Theoritical Prediction
Using Modified Factor
dσ/dΩ (nb/sr)
1
2
3
0.5
0.6
0.7
0.8
Q² (Gev/c)²

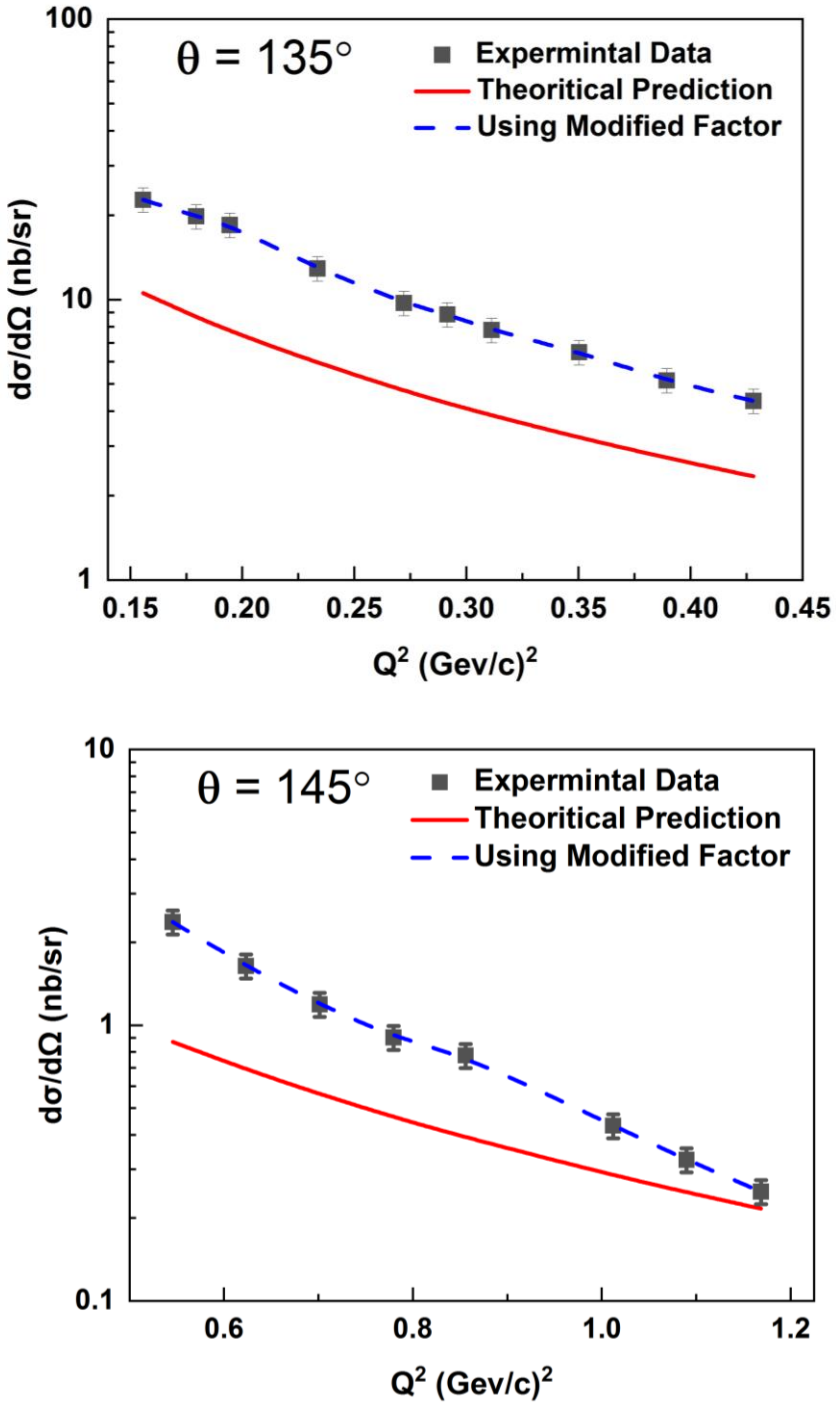

Figure 4.2: Variation of cross-section of e-p elastic scattering with Q^2 at different scattering angles in backward directions. The solid line is the predictions of Mott formula while dashed line at modified factor.

By The same common observations, one can conclude that the cross-section decreases with Q^2 for all backward angles. Theoretical predictions are similar but not identical with experimental data. The theoretical calculated values are greater than the experimental data in the forward directions (figure 4.1) and less in the backward one (figure 4.2) except for angle 110^o. This may be due to low statistics or a mixture between the two assumed kinematics (forward and backward). Also, the same divergence between experimental data and theoretical prediction depends on both θ and Q^2. Again, the additional modified factor MF is applied to reduce this divergence to match the data and is represented by dashed line. The variety in θ could be explained in terms of the dynamical parameters E, E', Q^2 and the possible magnitudes of the impact parameter b. If the scattering is in backward direction, the impact parameter is less than the radius of proton and, the electron encounters the proton to transfer sufficient momentum and undergoes reverse scattering.

Second, scattering cross-section at relatively high values of Q^2 in the range 1-25$(GeV/c)^2$ is studied for the same experimental parameters. At relatively high values of Q^2 where $Q^2 \geq 1$ $(GeV/c)^2$, the same comparisons are shown in figure 4.3. There is a similar divergence between experimental data [14,15] and the calculated one. For all values of Q^2, there is no elastic scattering in backward directions and all recorded experimental data are forward where $\theta \leq 90^o$. So, the modified factor must be added to Mott formula and becomes in good agreement with the experimental data, which is represented by dashed lines. The physics of these factors will be discussed in the next section.

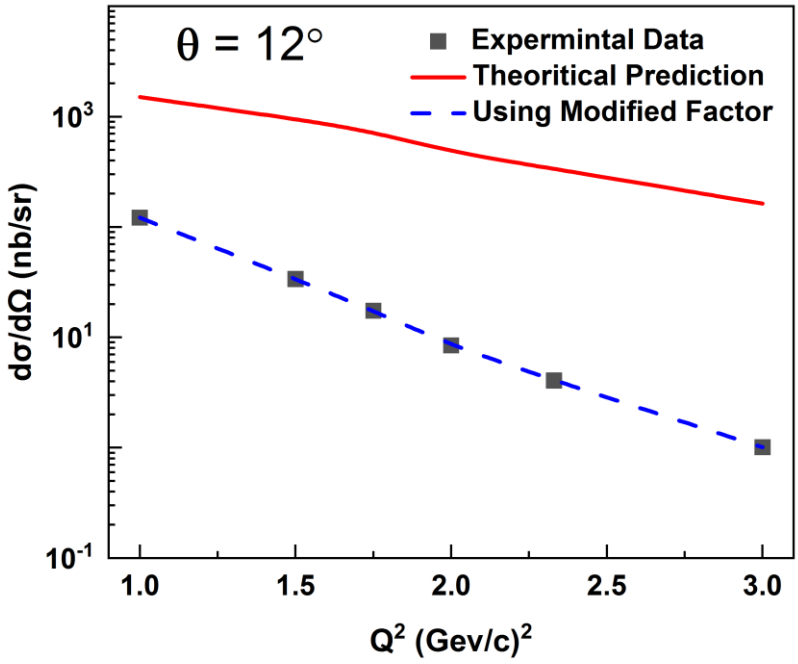
θ = 12°
Expermintal Data
Theoritical Prediction
Using Modified Factor
dσ/dΩ (nb/sr)
10^3
10^1
10^-1
1.0
1.5
2.0
2.5
3.0
Q^2 (Gev/c)^2

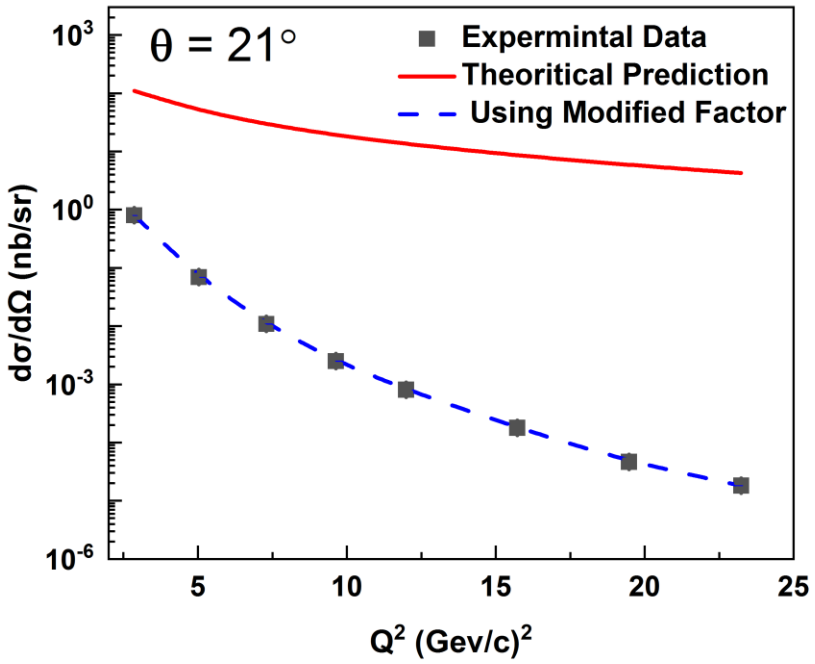
θ = 21°
Expermintal Data
Theoritical Prediction
Using Modified Factor
dσ/dΩ (nb/sr)
10^3
10^0
10^-3
10^-6
5
10
15
20
25
Q^2 (Gev/c)^2

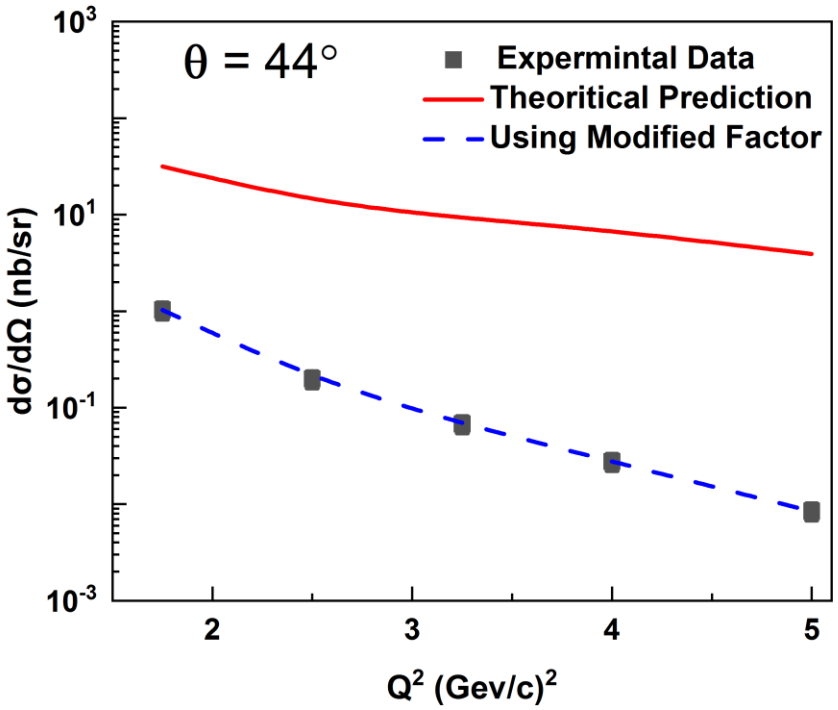
θ = 44°
Expermintal Data
Theoritical Prediction
Using Modified Factor
dσ/dΩ (nb/sr)
Q² (Gev/c)²

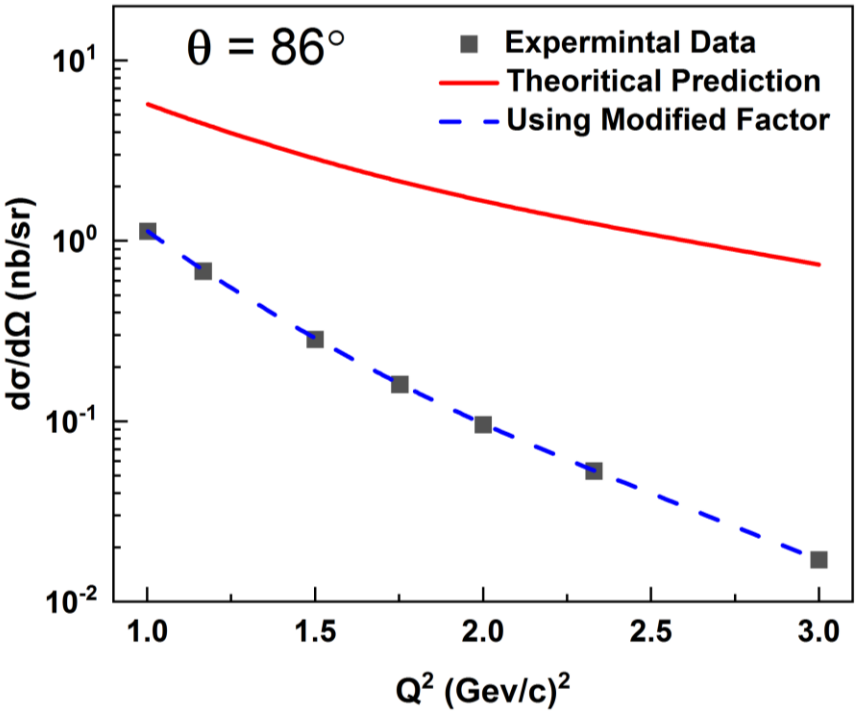
θ = 86°
Expermintal Data
Theoritical Prediction
Using Modified Factor
dσ/dΩ (nb/sr)
Q² (Gev/c)²

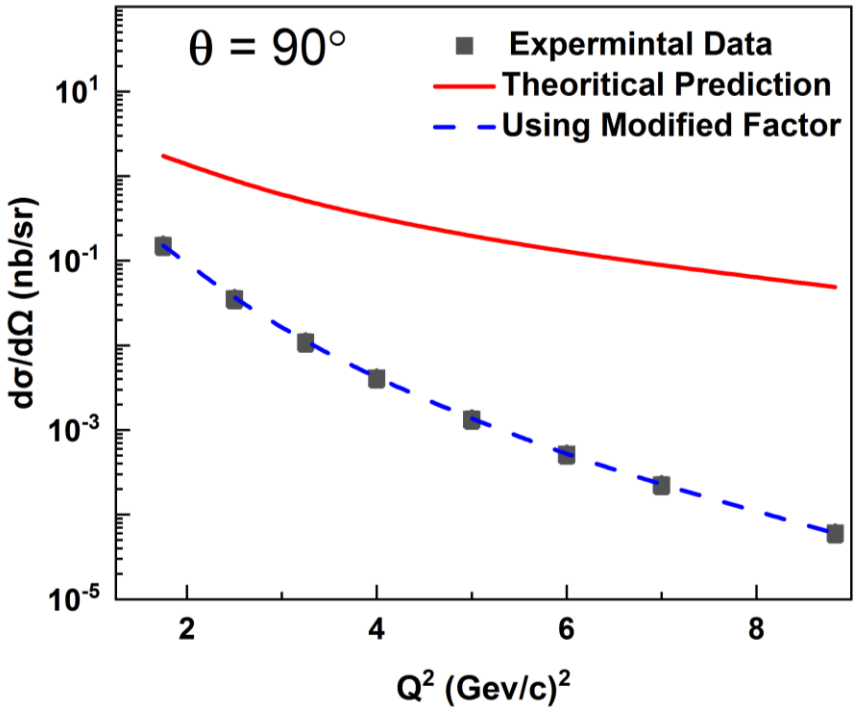

Figure 4.3 : Variation of cross-section of e-p elastic scattering at relatively high-values of $Q^2$and at different scattering angles the solid line is the predictions of Mott formula while dashed line at modified factor.

4.2.2 Electromagnetic Form Factors

Electromagnetic form factors MF are assumed parameters added to Mott formula to match experimental data of e-p elastic scattering for both low and high values of Q^2. The dashed line in figures (4.1), (4.2) and (4.3) represents these predictions. The predicted MF gives information on the electric and magnetic properties of proton constituents, and mathematically represented by $F(Q^2)$. They could be described in terms of the charge distribution and magnetization of the proton. The variation of MF for all possible values of Q^2 in forward and backward angles is shown in figure 4.4 (a) and (b) respectively and given in table 4.1. Also, their dependance on θ is shown in figure (4.5).

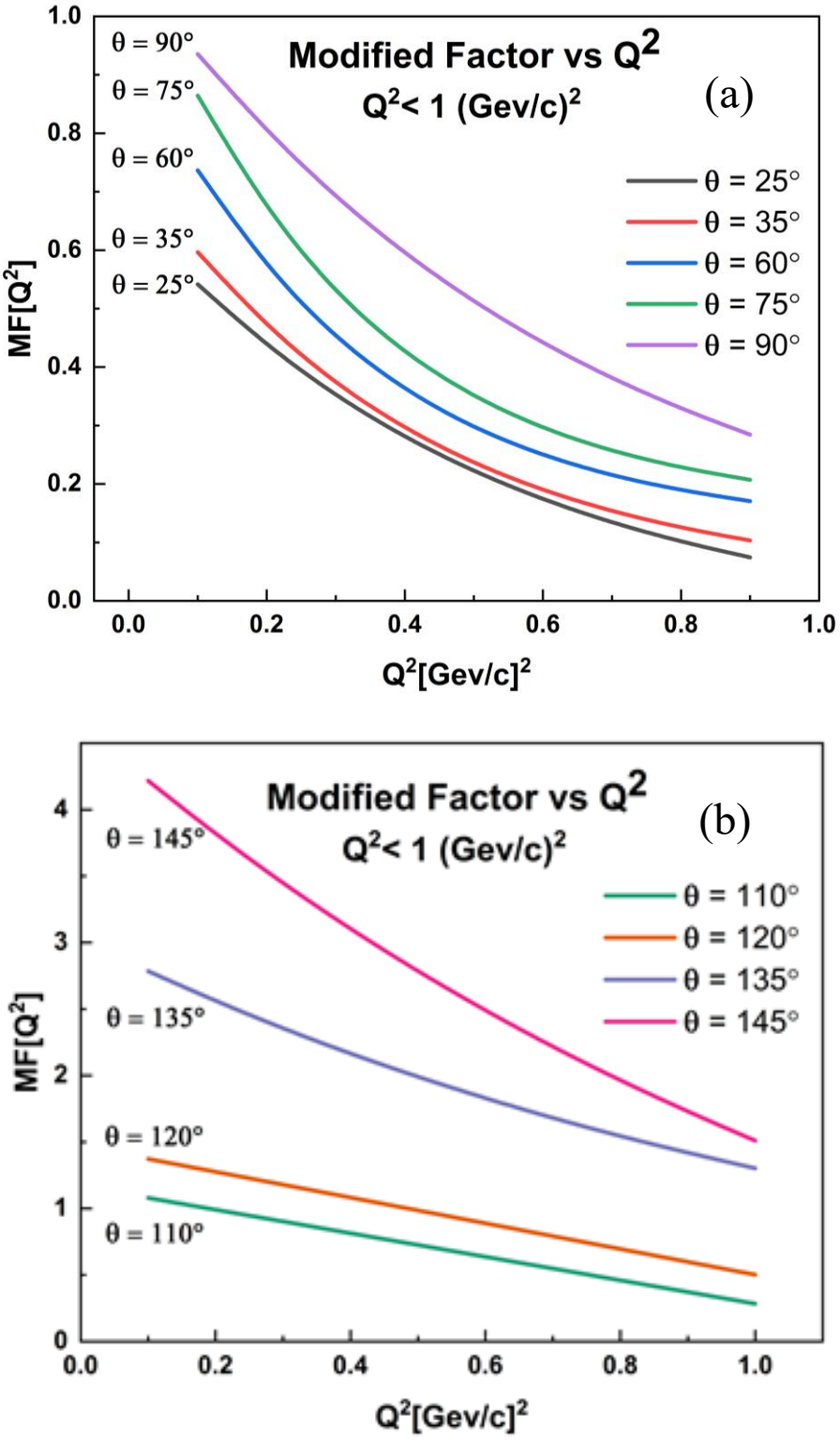

Figure 4.4: Modified factor dependence on Q^2 for forward angles (a) and for backward angles (b).

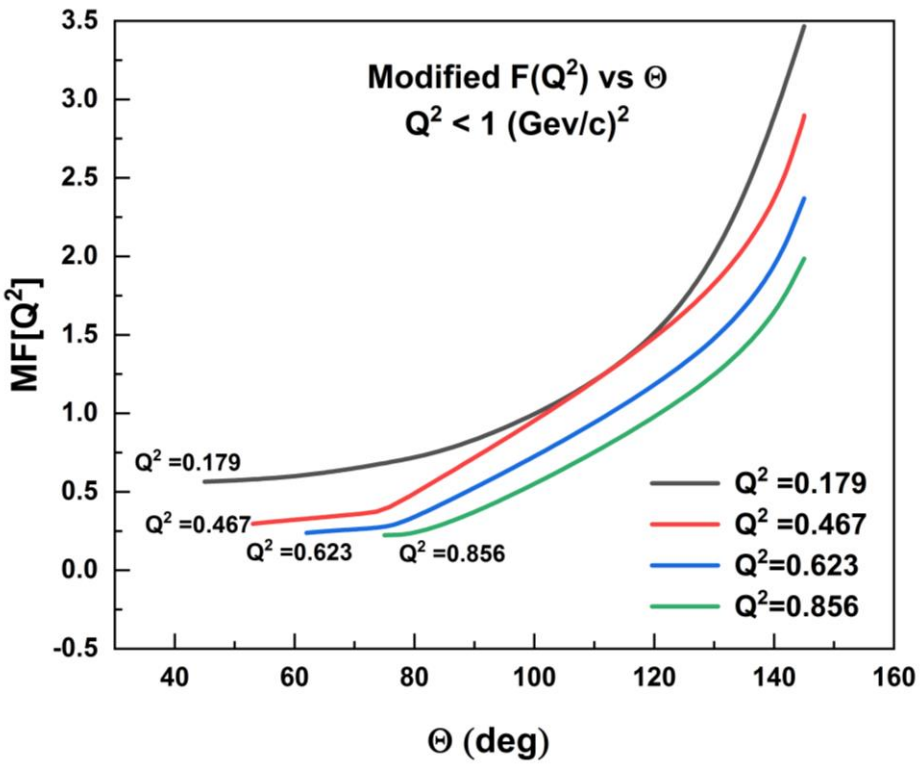

Figure 4.5 : Modified factor dependence on scattering angles at different Q^2.

Table 4.1: Modified Factor for Low Q^2 (Forward and backward angles) and for relative high values of Q^2.

At small values of Q^2				Relative high values of Q2	
Q^2 $[Gev/c]^2$	$MF(Q^2)$ for $\theta \leq 90^o$	Q^2 $[Gev/c]^2$	$MF(Q^2)$ for $\theta > 90^o$	Q^2 $[Gev/c]^2$	$MF(Q^2)$
0.1555	0.7317	0.1794	2.2850	1.0002	0.0807
0.1794	0.5888	0.1944	2.3842	1.0021	0.1972
0.1794	0.6782	0.2335	2.1720	1.1673	0.1536
0.1947	0.7199	0.2721	2.0532	1.1682	0.0626
0.2335	0.6105	0.2915	2.0730	1.4987	0.0356
0.2339	0.5407	0.2915	2.0633	1.5005	0.0354
0.2728	0.4903	0.2916	1.1874	1.5007	0.1004
0.2730	0.5709	0.3112	2.0157	1.7500	0.0325
0.2916	0.5387	0.3503	2.0169	1.7505	0.0239
0.2916	0.5344	0.3503	2.0062	1.7522	0.0259
0.2922	0.4631	0.3893	1.8897	1.7525	0.0752
0.2922	0.4652	0.3893	1.8791	1.9983	0.0186
0.3113	0.4235	0.3898	1.0924	2.0002	0.0177
0.3498	0.3909	0.4280	1.8572	2.0006	0.0578
0.3500	0.4738	0.5064	1.6301	2.0030	0.0254
0.3500	0.4698	0.5064	1.6194	2.3306	0.0120
0.3891	0.3714	0.5445	1.5681	2.3307	0.0430
0.3891	0.3734	0.5445	1.5574	2.4970	0.0149
0.3892	0.3018	0.5456	2.7220	2.5000	0.0146
0.3894	0.3005	0.5833	1.5261	2.5011	0.0101
0.3897	0.4402	0.5833	1.5155	2.7257	0.0093
0.3897	0.4364	0.6226	1.4197	2.8620	0.0073
0.3903	0.2859	0.6232	2.3693	2.9204	0.0069
0.4287	0.4103	0.6624	1.4475	3.0003	0.0230
0.4677	0.3771	0.7012	1.2655	3.0004	0.0062
0.4677	0.3735	0.7012	1.2552	3.0070	0.0089
0.4865	0.3537	0.7013	2.1170	3.2500	0.0074
0.5066	0.3381	0.7404	1.2747	3.5045	0.0047
0.5066	0.3347	0.7784	1.3589	3.7557	0.0032
0.5072	0.2175	0.7795	1.9435	3.8939	0.0036
0.5452	0.2690	0.8559	1.9852	4.0000	0.0040
0.5453	0.3116	0.8571	1.2409	4.4779	0.0023
0.5837	0.2935	1.0120	1.5126	5.0000	0.0022
0.5837	0.2905	1.0899	1.3124	5.0270	1.37E-03
0.5840	0.2618	1.1686	1.1518	5.0620	1.64E-03
0.5841	0.1800			5.0751	1.22E-03
0.5843	0.1951			7.3000	3.72E-04
0.5847	0.1799			9.6290	1.31E-04
0.6228	0.2697			9.9839	1.16E-04
0.6613	0.2653			11.9900	6.02E-05
0.6809	0.2667			15.7200	2.10E-05
0.7005	0.2582			19.4700	7.98E-06
0.7005	0.2553			23.2400	4.29E-06

In both directions, MF decreases with Q^2 and takes fraction values in the forward angles and is weakly dependent on θ. It suddenly increases to become greater than unity for the backward angles. The backward scattering is more sensitive to both Q^2 and θ. This process is hard elastic scattering and strongly affected by the internal proton constituents. It may be explained by considering that the two scattering patterns for both forward and backward directions have limited criteria namely, small values of Q^2, and long wavelength for the incident electron wave compared to proton radius r_p. These observations prove that there are different kinematics for elastic scattering process according to the impact parameter b. Firstly, at forward angles in which $b \geq r_p$, the center of scattering is located just outside the volume of the proton. Secondly, process produces scattering in backward angles at $b < r_p$, in which the scattering center is located inside the proton volume and sensitive to the internal constituent of proton. In both cases, the scattering electron can feel the proton as integrated particle say point-like or collected particle with homogenous distributions of mass, charge, and magnetization. The transfer momentum Q^2 is consumed in a form of limited excitation for proton constituents and proton still conserves its elastic components. At $Q^2 \approx 0$, it is suitable to investigate the properties of the initial phase of the nuclear materials and their constituents.

At relatively high values of Q^2, the magnitudes of MF are much lower than the corresponding values at low values of Q^2 and become strongly dependent on the scattering angle. This behavior is noticed before at the backward scattering for low Q^2. It may be acceptable due to suitable reasons in which the electron becomes more sensitive and affected by the electric and magnetic properties of internal contents of proton. It is possible to conclude that for both

backward scattering at low Q^2 and all angles at high Q^2 the electron becomes strongly affected by the electric and magnetic fields that are produced from the internal proton constituents. The effect of these fields increases with Q^2 and it becomes the experimental tool to discover the internal constituents of the proton. The variation of MF with different Q^2 at range $Q^2 > 1$ $(GeV/c)^2$ is shown in figure (4.6).

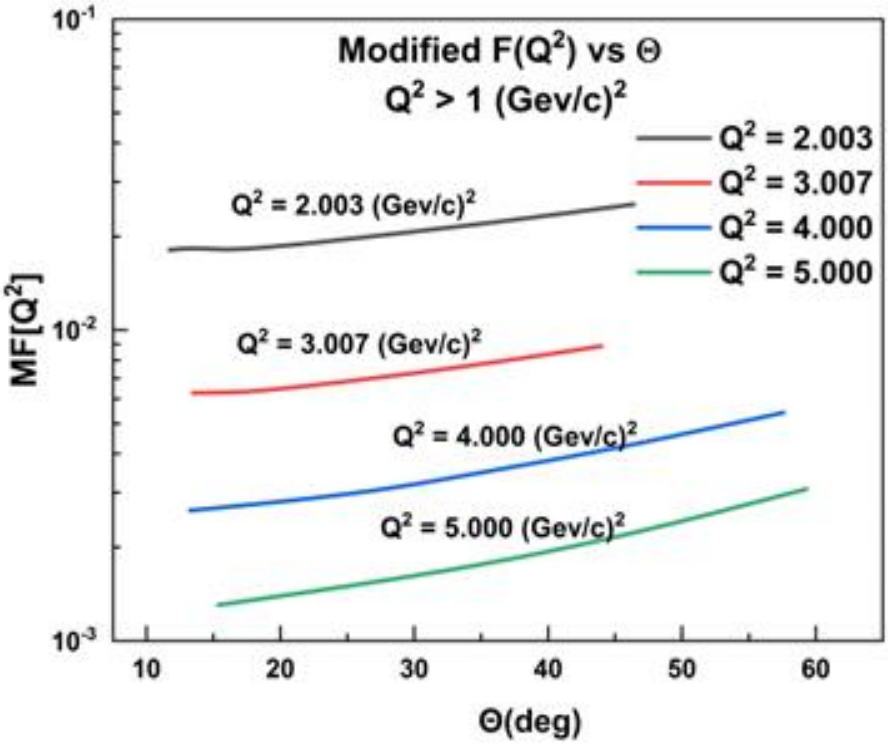

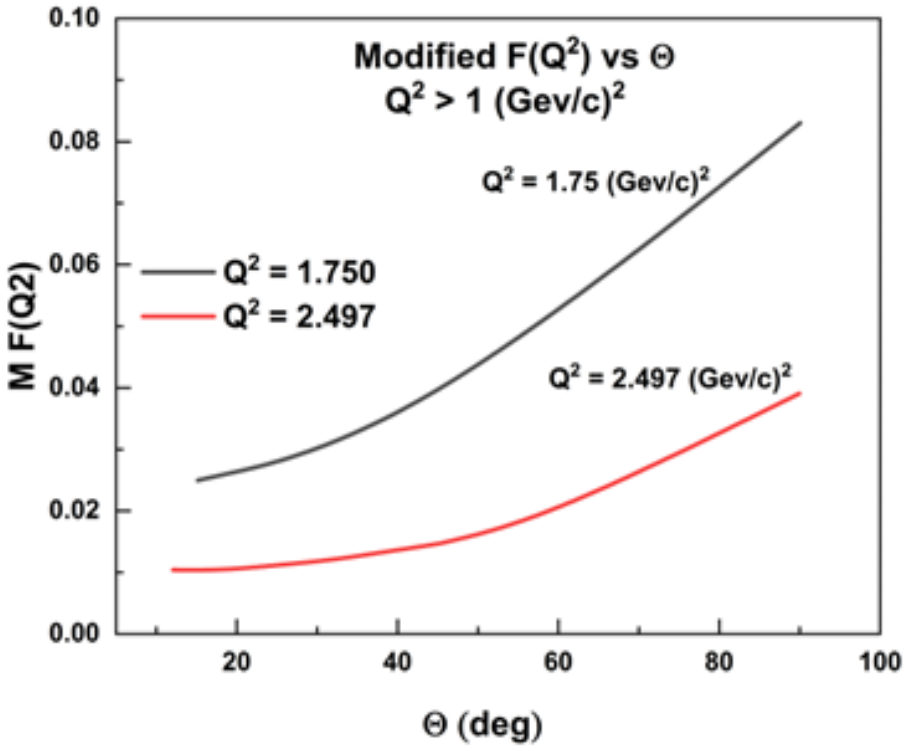

Figure 4.6: Modified factor dependence on Q^2 and angles of scattering.

It is very clear from the above figures that the Modified factor must be introduced to match the experimental measurements with theoretical predictions. Elastic scattering of electrons from protons reveals information about the distribution of the charge and the magnetism. In general, proton static properties, including mass, electric charge, and magnetic moment, have been measured precisely [16]. The fundamental electromagnetic properties of the proton are described by the dynamical physical quantities called electromagnetic form factors, which give information about the proton structure. It plays an important role in providing information about the volume of static proton and strong interaction of many body systems of quarks and gluon. One of the form factors is sensitive to the charge distribution in the proton $G_E(Q^2)$ and is called point-like electric form factor. The other is sensitive to distribution of the magnetization current, and the magnetic

moment of the proton $G_M(Q^2)$ and it is called point-like magnetic form factor. They are real-valued functions of the four-momentum transfer squared, $Q^2=-q^2 > 0$. These can be measured from elastic electron-proton scattering experiments. These factors provide valuable information on the nuclear material at states close to ground state of the internal nuclear materials that constituent of the proton. These form factors were determined by making Rosenbluth separations [17, 18] of cross-section results. Experimentally, the number of scattered electrons in a specific direction determines the form factor and then compares the results with the corresponding theoretical predictions. The equation (3.24) in chapter 3 which is called Rosenbluth formula includes this modification. This can be simplified to another form by introducing the electric form factor G_E and the magnetic form factor G_M to a new form.

$$\frac{d\sigma}{d\Omega} = \frac{\alpha^2}{4E^2 \sin^4\left(\frac{\theta}{2}\right)} \frac{E'}{E} \left(\frac{G_E^2 + \tau G_M^2}{(1+\tau)} \cos^2\left(\frac{\theta}{2}\right) + 2\tau G_M^2 \sin^2\left(\frac{\theta}{2}\right) \right) \quad (4.2)$$

Where $K_1 = \tau G_M^2$ and $K_2 = \frac{G_E^2 + \tau G_M^2}{(1+\tau)}$ and τ is Lorentz invariant quantity $\tau = \frac{Q^2}{4M_p^2}$. Here, a brief note on this equation is observed as a combination of multi-quantities. The first one is $\frac{\alpha^2}{4E^2 \sin^4\left(\frac{\theta}{2}\right)}$ which is called Rutherford cross-section and $\frac{E'}{E}$ due to recoiling of proton. The second two quantities are responsible for electromagnetic form factors, in which $2\tau G_M^2 \sin^2\left(\frac{\theta}{2}\right)$ is the magnetic term due to spin interaction while $\frac{G_E^2 + \tau G_M^2}{(1+\tau)} \cos^2\left(\frac{\theta}{2}\right)$ is responsible for electric and magnetic scattering.

4.2.3 Rosenbluth Separation Method

In this section, it will be illustrated the method of separation of the Rosenbluth equation to get the electric form factor G_E and the magnetic form factor G_M separately. It shows the dependence of both factors on a wide range of momentum transfer Q^2. In addition, it will be compared with other data for other co-workers.

$$\frac{d\sigma}{d\Omega} = \left(\frac{d\sigma}{d\Omega}\right)_{NS} \left\{ \frac{G_E^2(Q^2) + \tau G_M^2(Q^2)}{1+\tau} + 2\tau G_M^2(Q^2)\tan^2\left(\frac{\theta}{2}\right) \right\} \qquad (4.3)$$

Where $\left(\frac{d\sigma}{d\Omega}\right)_{NS}$ is the non-spin elastic cross-section is given as

$$\left(\frac{d\sigma}{d\Omega}\right)_{NS} = \frac{(\alpha\hbar c)^2\cos^2\left(\frac{\theta}{2}\right)}{4E^2\sin^4\left(\frac{\theta}{2}\right)\left[1+2\left(E/M_p\right)\sin^2\left(\frac{\theta}{2}\right)\right]} \qquad (4.4)$$
$$= \left(\frac{d\sigma}{d\Omega}\right)_{\text{Mott}} \frac{E'}{E}$$

In the one photon exchange approximation, the experimental un-polarized e-p differential cross-section can be written in the rest frame of the initial proton as

$$\frac{d\sigma}{d\Omega_e} = \sigma_{Mott} \frac{\tau G_M^2(Q^2) + \epsilon G_E^2(Q^2)}{\epsilon(1+\tau)} \qquad (4.5)$$

The elastic cross-section, $\frac{d\sigma}{d\Omega_e}$, is differential with respect to a single variable, chosen to be the scattered electron angle. And ϵ is the degree of virtual photon linear polarization where

$$\epsilon = \left[1 + 2(1+\tau)\tan^2\left(\frac{\theta}{2}\right)\right]^{-1}$$

and $$Q^2 = \frac{2ME^2(1-\cos\,\theta)}{M+E(1-\cos\,\theta)}$$

These two form factors encapsulate the elastic structure of the proton. The combination $\frac{\epsilon G_E^2}{\tau} + G_M^2$ appearing in equation (4.3) is often called the reduced cross-section σ_{red} defined by

$$\sigma_{red} = \left(\frac{\epsilon(1+\tau)}{\tau}\frac{E'}{E}\left(\frac{d\sigma}{d\Omega}\right)_e\right) / \left(\frac{d\sigma}{d\Omega}\right)_{Mott} \tag{4.6}$$

$$\sigma_{red} \equiv \frac{d\sigma}{d\Omega} \cdot \frac{\epsilon(1+\tau)}{\tau\sigma_{Mott}} \tag{4.7}$$

and is represented in a linear equation as

$$\sigma_{red} = \frac{\epsilon}{\tau} G_{E_p}^2(Q^2) + G_{Mp}^2(Q^2) \tag{4.8}$$

The reduced cross-section σ_{red} described in equation **(**4.8**)** is a function in both polarization ϵ and τ, which are related to the experimental kinematic parameters. Their values are obtained from experimental measurements [12, 14, 15, 19] at different values of Q^2 and shown in figure (4.7).

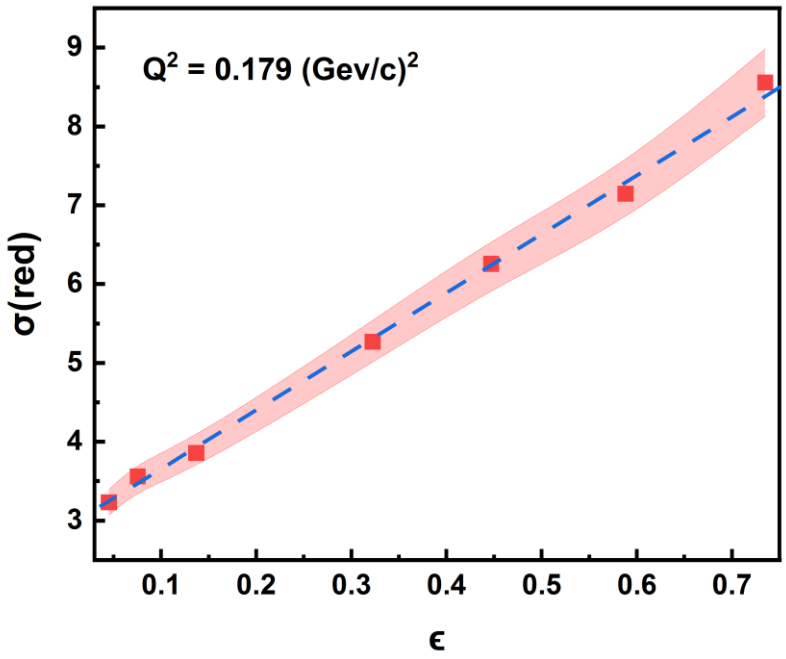
Q^2 = 0.179 (Gev/c)^2
σ(red)
ϵ
9
8
7
6
5
4
3
0.1
0.2
0.3
0.4
0.5
0.6
0.7

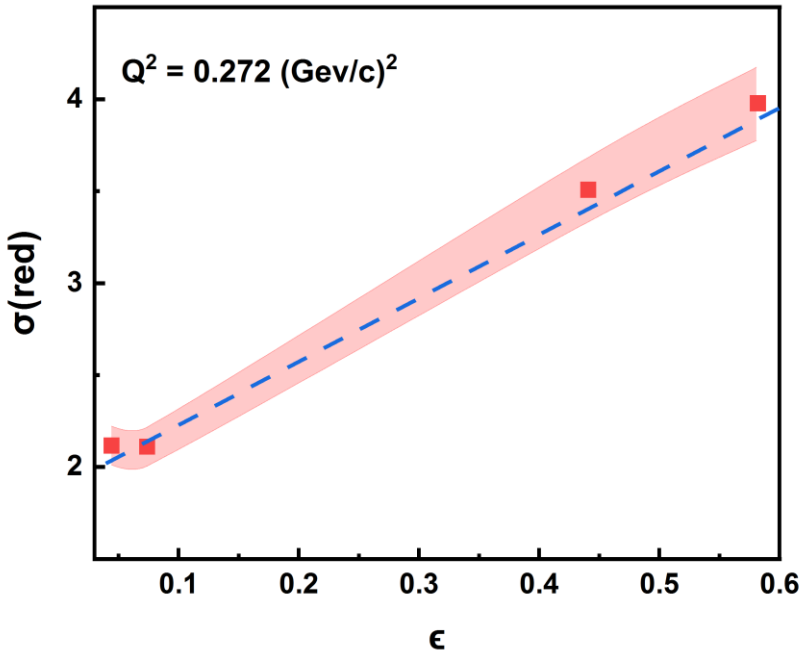
Q^2 = 0.272 (Gev/c)^2
σ(red)
ϵ
4
3
2
0.1
0.2
0.3
0.4
0.5
0.6

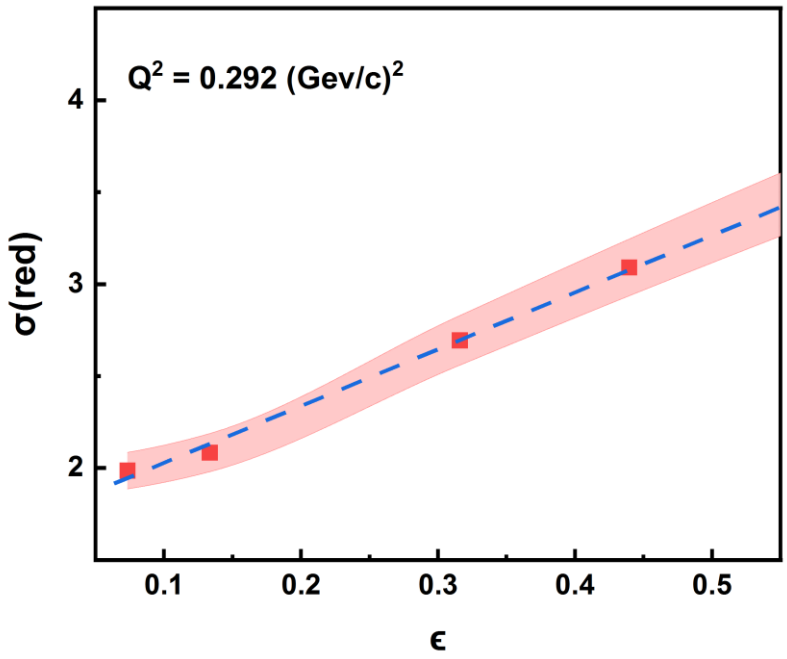
Q^2 = 0.292 (Gev/c)^2
σ(red)
ϵ
4
3
2
0.1
0.2
0.3
0.4
0.5

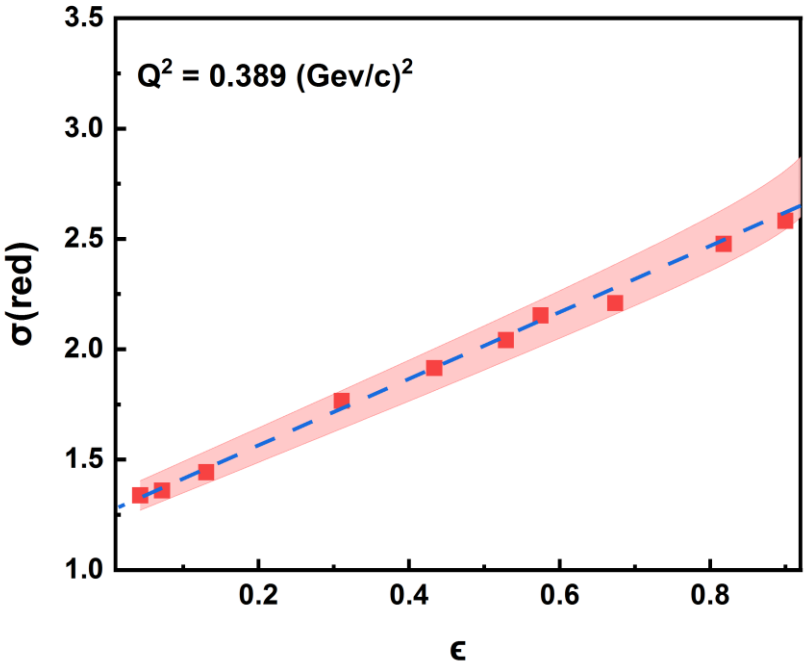
Q^2 = 0.389 (Gev/c)^2
σ(red)
ϵ
3.5
3.0
2.5
2.0
1.5
1.0
0.2
0.4
0.6
0.8

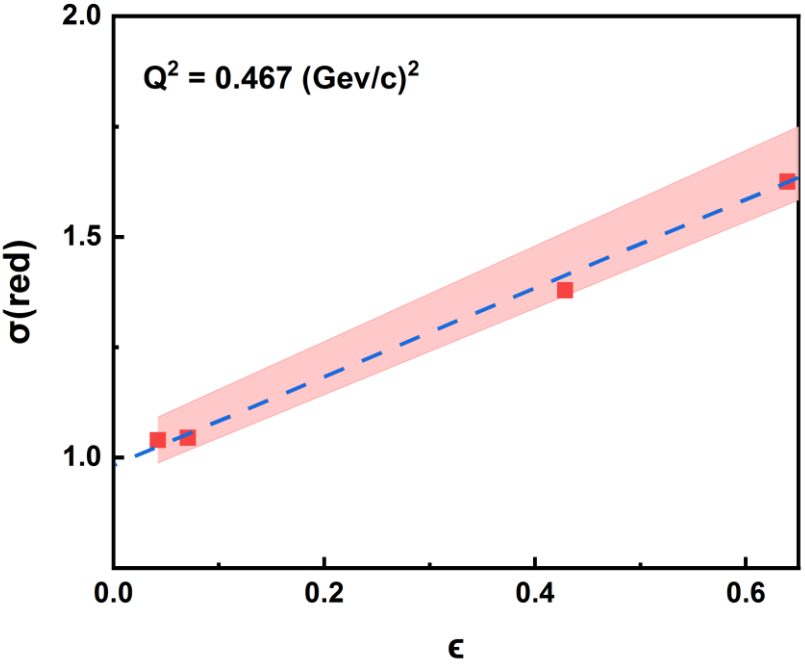
Q^2 = 0.467 (Gev/c)^2
σ(red)
ϵ
2.0
1.5
1.0
0.0
0.2
0.4
0.6

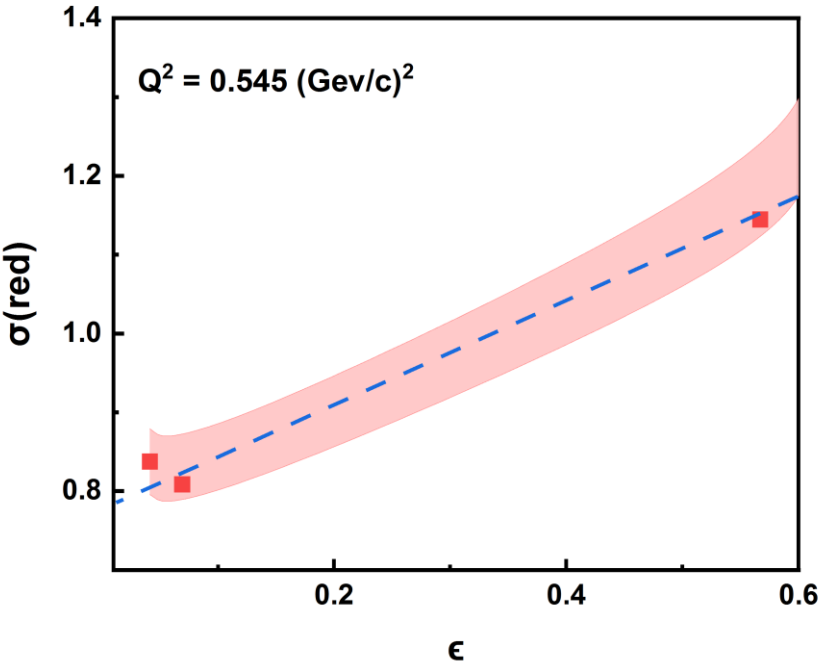
Q^2 = 0.545 (Gev/c)^2
σ(red)
ϵ
1.4
1.2
1.0
0.8
0.2
0.4
0.6

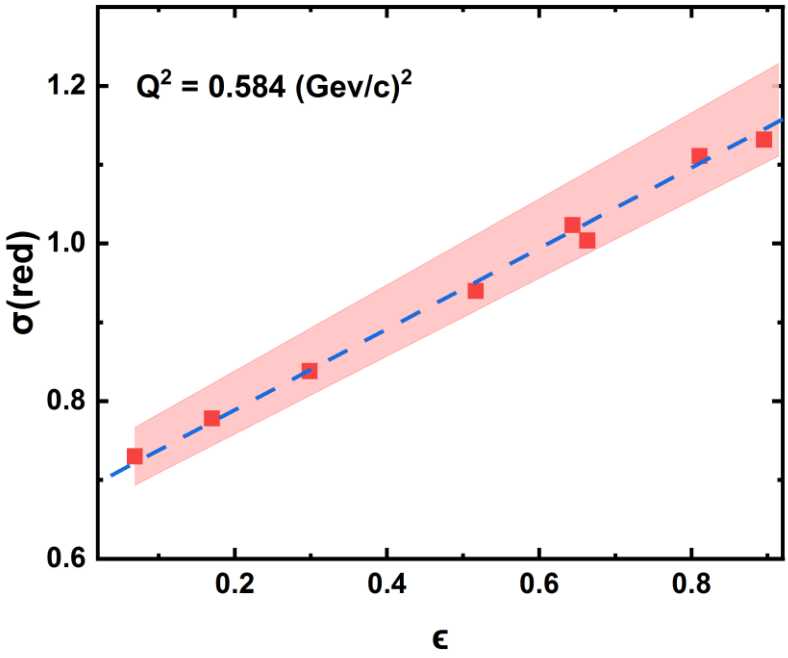
Q^2 = 0.584 (Gev/c)^2
σ(red)
ϵ
1.2
1.0
0.8
0.6
0.2
0.4
0.6
0.8

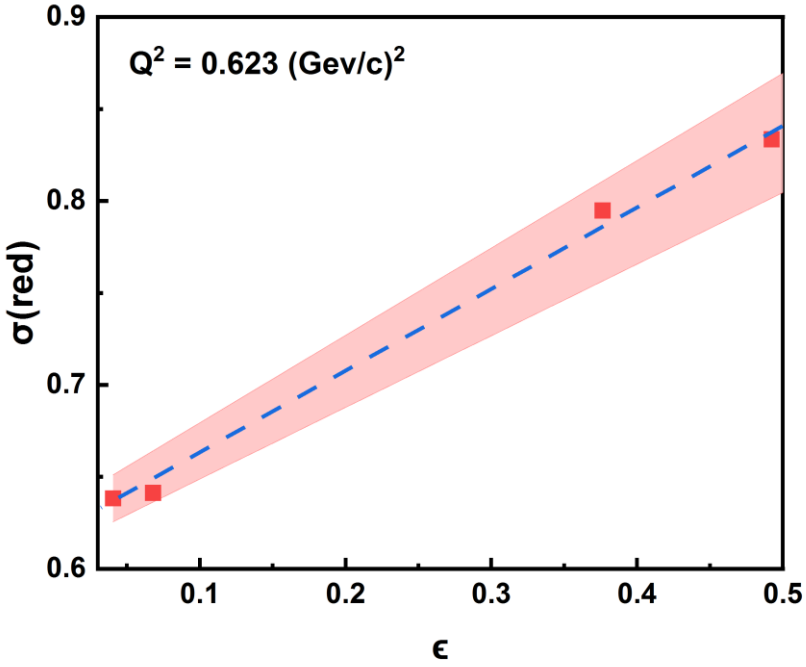
Q^2 = 0.623 (Gev/c)^2
σ(red)
ϵ
0.9
0.8
0.7
0.6
0.1
0.2
0.3
0.4
0.5

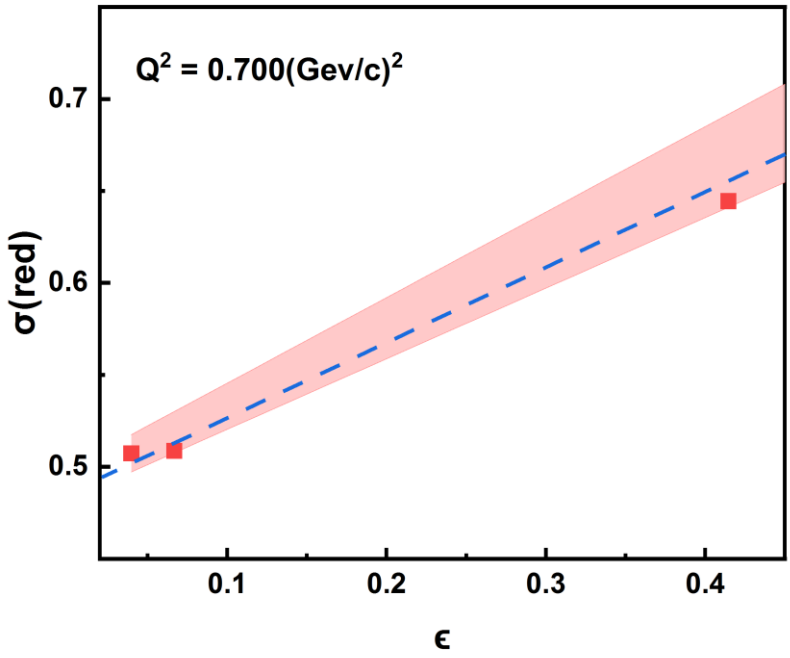
Q^2 = 0.700(Gev/c)^2
σ(red)
0.7
0.6
0.5
0.1
0.2
0.3
0.4
ϵ

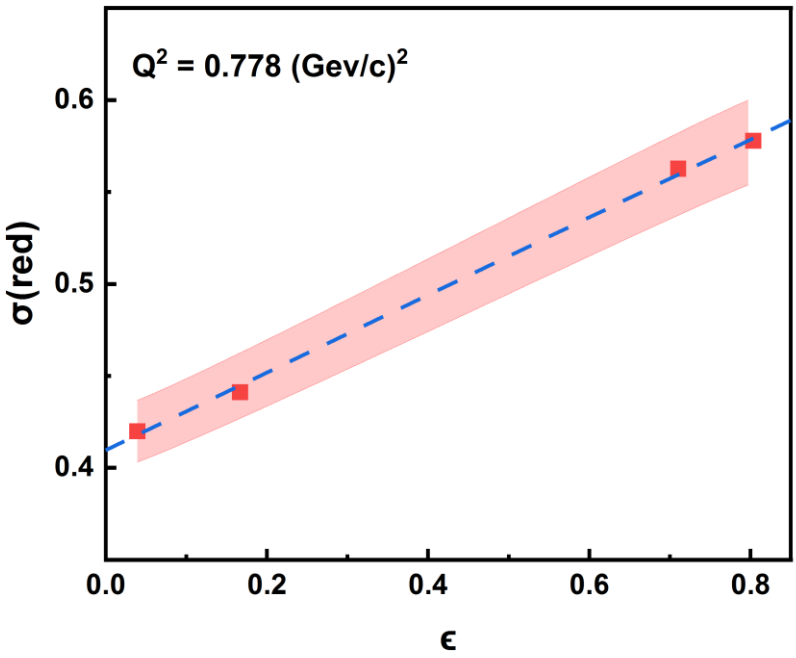
Q^2 = 0.778 (Gev/c)^2
σ(red)
0.6
0.5
0.4
0.0
0.2
0.4
0.6
0.8
ϵ

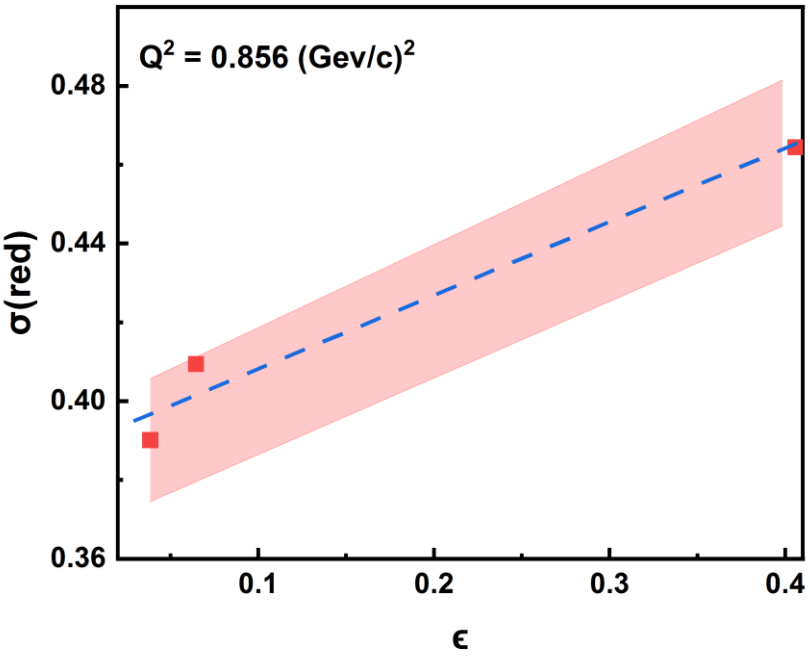
Q^2 = 0.856 (Gev/c)^2
0.48
0.44
0.40
0.36
σ(red)
0.1
0.2
0.3
0.4
ϵ

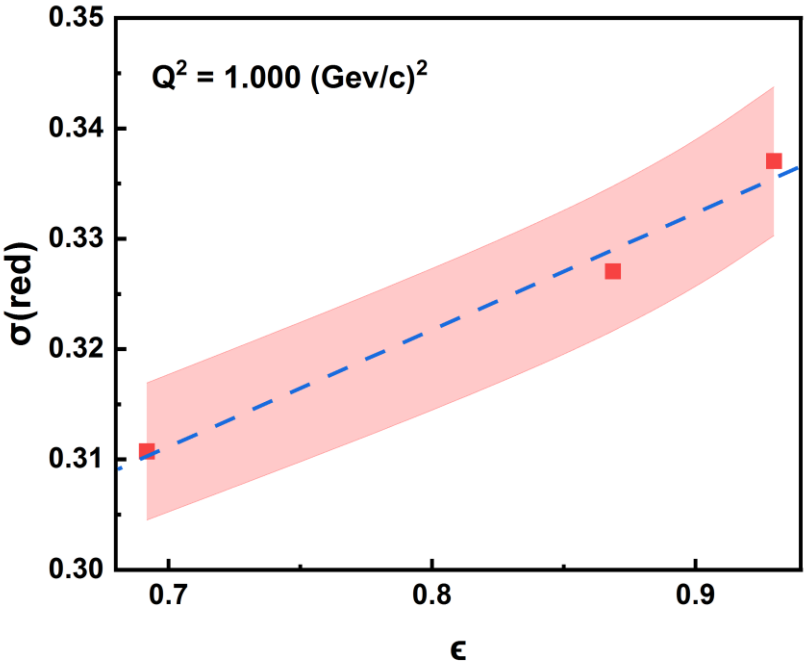
Q^2 = 1.000 (Gev/c)^2
0.35
0.34
0.33
0.32
0.31
0.30
σ(red)
0.7
0.8
0.9
ϵ

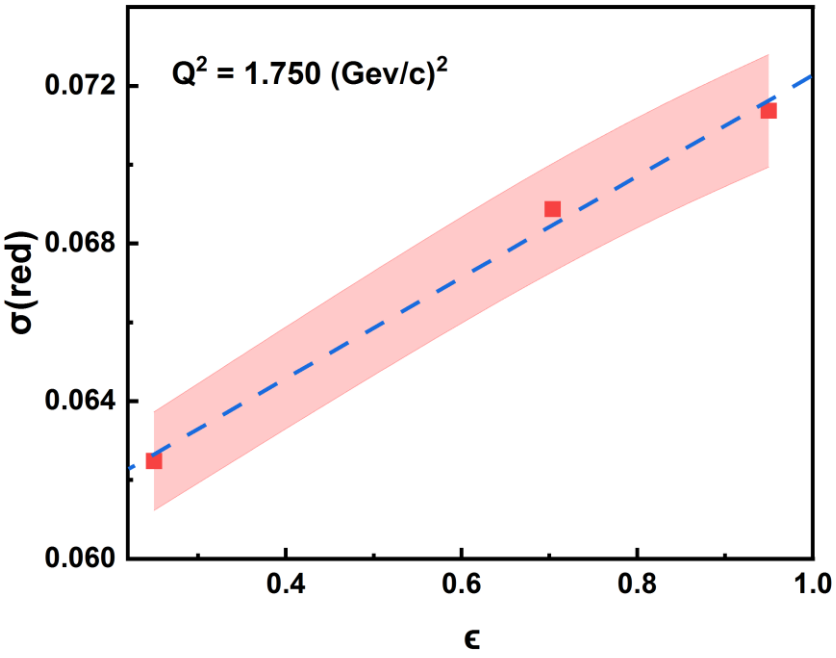
Q^2 = 1.750 (Gev/c)^2
0.072
0.068
0.064
0.060
σ(red)
0.4
0.6
0.8
1.0
ϵ

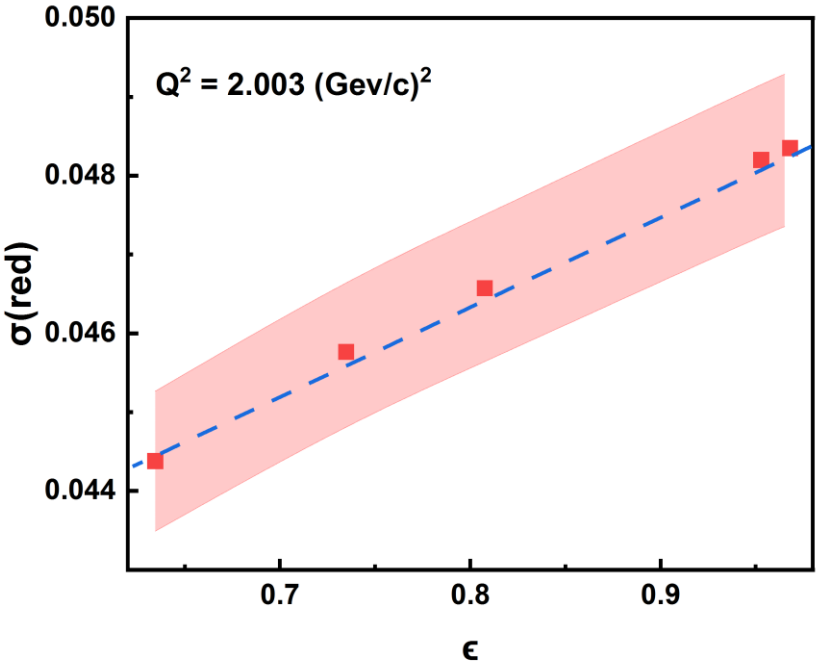
Q^2 = 2.003 (Gev/c)^2
0.050
0.048
0.046
0.044
σ(red)
0.7
0.8
0.9
ϵ

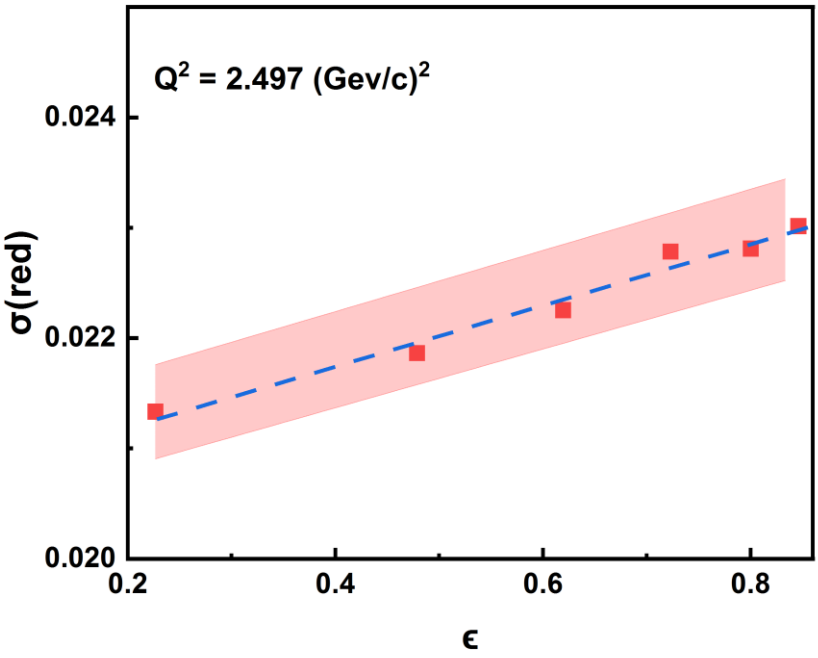
Q^2 = 2.497 (Gev/c)^2
0.024
0.022
0.020
σ(red)
0.2
0.4
0.6
0.8
ϵ

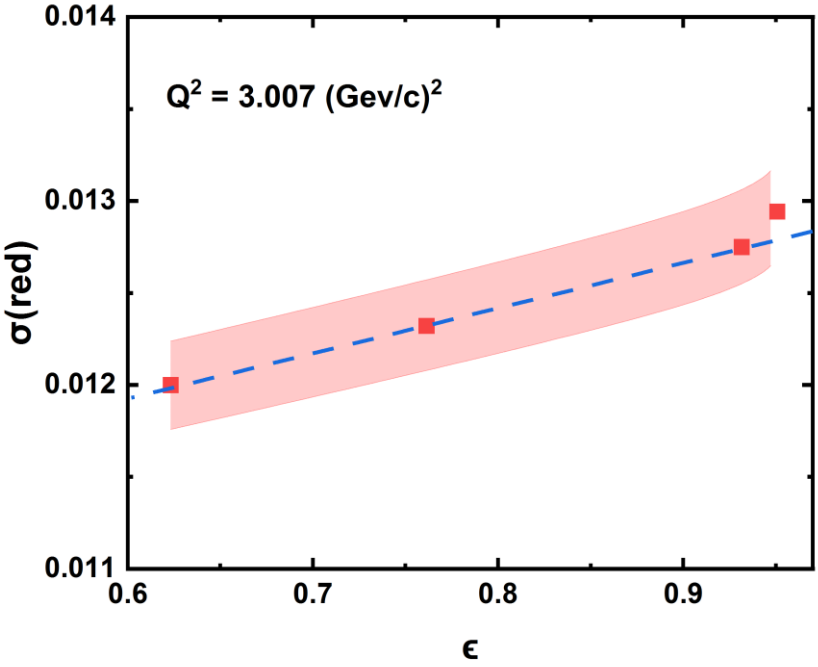
Q^2 = 3.007 (Gev/c)^2
0.014
0.013
0.012
0.011
σ(red)
0.6
0.7
0.8
0.9
ϵ

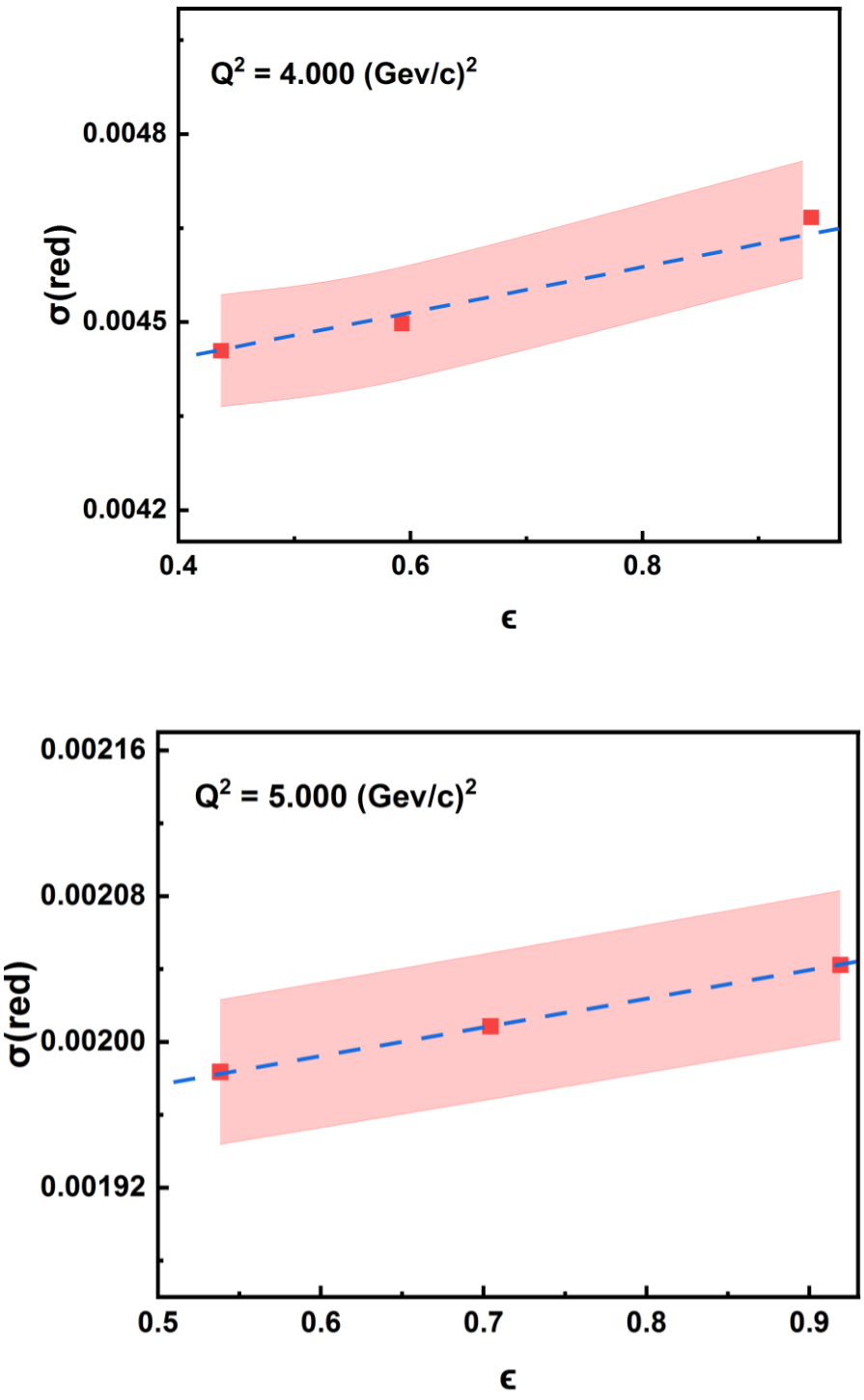

Figure 4.7 : Reduced cross-section σ_r at different polarization ϵ for different values of Q^2.

By varying beam energies and scattering angles, one can measure the reduced cross-section at a fixed values of Q^2, but for different values of ϵ [12, 14, 15, 19]. Then, performing a linear fit of these cross-section data as a function of ϵ, as shown in figure (4.8).

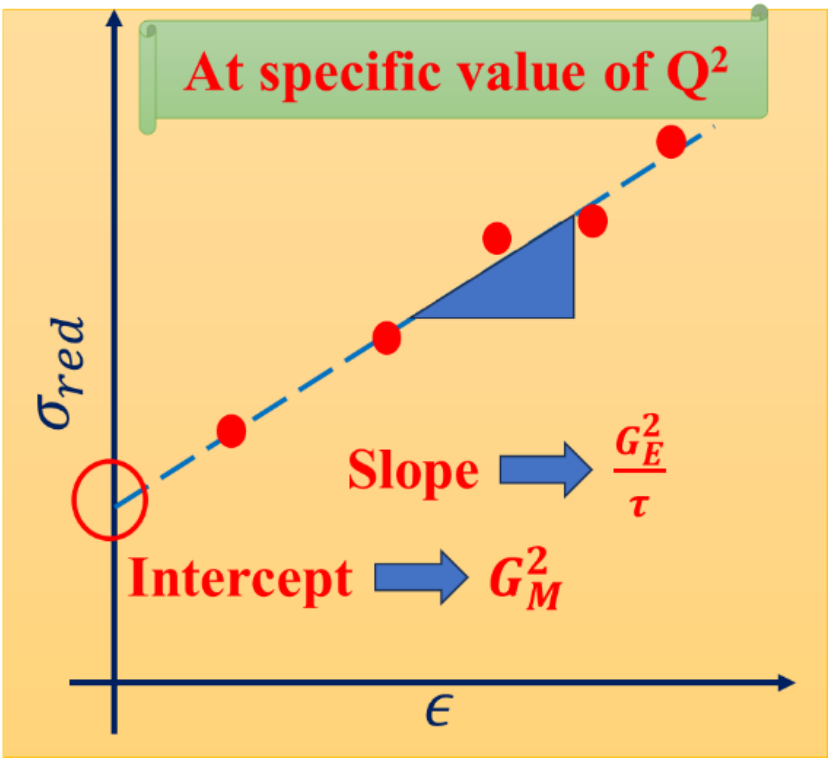

Figure 4-8 : Rosenbluth Separation Method

One can determine G_E^2/τ as the slope and $G^2{}_M$ as the intercept. The magnitudes of both the electric and the magnetic form factors are calculated for each value of Q^2. The data of this work is represented by star sign (*) in table 4.2 and is compared with the corresponding values from different groups given in reference[20]. These comparisons are shown in figure (4.9), and their values are given in table 4.2.

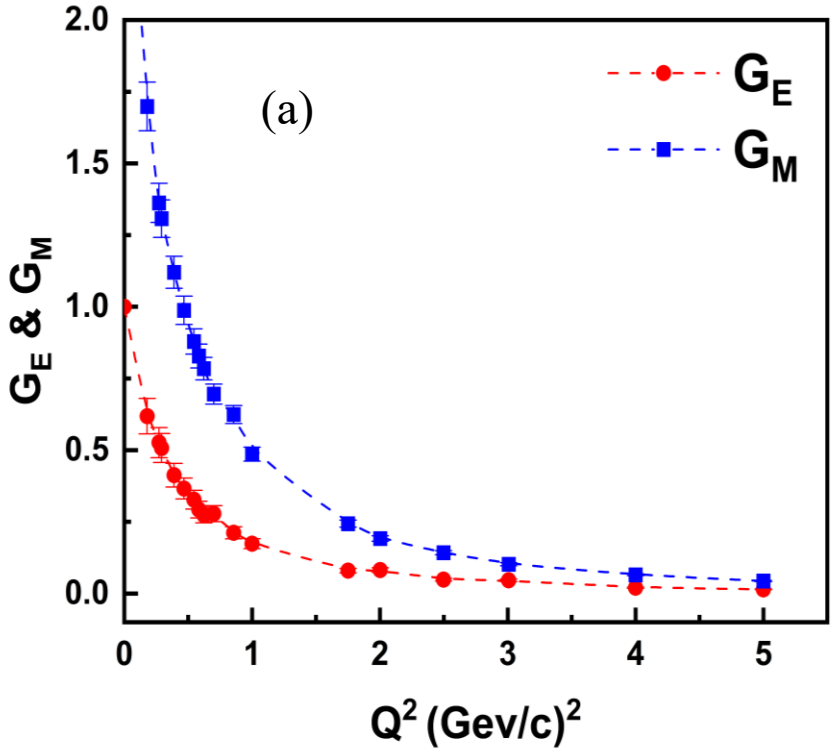
(a)
G_E
G_M
G_E & G_M
Q^2 (Gev/c)^2
2.0
1.5
1.0
0.5
0.0
0
1
2
3
4
5

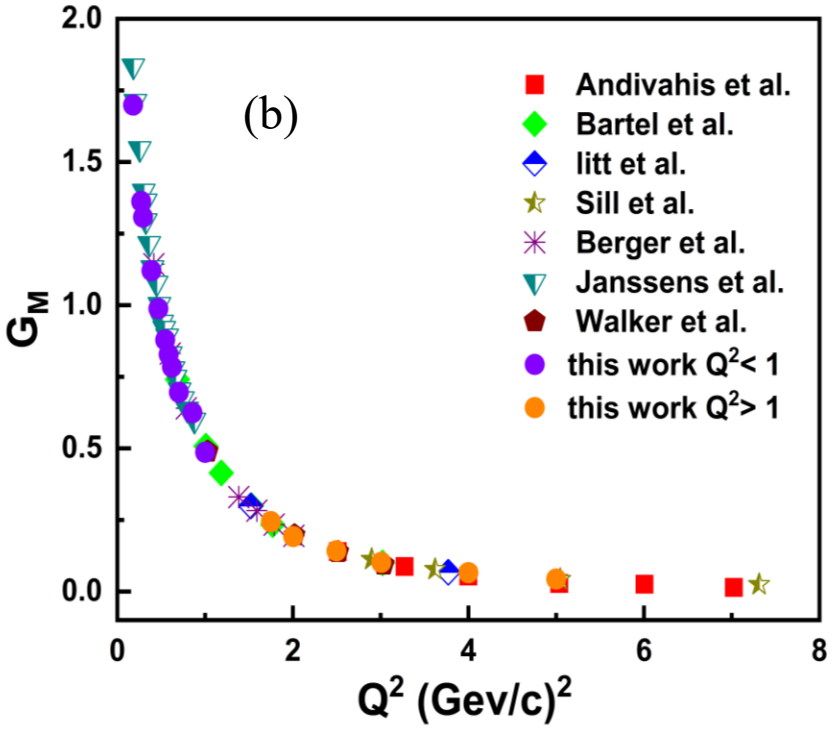
(b)
Andivahis et al.
Bartel et al.
litt et al.
Sill et al.
Berger et al.
Janssens et al.
Walker et al.
this work Q^2< 1
this work Q^2> 1
G_M
Q^2 (Gev/c)^2
2.0
1.5
1.0
0.5
0.0
0
2
4
6
8

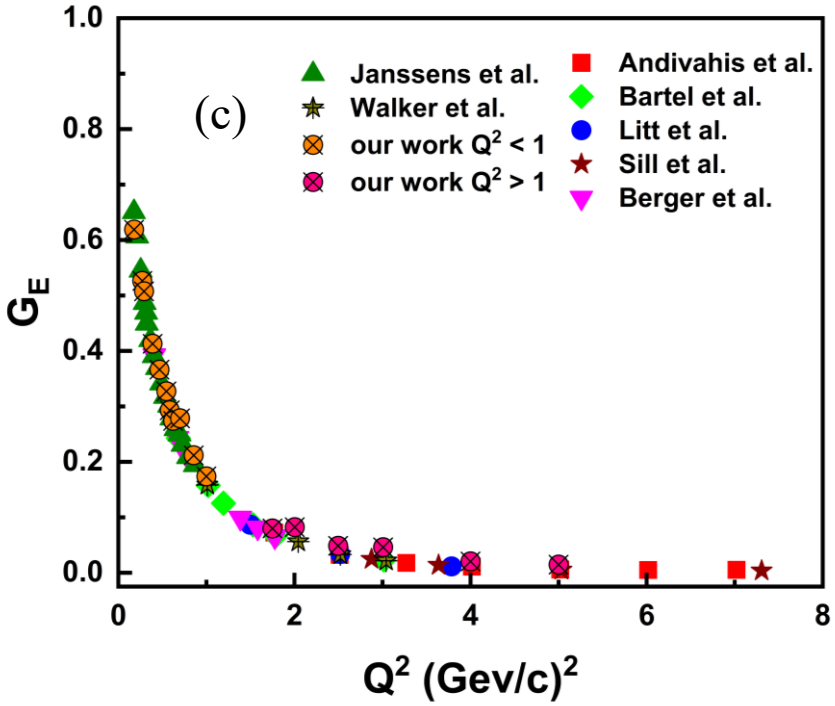

Figure 4.9: (a) Dependence of both electric and magnetic form factors on Q^2. (b) and (c) are for magnetic and electric form factors respectively compared with other references [20].

Table 4.2 : Values of electric and magnetic form factors with R-ratio at possible Q^2.

Q^2 (Gev/c)^2	G_E	G_M	R-ratio	Ref.
0.179	0.6187 ± 0.0309	1.6988 ± 0.0849	1.0162 ± 0.0508	*
	(0.6472± 0.0178)	(1.6317± 0.0532)	__	24
0.272	0.5262 ± 0.0263	1.3623 ± 0.0681	1.0776 ± 0.0539	*
	(0.4982± 0.0100)	(1.4147 ± 0.0116)	(0.9830 ±0.0140)	25
0.292	0.5074 ± 0.0254	1.3076 ± 0.0654	1.0827 ± 0.0541	*
	(0.5005± 0.0226)	(1.3041± 0.0336)	__	24
0.389	0.4129 ± 0.0206	1.1202 ± 0.0560	1.0283 ± 0.0514	*
	(0.4020± 0.0046)	(1.1542± 0.0093)	(0.9720 ±0.0170)	25
0.467	0.3662 ± 0.0183	0.9879 ± 0.0493	1.0344 ± 0.0517	*
	(0.3522± 0.0203)	(0.9777± 0.0212)	__	25
0.545	0.3273 ± 0.0164	0.8789 ± 0.0439	1.0390 ± 0.0519	*
	(0.3136± 0.0227)	(0.8742± 0.0196)	__	24
0.584	0.2929 ± 0.0146	0.8285 ± 0.0414	0.9865 ± 0.0493	*
	(0.2911± 0.0039)	(0.8458± 0.0058)	(0.9600 ±0.0160)	25
0.623	0.2738 ± 0.0137	0.7845 ± 0.0392	0.9738 ± 0.0487	*
0.701	0.2785 ± 0.0139	0.6958 ± 0.0348	1.1169 ± 0.0558	*
	(0.2723±0.0218)	(0.6925± 0.0155)	__	24
0.856	0.2118 ± 0.0106	0.6244 ± 0.0312	0.9467 ± 0.0473	*
1.000	0.1738 ± 0.0087	0.4863 ± 0.0243	0.9975 ± 0.0498	*
	(0.1710± 0.0044)	(0.4915± 0.0043)	(0.9710± 0.0260)	24
1.750	0.0799 ± 0.0039	0.2437 ± 0.0122	0.9157 ± 0.0458	*
	(0.0708± 0.0017)	(0.2523± 0.0010)	(0.7840 ±0.0200)	25
2.003	0.0821 ± 0.0041	0.1920 ± 0.0096	1.1935 ± 0.0596	*
2.497	0.0486 ± 0.0024	0.1425 ± 0.0071	0.9518 ± 0.0476	*

Continued table 4.2

Q^2 (Gev/c)^2	G_E	G_M	R-ratio	Ref.
	(0.0439 ±0.0016)	(0.1325±0.0019)	(0.9240±0.0349)	26
3.007	0.0461 ± 0.0023	0.1021 ± 0.0051	1.2600 ± 0.0630	*
4.000	0.0205 ± 0.0010	0.0655 ± 0.0033	0.8711 ± 0.0435	*
	(0.0245± 0.0019)	(0.0648± 0.0005)	(1.0580 ±0.0890)	24
	(0.0266±0.0017)	(0.0629±0.0009)	(1.1837±0.0787)	26
5.000	0.0148 ± 0.0007	0.0439 ± 0.0022	0.9467 ± 0.0473	*
	(0.0157± 0.0022)	(0.0436± 0.0009)	(1.0060± 0.1400)	24

It is noticed that at all given values of Q^2, the magnitudes of the magnetic form factor $G_M(Q^2)$ are higher in value than the corresponding value for the electric factor $G_E(Q^2)$. With increasing Q^2, the two factors decrease gradually. This is in good agreement with experimental data [21]. This behavior proves that all possible systems that describe the internal charge distribution of the proton are mostly dynamical. The calculations predicted by different research groups [20] are in good agreement and may be represented by a unified general curve within the given range of Q^2.

4.2.4 R-Ratio

The R-ratio is defined as the quantity of transverse to longitudinal polarizations and thus from the phase shift of the azimuthal scattering distribution of the experimental data. This ratio is useful for cross-section measurements. The electromagnetic form factor interest stems from the fact that changes of just a few percent in the nucleon form factors at low Q^2 have direct implications on our understanding of the nucleon structure [22, 23]. In

Born approximation the ratio R is related to the electromagnetic form factors by the equation:

$$R \equiv \mu_p \frac{G_E^P}{G_M^P} = -\mu_p \frac{E_e + E'_e}{2M} \tan\left(\frac{\theta}{2}\right) \frac{P_T}{P_L} \qquad (4.9)$$

where P_T and P_L are the recoil proton polarization transverse and longitudinal to the proton momentum. The magnitudes of R-ratio at different values of Q^2 and the corresponding values of G_E and G_M are also given in table 4.2 and its variation with Q^2 is shown in figure (4.10). The corresponding values from many references [24, 25]are shown in the same figure. In this work, most of extracted values of G_E and G_M at different values of Q^2 are agree with corresponding values calculated by different groups in Refs. [24, 26, 27] which used different tools of data analysis. Differences in the allowed region may be due to the errors of fitting parameters used in these tools.

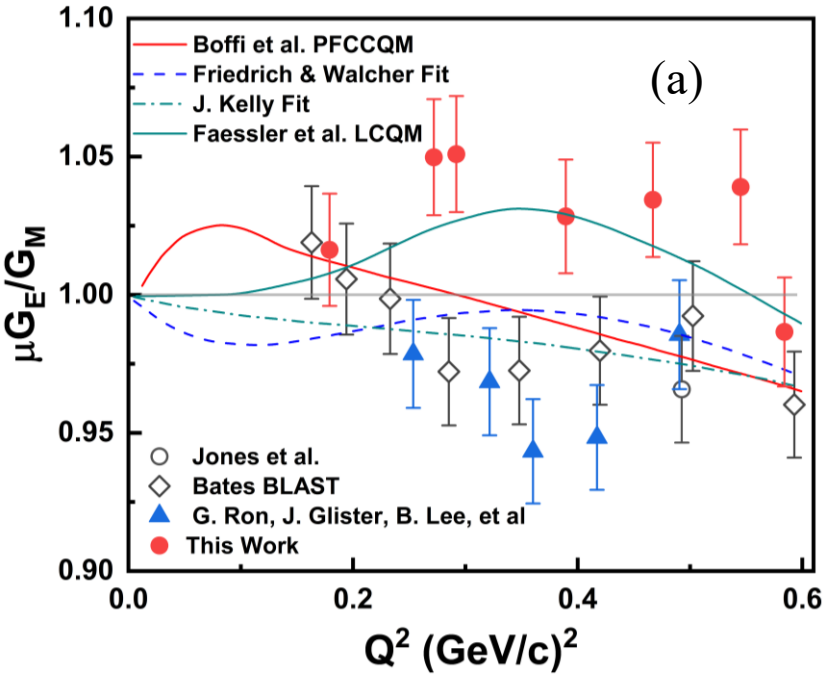

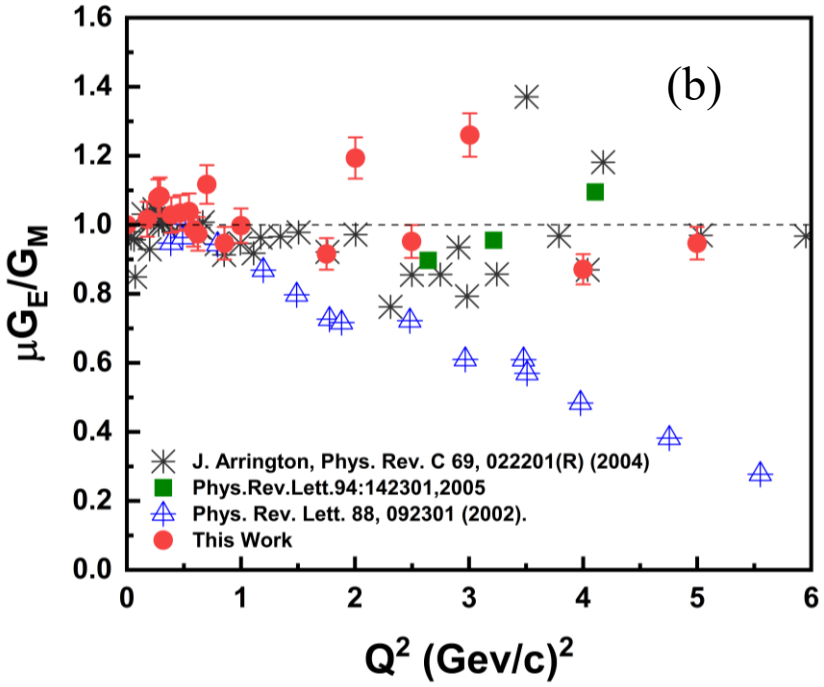

Figure 4.10 : Dependence of R-ratio on the electromagnetic form factors and Q^2 (a) at small values of Q^2 and (b) at relatively high-values of Q^2.

This dependence can be divided into two ranges. First, at low values of Q^2 up to 0.6 $(GeV/c)^2$ as shown in figure 4.10 (a) second, at high values up to 6 $(GeV/c)^2$ as shown in figure 4.10 (b). In the two ranges, the values of R-ratio are fluctuated around unity with acceptable range for all compared data. In figure 4.10 (a), the R-ratio becomes R>1, which means that the medium constituent of the proton is most parabolic toward electric form factor and inverted for high Q^2 (figure 4.10 b) towards the magnetic form factor. This indicates that a suitable nature of the medium inside proton, in which both electric and magnetic properties fluctuate at possible excitation energies. It proves that the medium in the ground state is mostly static constituents and directed dynamically with increasing the square momentum transfer [29].

4.2.5 Charge Proton Radius

Proton radius and volume are important quantities to describe the structure of hadrons. There are many experimental techniques used to measure the radius of proton, including *e–p* scattering[28]. Experimentally, the charge radius of the proton can be determined using two different techniques. First, is the measurements of electron–proton elastic scattering cross-sections. Second, is the high-resolution spectroscopy of the hydrogen atom. A decade ago, the precision of the atomic spectroscopy method was greatly improved using muonic hydrogen atoms, wherein the electron is replaced by a muon. However, the value of the proton radius disagreed with previous determinations, giving rise to the "proton-radius puzzle". Electric and magnetic form factors are associated with the hadronic matter distribution in hadron volume. So, there is good relationship between the volume of proton and electric and magnetic form factors especially at small values of Q^2. The root mean square radius of the elastically scattering hadrons can be calculated by the following relation [30]:

$$\langle r^2 \rangle = -\frac{6}{G(0)} \frac{\mathrm{d}G(Q^2)}{\mathrm{d}Q^2}\bigg|_{Q^2=0} \tag{4.10}$$

Therefore, the charge radius can be determined from the slope of the form factors dG_E/dQ^2 at $Q^2=0$. Previously it showed in figure 4.9 (a) the dependence of both the electric and the magnetic form factors on Q^2. This dependence is fitted to the following equation

$$G_{dipole}(Q^2) = \left[1 + \frac{Q^2}{0.71}\right]^{-2} \tag{4.11}$$

This equation is described up to 10 (Gev/c)^2 by the dipole approximation expression and its derivative with respect to Q^2 is

$$\frac{dG(Q^2)}{dQ^2} = \frac{-2.8169}{[1 + 1.4084\ Q^2]^{-3}} \tag{4.12}$$

Then it is applied when Q^2 tends to zero. In this analysis, the root mean square value of the scattering proton radius is calculated using equation (4.10), note that $1\ GeV/c\ =\ 5.068\ fm^{-1}$. The corresponding value of r_p is equal to 0.81±0.04 fm. The errors are obtained from the fitting parameters. The comparison of this value with the previous measurements at different techniques is shown in figure (4.11).

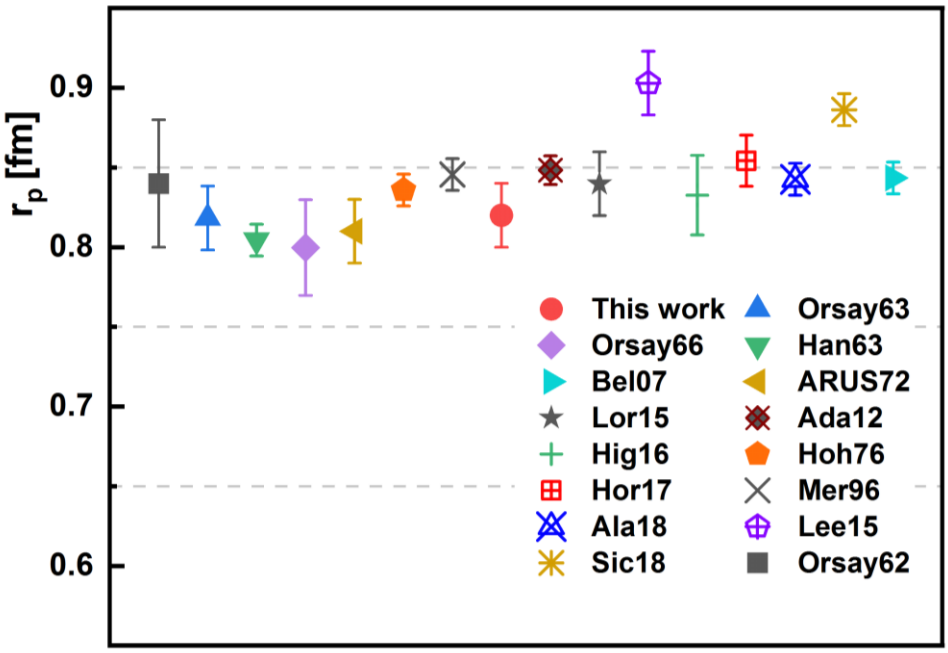

Figure 4.11: Proton radius from different theoretical and experimental procedures.

In figure 4.9(a), the slope of the form factors dG_E/dQ^2 at different values of Q^2 gives the possibility to calculate the radius at which the electron explores the proton and is responsible for scattering called radius of scattering r_s where

$r_s \leq r_p$. The root mean square value of the scattering radius can be derived from equations (4.10, 4.11 and 4.12) at different values of Q^2. The corresponding calculations of the scattering radius at each value of Q^2 are shown in figure (4.12). Its magnitudes are decreased with increasing the transfer square momentum in regular and continuous radius. It can be fitted by the exponential decay curve represented by the dash curve. There is similar dependence of the wavelength λ for photon which responsible for the energy carriers on Q^2 and may be fitted by similar exponential function but with different fitting parameters represented by dashed line in figure (4.12). The proton scattering area decreases with Q^2 and is simply represented in figure (4.13).

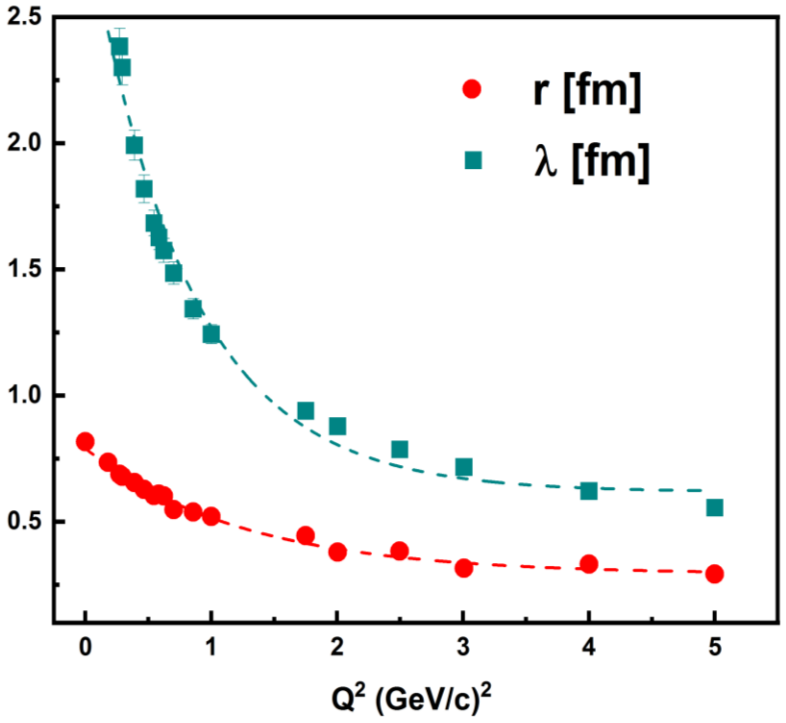

Figure 4.12: Variation of scattering radius and wavelength of photon with Q^2.

Figure 4.13: Scattering area decreases with increasing in Q^2.

It concludes that, with increasing Q^2, both scattering radius and the wavelength of the photon are decreasing to allow the scattering process to take place from a single or group of constituents of the internal proton contents. This allows the production of the fine image of the internal proton structure and hence discovering the physical properties of its constituents. The resolution of the resulting image increases with the increase in Q^2, and this leads to discovering the nature of the initial nuclear material in its primitive phase.

CONCLUSION

This thesis studies the physical properties of nuclear materials which are the main constituents of hadron like proton. Electron-proton scattering can satisfy this aim, and the following conclusion can be summarized as:

1. There are two mechanisms of electron scattering off proton, one of them is in a forward direction where $\theta \leq 90°$ and the other is backward $\theta > 90°$. This is explained by considering scattering in the forward due to a single point-like particle in which the impact parameter is greater than the proton radius. Scattering in backward direction is explained due to internal components of the proton where impact parameter is less than the proton radius.

2. Two ranges of momentum transfer Q^2 are investigated. First, at low $Q^2 < 1\ (GeV/c)^2$, there are two mechanisms are found (forward and backward). Second, at high $Q^2 > 1\ (GeV/c)^2$ the forward scattering only is found.

3. There is a regular spacing between theoretical cross-section (Mott Formula) and experimental data for all ranges of momentum transfer Q^2.

4. Modified Factor (MF) is added to Mott formula to make an agreement between theoretical prediction and experimental data.

5. This MF is explained as the electric and magnetic form factors which describes the charge distribution and magnetization distribution of the proton components.

6. Electric and magnetic form factors G_E, G_M are calculated from reduced cross-section σ_r by using Rosenbluth separation method and agree with other theoretical techniques. They depend on the angle of scattering and values of momentum-transfer.

7. At low values of momentum transfer, the majority of these factors are for electric rather than magnetic. It proves that the medium in (or near) the ground state is mostly static constituents and becomes dynamically with increasing the momentum transfer. At $Q^2 \approx 0$, it is suitable to investigate the properties of the initial phase of the nuclear materials and their constituents.

8. The charge radius of the proton is calculated to be $r_p \approx 0.81\ fm$ and it is found to be acceptable with the previous measurements at different techniques.

9. The scattering radius is also calculated and is found to be as an exponential decay with momentum transfer.

10. The photon wavelength is decreasing with increasing Q^2. It allows giving a fine image of proton components and increases the possibility of scanning proton constituents.

These points are concluded to investigate the physical properties of the initial phase of nuclear matter, which are the main constituents of hadrons like proton. Quantum electro-dynamic theory gives a reasonable description for electron-proton scattering and gives quantitative formula for elastic cross-section. At low-values of momentum transfer, the scattering process is explained by considering proton is a single point-like particle, while at high-

values, scattering is due to the components of proton constituents. Comparison with experimental data shows regular spacings which require an additional modified factor MF must be added to introduce good agreement with experimental results. These MFs depend on both the angle of scattering and the four-momentum transfer. The obtained values of electric and magnetic form factors agree with the different values that obtained by other theoretical techniques. The charged proton radius is found to be 0.81±0.04 fm, which is the upper limit of the scattering radius. Finally, the scattering radius and the wavelength of the photon decrease with increasing Q^2 at which the electron can scope the fine constituents of the internal structure of the proton.

REFERENCES

[1] K. S. Krane, J. Wiley, N. York, C. Brisbane, and T. Singapore, *Introductory Nuclear Physics*, 1988.

[2] F. Francis Halzen and A. D. Alan D. Martin, *Quarks and leptons: an introductory course in modern particle physics*, 1984.

[3] B. (Bogdan) Povh and M. J. Lavelle, *Particles and nuclei: an introduction to the physical concepts*. Springer, 2008.

[4] D. Griffiths, *Introduction to Elementary Particles*, 2004.

[5] UC Santa Barbara, "scattering cross-section." Accessed: Jun. 18, 2024. [Online]. Available: https://web.physics.ucsb.edu/~fratus/phys103/LN/Scattering.pdf

[6] Corina Andreoiu, "Rutherford scattering Introduction to Nuclear Science," 2011. Accessed: Jun. 18, 2024. [Online]. Available: https://web-docs.gsi.de/~wolle/TELEKOLLEG/KERN/LECTURE/Fraser/L22.pdf

[7] D. J. Griffiths and D. F. Schroeter, "Introduction to Quantum Mechanics.", 3rd edition, 2018.

[8] University of Gothenburg, "The Dirac Equation and Spinors." Accessed: Jun. 18, 2024. [Online]. Available: https://physics.gu.se/~tfkhj/TOPO/DiracEquation.pdf

[9] A. M. Abdalla, A. M. Eltanany, and A. Saber, "Electromagnetic form factors at low energy elastic electron–proton scattering," *International Journal of Modern Physics E*, vol. 32, no. 12, Dec. 2023. doi: 10.1142/S0218301323500623.

[10] S. Pacetti and E. Tomasi-Gustafsson, "Sensitivity of the elastic electron–proton cross-section to the proton radius," *The European Physical Journal A*, vol. 56, no. 3, p. 74, 2020. doi: 10.1140/epja/s10050-020-00076-1.

[11] R. Nave, "Hyperphysics. Retrieved June 17, 2024, from http://hyperphysics.phy-astr.gsu.edu/hphys.html." Accessed: Jun. 17,

2024. [Online].
Available: http://hyperphysics.phy-astr.gsu.edu/hphys.html

[12] T. Janssens, R. Hofstadter, E. B. Hughes, and M. R. Yearian, "Proton Form Factors from Elastic Electron-Proton Scattering," *Physical Review*, vol. 142, no. 4, pp. 922–931, Feb. 1966.
doi: 10.1103/PhysRev.142.922.

[13] X. Zhan *et al.*, "High-precision measurement of the proton elastic form factor ratio $\mu_p G_E/G_M$ at low Q^2," *Physics Letters B*, vol. 705, no. 1, pp. 59–64, 2011.
doi: https://doi.org/10.1016/j.physletb.2011.10.002.

[14] W. Bartel *et al.*, "Measurement of proton and neutron electromagnetic form factors at squared four-momentum transfers up to 3 $(GeV/c)^2$," *Nucl Phys B*, vol. 58, no. 2, pp. 429–475, Jul. 1973 doi: 10.1016/0550-3213(73)90594-4.

[15] L. Clogher, "A Precise Measurement of the Proton Elastic Form Factors for $1.75 \leq Q^2 \leq 8.83$ $(GeV/c)^2$.", PhD thesis, 1993.

[16] M. Kohl, "EM Form Factors and OLYMPUS," *EPJ Web Conf*, vol. 81, p. 01006, Nov. 2014, doi: 10.1051/epjconf/20148101006.

[17] M. N. Rosenbluth, "High Energy Elastic Scattering of Electrons on Protons," *Physical Review*, vol. 79, no. 4, pp. 615–619, Aug. 1950. doi: 10.1103/PhysRev.79.615.

[18] J. Arrington, "Evidence for two-photon exchange contributions in electron-proton and positron-proton elastic scattering," *Phys Rev C*, vol. 69, no. 3, p. 032201, Mar. 2004, doi: 10.1103/PhysRevC.69.032201.

[19] A. F. Sill *et al.*, "Measurements of Elastic Electron-Proton Scattering at Large Momentum Transfer*," 1993.

[20] E. Santopinto, A. Vassallo, M. M. Giannini, and M. De Sanctis, "High Q^2 behavior of the electromagnetic form factors in the relativistic hypercentral constituent quark model," *Phys Rev C*, vol. 82, no. 6, p. 065204, Dec. 2010, doi: 10.1103/PhysRevC.82.065204.

[21] J. Arrington, K. De Jager, and C. F. Perdrisat, "Nucleon form factors - A Jefferson Lab perspective," in *Journal of Physics: Conference Series*, Institute of Physics Publishing, 2011. doi: 10.1088/1742-6596/299/1/012002.

[22] C. Adamuscin, S. Dubnicka, and A. Z. Dubnickova, "New value of the proton charge root mean square radius," *Prog Part Nucl Phys*, vol. 67, no. 2, pp. 479–485, Apr. 2012. doi: 10.1016/j.ppnp.2012.01.014.

[23] A. Akhiezer and M. P. Rekalo, "Dokl. AN USSR J. Part. Nucl, 4, 277".

[24] I. A. Qattan *et al.*, "Precision Rosenbluth Measurement of the Proton Elastic Form Factors," *Phys Rev Lett*, vol. 94, no. 14, p. 142301, Apr. 2005. doi: 10.1103/PhysRevLett.94.142301.

[25] G. Ron *et al.*, "Measurements of the Proton Elastic-Form-Factor Ratio at Low Momentum Transfer," *Phys Rev Lett*, vol. 99, no. 20, p. 202002, Nov. 2007. doi: 10.1103/PhysRevLett.99.202002.

[26] R. C. Walker *et al.*, "Measurements of the proton elastic form factors for $1 \leq Q^2 \leq 3$ $(\mathrm{GeV/c})^2$ at SLAC," *Physical Review D*, vol. 49, no. 11, pp. 5671–5689, Jun. 1994. doi: 10.1103/PhysRevD.49.5671.

[27] J. Arrington, W. Melnitchouk, and J. A. Tjon, "Global analysis of proton elastic form factor data with two-photon exchange corrections," Jul. 2007, doi: 10.1103/PhysRevC.76.035205.

[28] J.-P. Karr, D. Marchand, and E. Voutier, "The proton size," *Nature Reviews Physics*, vol. 2, no. 11, pp. 601–614, Sep. 2020. doi: 10.1038/s42254-020-0229-x.

[29] M. V Galynskii and E. A. Kuraev, "On the physical meaning of Sachs form factors and on the violation of the dipole dependence of G_E and G_M on Q^2," JETP Lett, vol. 96, no. 1, pp. 6–12, 2012,

doi: 10.1134/S0021364012130061.

[30] A. Bernauer et al., “Electric and magnetic form factors of the proton,” Phys Rev C, vol. 90, no. 1, p. 15206, Jul. 2014,

doi: 10.1103/PhysRevC.90.015206.

APPENDIX A

Before starting in explaining Casmir's trick, we introduced some notes about Dirac equation and its solutions. It is found that free electrons and positrons of momentum p = (E/c, p), with $E = \sqrt{m^2c^2 + p^2c^2}$, are represented by the wave functions

For Electrons

$$\psi(x) = ae^{-(i/\hbar)p\cdot x}u^{(s)}(p) \tag{A.1}$$

and positrons

$$\psi(x) = ae^{(i/\hbar)p\cdot x}v^{(s)}(p) \tag{A.2}$$

where s takes possible values as s = 1, 2 for the two spin states. The spinors $u^{(s)}$ and $v^{(s)}$ for particle and antiparticle respectively are satisfied the four momentum-space Dirac equations:

$$(\gamma^\mu p_\mu - mc)u = 0 \qquad \text{and} \qquad (\gamma^\mu p_\mu + mc)v = 0$$

and their adjoints, $\bar{u} = u^\dagger\gamma^0, \bar{v} = v^\dagger\gamma^0$, satisfy.

$$\bar{u}(\gamma^\mu p_\mu - \mathrm{mc}) = 0 \qquad and \qquad \bar{v}(\gamma^\mu p_\mu + \mathrm{mc}) = 0$$

They are orthogonal,

$$\bar{u}^{(1)}u^{(2)} = 0 \qquad \text{and} \qquad \bar{v}^{(1)}v^{(2)} = 0$$

normalized,

$$\bar{u}u = 2\mathrm{mc} \qquad \text{and} \qquad \bar{v}v = -2\mathrm{mc}$$

and complete, in the sense that

$$\sum_{s=1,2} u^{(s)}\bar{u}^{(s)} = \left(\gamma^{\mu}p_{\mu} + mc\right) \tag{A.3}$$

$$\sum_{s=1,2} v^{(s)}\bar{v}^{(s)} = \left(\gamma^{\mu}p_{\mu} - mc\right) \tag{A.4}$$

Meanwhile, a free photon of momentum p = (E/c, p), with $E = |p|c$ is represented by the wave function of Photons.

$$A^{\mu}(x) = ae^{-(i/\hbar)p\cdot x}\epsilon^{\mu}_{(s)} \tag{A.5}$$

where s = 1, 2 for the two spin states is replaced and represents two states of polarizations of the photon. The polarization vectors $\epsilon^{\mu}_{(s)}$ satisfy the momentum space Lorentz condition:

$$\epsilon^{\mu}p_{\mu} = 0$$

They are orthogonal, in the sense that.

$$\epsilon^{\mu*}_{(1)}\epsilon_{\mu(2)} = 0$$

And normalized.

$$\epsilon^{\mu*}\epsilon_{\mu} = 1$$

In the Coulomb gauge

$$\epsilon^{0} = 0 \qquad and \qquad \epsilon.p = 0$$

and the polarization three-vectors obey the completeness relation.

$$\sum_{s=1,2} \left(\epsilon_{(s)}\right)_i \left(\epsilon^{*}_{(s)}\right)_j = \delta_{ij} - \hat{p}_i\hat{p}_j \tag{A.6}$$

In some experiments the incoming and outgoing electron (or positron) spins are specified, and the photon polarizations are given. If so, the next thing to do is insert the appropriate spinors and polarization vectors into the expression

and compute the matrix element $|\mathcal{M}|^2$, the quantity we need to determine cross-sections and lifetimes. More often, however, we are not interested in spins. A typical experiment starts out with a beam of particles whose spin orientations are random, and simply counts the number of particles scattered in a given direction. In this case the relevant cross-section is the average over all initial spin configurations, i, and the sum over all final spin configurations, f: In principle, $|\mathcal{M}(i \to f)|^2$

we could compute for every possible combination, and then do the summing and averaging:$\langle|\mathcal{M}|^2\rangle average\ over\ intial\ spins, sum\ over\ final\ spins, of$

$$|\mathcal{M}(i \to f)|^2$$

let us introduce some convenient notation known as Feynman slash notation.

$$\not{a} \equiv a^\mu \gamma_\mu\,, \qquad \not{a}^* \equiv \gamma^\mu a_\mu^*\,, \quad \text{and} \quad \bar{\Gamma} \equiv \gamma^0 \Gamma^\dagger \gamma^0$$

In practice, it is much easier to compute $\langle|\mathcal{M}|^2\rangle$ directly, without ever evaluating the individual amplitudes. Consider, for instance, the electron-proton elastic scattering will be represented by Feynman diagram 1.

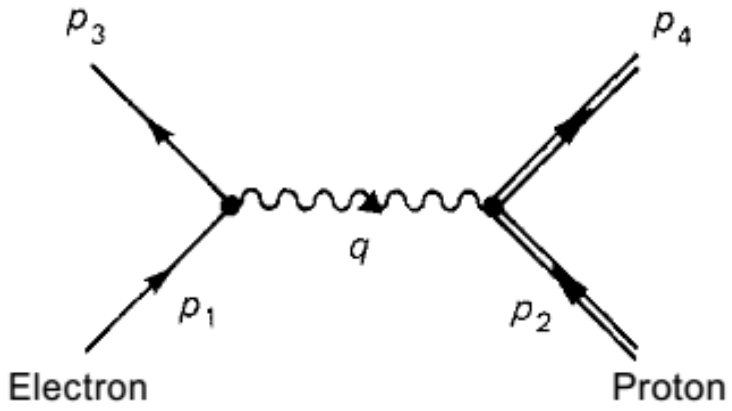

Figure 1 Feynman diagram with single photon of electron-proton scattering

Squaring amplitude, we have

$$|\mathcal{M}|^2 = \frac{g_e^4}{(p_1 - p_3)^4}[\bar{u}(3)\gamma^\mu u(1)]\big[\bar{u}(4)\gamma_\mu u(2)\big] \qquad \text{(A.7)}$$
$$\times [\bar{u}(3)\gamma^\nu u(1)]^*[\bar{u}(4)\gamma_\nu u(2)]^*$$

We must handle quantities of the general form.

$$\mathrm{G} \equiv [\bar{u}(a)\Gamma_1 u(b)][\bar{u}(a)\Gamma_2 u(b)]^* \qquad \text{(A.8)}$$

where (a) and (b) stand for the appropriate spins and momenta, and Γ_1 , and Γ_2 are two 4 x 4 matrices. To begin, we evaluate the complex conjugate (which is the same as the Hermitian conjugate, since the quantity in brackets is a 1 x 1 "matrix"):

$$[\bar{u}(a)\Gamma_2 u(b)]^* = [u(a)^\dagger \gamma^0 \Gamma_2 u(b)]^\dagger = u(b)^\dagger \Gamma_2^\dagger \gamma^{0\dagger} u(a)$$

Now, $\gamma^{0\dagger} = \gamma^0$, and $(\gamma^0)^2 = 1$, so

$$[\bar{u}(a)\Gamma_2 u(b)]^* = u(b)^\dagger \gamma^0 \gamma^0 \Gamma_2^\dagger \gamma^0 u(a) = \bar{u}(b)\bar{\Gamma}_2 u(a)$$

Where $\bar{\Gamma}_2 \equiv \gamma^0 \Gamma_2^\dagger \gamma^0$

$$\mathrm{G} = [\bar{u}(a)\Gamma_1 u(b)][\bar{u}(b)\bar{\Gamma}_2 u(a)] \qquad \text{(A.9)}$$

We are ready now to sum over the spin orientations of particle (b). Using the completeness relation

$$\sum_{b \text{ spins}} G = \bar{u}(a)\Gamma_1 \left\{ \sum_{s_b=1,2} u^{(s_b)}(p_b)\bar{u}^{(s_b)}(p_b) \right\} \bar{\Gamma}_2 u(a) \qquad \text{(A.10)}$$
$$= \bar{u}(a)\Gamma_1 \big(\not{p}_b + m_b c\big)\bar{\Gamma}_2 u(a) = \bar{u}(a) Q u(a)$$

where Q is a temporary shorthand for the 4 X 4 matrix

$$Q \equiv \Gamma_1 \big(\not{p}_b + m_b c\big)\bar{\Gamma}_2 \qquad \text{(A.11)}$$

Next, we do the same for particle (a):

$$\sum_{\text{a spins}} \sum_{\text{b spins}} G = \sum_{s_a 1,2} \bar{u}^{(s_a)}(p_a) Q u^{(s_a)}(p_a) \tag{A.12}$$

$$\sum_{s_a=1,2} \bar{u}^{(s_a)}(p_a)_i Q_{ij} u^{(s_a)}(p_a)_j$$

$$= Q_{ij} \left\{ \sum_{s_a=1,2} u^{(s_a)}(p_a) \bar{u}^{(s_a)}(p_a) \right\}_{ji} \tag{A.13}$$

$$= Q_{ij} \left(\not{p}_{\text{a}} + m_a c \right)_{ji} = \text{Tr} \left(Q \left(\not{p}_{\text{a}} + m_a c \right) \right)$$

Or, writing out the matrix multiplication explicitly (i and j are summed from 1to 4): where Tr denotes the trace of the matrix (the sum of its diagonal elements):

$$\text{Tr}\,(A) \equiv \sum_i A_{ii}$$

Conclusion

$$\sum_{\text{all spins}} [\bar{u}(a)\Gamma_1 u(b)][\bar{u}(a)\Gamma_2 u(b)]^* \tag{A.14}$$

$$= Tr \left[\Gamma_1 \left(\not{p}_b + m_b c \right) \bar{\Gamma}_2 \left(\not{p}_a + m_a c \right) \right]$$

This may not look like much of a simplification but notice that there are no spinors left; once we do the summation over spins, it all reduces to matrix multiplication and taking the trace. For want of a better name, it is called "Casimir's trick," since Casimir was apparently the first one to use it.

In the case of electron-proton scattering, Casimir's trick will be applied twice as the matrix element squared is

$$|\mathcal{M}|^2 = \frac{g_e^4}{(p_1 - p_3)^4}[\bar{u}(3)\gamma^\mu u(1)]\left[\bar{u}(4)\gamma_\mu u(2)\right] \times [\bar{u}(3)\gamma^\nu u(1)]^*[\bar{u}(4)\gamma_\nu u(2)]^* \quad \text{(A.15)}$$

So, Casimir's trick will be applied for the term $[\bar{u}(3)\gamma^\mu u(1)][\bar{u}(3)\gamma^\nu u(1)]^*$

to become $Tr\left[\gamma^\mu(\not{p}_1 + mc)\gamma^\nu(\not{p}_3 + mc)\right]$

then applying it to the second term $\left[\bar{u}(4)\gamma_\mu u(2)\right][\bar{u}(4)\gamma_\nu u(2)]^*$

to become $Tr\left[\gamma_\mu(\not{p}_2 + Mc)\gamma_\nu(\not{p}_4 + Mc)\right]$

So, the final result will be

$$\langle|\mathcal{M}|^2\rangle = \frac{g_e^4}{4(p_1 - p_3)^4} Tr\left[\gamma^\mu(\not{p}_1 + mc)\gamma^\nu(\not{p}_3 + mc)\right] \times Tr\left[\gamma_\mu(\not{p}_2 + Mc)\gamma_\nu(\not{p}_4 + Mc)\right] \quad \text{(A.16)}$$

where *m* is the mass of the electron and *M* is the mass of the proton. The factor of ¼ is included because we want the average over the initial spins; since there are two particles, each with two allowed spin orientations, the average is a quarter of the sum. Casimir's trick reduces everything down to a problem of calculating the trace of some complicated product of γ matrices. This algebra is facilitated by a number of theorems. Thus

$$\text{Tr}\left(\gamma^\mu(\not{p}_1 + mc)\gamma^\nu(\not{p}_3 + mc)\right] = 4\left[p_1^\mu p_3^\nu + p_3^\mu p_1^\nu + g^{\mu\nu}\left((mc)^2 - (p_1 \cdot p_3)\right)\right] \quad \text{(A.17)}$$

The second trace is the same with $m \longrightarrow M$, $1 \longrightarrow 2$, $3 \longrightarrow 4$ and Greek indices are lowered.

$$Tr\left[\gamma_\mu(\not{p}_2 + Mc)\gamma_\nu(\not{p}_4 + Mc)\right] = 4\left[p_{2_\mu}p_{4\nu} + p_{4_\mu}p_{2_\nu} + g_{\mu\nu}\left((Mc)^2 - (p_2 \cdot p_4)\right)\right] \quad \text{(A.18)}$$

So, the result of average matrix element squared is.

$$\langle|\mathcal{M}|^2\rangle = \frac{4g_e^4}{(p_1 - p_3)^4}\left[p_1^\mu p_3^\nu + p_3^\mu p_1^\nu + g^{\mu\nu}\left((mc)^2 - (p_1 \cdot p_3)\right)\right] \times \left[p_{2_\mu}p_{4\nu} + p_{4_\mu}p_{2_\nu} + g_{\mu\nu}\left((Mc)^2 - (p_2 \cdot p_4)\right)\right] \quad \text{(A.19)}$$

$$\langle|\mathcal{M}|^2\rangle = \frac{8g_e^4}{(p_1 - p_3)^4}[(p_1 \cdot p_2)(p_3 \cdot p_4) + (p_1 \cdot p_4)(p_2 \cdot p_3) - (p_1 \cdot p_3)(Mc)^2 - (p_2 \cdot p_4)(mc)^2 + 2(mMc^2)^2]$$

Note that this is independent of the reference frame. To consider the problem in a specific reference frame, write out the relevant four vectors in that reference frame and do the calculation. Consider the case of electron scattering from a heavy proton at rest:

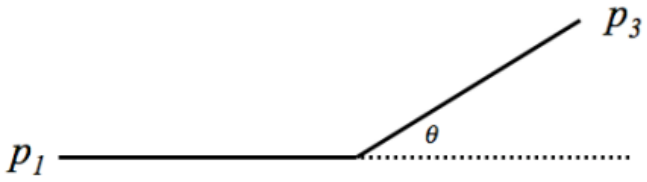

Figure 2 Kinematics of lap System

Assume M >> m so that we can ignore the recoil of the heavy spin ½ particle.

From the given figure

$$p_1 = \left(\frac{E}{c}, \vec{p}_1\right), \qquad p_2 = \left(Mc, \vec{0}\right), \quad p_3 = \left(\frac{E}{c}, \vec{p}_3\right) \ \ and \quad p_4 = (Mc, \vec{0})$$

$$|\vec{p}_1| = |\vec{p}_3| \equiv p$$

$$\vec{p}_1 \cdot \vec{p}_3 = p^2 \cos\,\theta$$

And the differential cross-section is given by

$$\frac{d\sigma}{d\Omega} = \frac{\hbar}{8\pi Mc}\langle|\mathcal{M}|^2\rangle$$

The average squared matrix element

$$\begin{aligned}\langle|\mathcal{M}|^2\rangle = 8\frac{g^4}{(p_1 - p_3)^4}\{&(p_1 \cdot p_2)(p_3 \cdot p_4) \\ &+ (p_2 \cdot p_3)(p_1 \cdot p_4) - (p_1 \cdot p_3)(Mc)^2 \\ &- (p_2 \cdot p_4)(mc)^2 + 2(mMc^2)^2\}\end{aligned} \tag{A.20}$$

$$\begin{aligned}(p_1 - p_3)^2 &= -(\vec{p}_1 - \vec{p}_3)^2 = -|\vec{p}_1|^2 - |\vec{p}_3|^2 + 2\vec{p}_1 \cdot \vec{p}_3 = -2p(1 - \cos\,\theta) \\ &= -4p^2\sin^2\,(\theta/2) \qquad \text{(a)}\end{aligned}$$

$$\begin{aligned}(p_1 \cdot p_3) &= \frac{E^2}{c^2} - (\vec{p}_1 \cdot \vec{p}_3) = p^2 + m^2c^2 - p^2\cos\,\theta \\ &= m^2c^2 + 2p^2\sin^2\,(\theta/2) \qquad \text{(b)}\end{aligned}$$

$$(p_1 \cdot p_2)(p_3 \cdot p_4) = (p_1 \cdot p_4)(p_2 \cdot p_3) = (ME)^2 \qquad (c)$$

$$and \quad (p_2 \cdot p_4) = (Mc)^2 \qquad (d)$$

Substitute with a, b, c, and d into (A.20) it becomes as

$$\begin{aligned}\langle|\mathcal{M}|^2\rangle = 8\frac{g^4}{(-4p^2\sin^2\,(\theta/2))^2}\{&(ME)^2 + (ME)^2 \\ &- (m^2c^2 + 2p^2\sin^2\,(\theta/2))(Mc)^2 - (Mc)^2(mc)^2 \\ &+ 2(mMc^2)^2\}\end{aligned}$$

$$\begin{aligned}\langle|\mathcal{M}|^2\rangle = 8\left(\frac{g^2}{4p^2\sin^2\,(\theta/2)}\right)^2\{&2(ME)^2 - (m^2c^2 + 2p^2\sin^2\,(\theta/2))(Mc)^2 \\ &- (Mc)^2(mc)^2 + 2(mMc^2)^2\}\end{aligned}$$

$$\langle|\mathcal{M}|^2\rangle = 8\left(\frac{g^2}{4p^2\sin^2(\theta/2)}\right)^2 \{2M^2(p^2c^2+m^2c^4) - 2(Mc)^2p^2\sin^2(\theta/2) - (m^2c^2)(Mc)^2 - (M^2c^2)(m^2c^2) + 2(mMc^2)^2\}$$

$$\langle|\mathcal{M}|^2\rangle = 2\left(\frac{2g^2}{4p^2\sin^2(\theta/2)}\right)^2 \{2M^2c^2(m^2c^2+p^2-p^2\sin^2(\theta/2))\}$$

$$= \left(\frac{g^2Mc}{p^2\sin^2(\theta/2)}\right)^2 \{m^2c^2+p^2\cos^2(\theta/2)\}$$

$$\langle|\mathcal{M}|^2\rangle = \left(\frac{g^2Mc}{p^2\sin^2(\theta/2)}\right)^2 \{m^2c^2+p^2\cos^2(\theta/2)\} \qquad \text{(A.21)}$$

Then substitute with this expression into the equation of differential cross-section.

$$\frac{d\sigma}{d\Omega} = \left(\frac{\alpha\hbar}{2p^2\sin^2(\theta/2)}\right)^2 \{(mc)^2+p^2\cos^2(\theta/2)\} \qquad \text{(A.22)}$$

Where $g = \sqrt{4\pi\alpha}$. This is called Mott formula of differential cross-section. This is a good approximation in low energy electron-proton scattering.

In the case that $p^2 << (mc)^2$ this means that the incident electron is non-relativistic, so the expression reduced to

$$\frac{d\sigma}{d\Omega} = \left(\frac{\alpha\hbar}{2p^2\sin^2(\theta/2)}\right)^2 (mc)^2 = \left(\frac{\alpha\hbar mc}{2p^2\sin^2(\theta/2)}\right)^2$$

Using $\alpha = \frac{e^2}{\hbar c}$ and $p = mv$ the expression becomes

$$\frac{d\sigma}{d\Omega} = \left(\frac{e^2}{2mv^2 \sin^2(\theta/2)}\right)^2$$

which is Rutherford formula that is used in classical mechanics in non-relativistic regions.

الملخص

تدرس هذه الرسالة الخصائص الفيزيائية للمواد النووية التي هي المكونات الرئيسية للهدرونات مثل البروتون. وتعتبر تجارب التشتت للإلكترون مع البروتون من اهم الوسائل التي تساعدنا في تلك الدراسة و تمكننا من تحقيق ذلك الهدف. دراسة الخصائص الفيزيائية الداخلية للهادرونات (البروتونات) مهمة جدا في الفيزياء ويتم التحقيق في هذه الخصائص باستخدام تقنيات مختلفة حيث ان تجارب التشتت المرنة هي واحدة من تلك التقنيات. تعد نظرية التشتت باستخدام الديناميكا الكهربائية الكمية (QED) طريقة مناسبة خاصة للتجارب ذات الطاقات العالية. وفى تلك الرسالة تم تطبيق قواعد فاينمان على تشتت لبتون–هادرون لإعطاء تعبير مناسب لمساحة مقطع التشتت المعروفة باسم صيغة Mott. وفى هذه الرسالة تم استنتاج مساحة مقطع التشتت المرن للإلكترون مع البروتون وتم مقارنة مساحة المقطع المحسوبة مع القياسات المعملية لهذا النوع من التشتت. وبالمقارنة تم ملاحظة استنتاجين أولا: يوجد تباعد منتظم بين قيم مساحة المقطع المحسوبة والمقاسة معمليا. ثانيا: انه عند القيم المنخفضة للطاقة (كمية الحركة)، يظهر البروتون كجسيم يشبه النقطة الواحدة ويحدث التشتت من على سطحه ككل بينما تبدأ مكوناته بالمشاركة والتأثير في عملية التشتت عند الطاقات العالية. ويخلص ذلك إلى أن هناك عاملا معدلا يجب إضافته إلى صيغة Mott لجعل القيم المحسوبة لمساحة المقطع تتوافق مع القيم المعملية. يرتبط هذا العامل بالخواص الكهربائية والمغناطيسية للمكونات الداخلية للبروتون . وتسمى هذه العوامل عوامل الشكل. تم حساب هذه العوامل بطريقة فصل روزنبلوث بالإضافة الى مقارنتها مع القيم التي تم الحصول عليها من تجارب أخرى حيث اتفقت القيم المحسوبة مع تلك. ومن ضمن اهداف الرسالة حساب نصف قطر توزيع الشحنات على البروتون حيث تم استخدام القيم

المحسوبة لعوامل الشكل في استنتاج قيمة نصف القطر للبروتون والتي كانت 0.81 فمتومتر. مع زيادة الطاقة الخاصة بالالكترون يتم الحصول على تفاصيل ادق لمكونات البروتون وذلك لانه مع زيادة الطاقة يقل الطول الموجي للحركة الموجية المرافقة لحركة الالكترون وكذلك للفوتون الحامل للطاقة بين الالكترون والبروتون والذي يسمى بوزون وذلك من شأنه التعمق في التفاصيل الدقيقة لمكونات البروتون.

جامعة بنها
كلية هندسة شبرا
قسم العلوم الأساسية

الخواص الفيزيائية للطّور الأوَّلِي للمادة النووية في ضوء القياسات المعملية ونظيراتها من النماذج النظرية

رسالة مقدمة كجزء من متطلبات الحصول على درجة الماجستير في الفيزياء الهندسية قسم العلوم الأساسية – بكلية الهندسة بشبرا – جامعة بنها

مقدمة من

المهندس / أحمد مصطفى بعد الرازق سيد

معيد الفيزياء الهندسية – قسم العلوم الأساسية –كلية هندسة شبرا – جامعة بنها

تحت اشراف

أ.د / أحمد محمد عبد الله

أستاذ الفيزياء الهندسية – قسم علوم أساسية – كلية هندسة شبرا – جامعة بنها

أ.م.د / عبد الناصر صابر عبد الفتاح

أستاذ مساعد الفيزياء الهندسية – قسم علوم أساسية – كلية هندسة شبرا – جامعة بنها

القاهرة - مصر
2024